Université d'Ottawa • University of Ottawa

Université d'Ottawa · University of Ottawa

FACULTÉ DES ÉTUDES SUPÉRIEURES ET POSTDOCTORALES

FACULTY OF GRADUATE AND POSTDOCTORAL STUDIES

Isil TÖRECI

AUTEUR DE LA THÈSE - AUTHOR OF THESIS

M. A. Sc. (Chemical Engineering)

GRADE - DEGREE

Department of Chemical Engineering

FACULTÉ, ÉCOLE, DÉPARTEMENT - FACULTY, SCHOOL, DEPARTMENT

TITRE DE LA THÈSE - TITLE OF THE THESIS

Adsorption Separation of Methyl Chloride from Air

H. Tezel

DIRECTEUR DE LA THÈSE - THESIS SUPERVISOR

CO-DIRECTEUR DE LA THÈSE - THESIS CO-SUPERVISOR

EXAMINATEURS DE LA THÈSE - THESIS EXAMINERS

M. Dubé

A. Macchi

J.-M. De Koninck, Ph.D.

LE DOYEN DE LA FACULTÉ DES ÉTUDES SUPÉRIEURES ET POSTDOCTORALES

SIGNATURE

DEAN OF THE FACULTY OF GRADUATE AND POSTDOCTORAL STUDIES

ADSORPTION SEPARATION OF METHYL CHLORIDE FROM AIR

By

Işıl Töreci

A thesis submitted to the Faculty of Graduate and Postdoctoral Studies in partial fulfillment of the requirement for the degree of

Master of Applied Science

In

Department of Chemical Engineering

UNIVERSITY OF OTTAWA

© Işıl Töreci, Ottawa, Canada, January 5th 2004

Library and Archives Canada

Published Heritage Branch

395 Wellington Street
Ottawa ON K1A 0N4
Canada

Bibliothèque et Archives Canada

Direction du Patrimoine de l'édition

395, rue Wellington
Ottawa ON K1A 0N4
Canada

Your file Votre référence
ISBN: 0-494-01619-1
Our file Notre référence
ISBN: 0-494-01619-1

NOTICE:
The author has granted a non-exclusive license allowing Library and Archives Canada to reproduce, publish, archive, preserve, conserve, communicate to the public by telecommunication or on the Internet, loan, distribute and sell theses worldwide, for commercial or non-commercial purposes, in microform, paper, electronic and/or any other formats.

The author retains copyright ownership and moral rights in this thesis. Neither the thesis nor substantial extracts from it may be printed or otherwise reproduced without the author's permission.

AVIS:
L'auteur a accordé une licence non exclusive permettant à la Bibliothèque et Archives Canada de reproduire, publier, archiver, sauvegarder, conserver, transmettre au public par télécommunication ou par l'Internet, prêter, distribuer et vendre des thèses partout dans le monde, à des fins commerciales ou autres, sur support microforme, papier, électronique et/ou autres formats.

L'auteur conserve la propriété du droit d'auteur et des droits moraux qui protège cette thèse. Ni la thèse ni des extraits substantiels de celle-ci ne doivent être imprimés ou autrement reproduits sans son autorisation.

In compliance with the Canadian Privacy Act some supporting forms may have been removed from this thesis.

While these forms may be included in the document page count, their removal does not represent any loss of content from the thesis.

Conformément à la loi canadienne sur la protection de la vie privée, quelques formulaires secondaires ont été enlevés de cette thèse.

Bien que ces formulaires aient inclus dans la pagination, il n'y aura aucun contenu manquant.

Canada

ABSTRACT

Volatile organic compounds (VOCs) are present ubiquitously and they are emitted in large amounts by especially semiconductor and aluminum industries each year. These compounds are very harmful to the environment, as well as to human health. Adsorption is one of the most efficient and practical separation techniques among all separation processes. Varieties of activated carbons and zeolites have been used as adsorbents for VOC emission control.

In this study methyl chloride was selected as the main adsorbate since it is one of the volatile organic compounds produced largely in industry. Nitrogen was the other adsorbate since air is composed of nitrogen by 79%. As adsorbents one in-house adsorbent; SBA-15 and three commercial adsorbents; HiSiv-3000 (ZSM-5 zeolite), activated carbon cloth, mesoporous activated carbon were used.

Experiments of constant volume technique were performed in order to obtain adsorption isotherms of methyl chloride and nitrogen with the adsorbents mentioned above up to 1.6 atm in the temperature range of 21.5 and 80 °C. Langmuir, Freundlich, Sips and Toth isotherm models were fitted to these isotherms. By using the Toth isotherm parameters adsorption isosteres were obtained. Henry's Law constants and heat of adsorption values were calculated. Expected working capacities for pressure swing adsorption (PSA), vacuum swing adsorption (VSA), temperature swing adsorption (TSA) were obtained and feasibility of these processes was discussed. The binary system behavior was also predicted for HiSiv-3000 and SBA-15 by using Extended Langmuir and Ideal Adsorbed Solution models.

Methyl chloride adsorption breakthrough curves with HiSiv-3000 and SBA-15 for vacuum swing adsorption application was produced. The effects of modeling parameters such as temperature, inlet concentration, flow rate and bed length were investigated.

It was concluded that mesocarbon is the best adsorbent to separate methyl chloride from air. Carbon cloth has the lowest heat of adsorption for methyl chloride. Prediction of binary system behavior showed that nitrogen adsorption is negligible. Mesocarbon shows the highest expected working capacities for PSA, VSA and TSA. VSA and TSA were found to be two promising processes for separation of methyl chloride from air.

RÉSUMÉ

Les materiaux organique volatiels sont present partout et sont emit engrande quantite par les industrie de semi conducteur et d'aluminum chaque annee.ces produit sont tres nocif a l'environment aussi bien pour la sante des humain. L'absortion est un des plus efficace et pratique moyen technique de separation de tout les methode de separation. Une variete de carbon active et zeolites ont ete utilise comme adsorbents pour le control les produit organique volatil.

Dans cette etude, le chlorure de methyl fut utiliser comme le gaz volatile a etre adsorber parce qu'il est largement produit par l'industrie. L'azote fut l'autre gaz etudie parce que l'air est compose de celui-ci a 79 %. Comme adsorbant, HiSiv-3000 (ZSM-zeolite), SBA-15, lige de carbone active et grain de carbon active a pore moyen furent utilise.

Des experience utilisant la technique a volume constant furent suivient afin d'obtenir des isotherm d'adsorption du chlorure de methyl et d'azote avec les adsorbant sus-mentionne jusqu'a 1.6 atmosphere et un champ de temperature de 21.5 et 80 °C. Les models isothermes de Langmuir, Freundlich, Sips and Toth marie a ces isothermes. En utilisant les parametre de l'isotherme Toth, des isostere d' adsorption furent obtenu. Les constantes de loi d'Henry et valeurs d'adsorption de chaleur furent calcules. Les capacites de fonctionnement prevues dans le balancement de l'adsortion par pression (APP), par vide (APV) et par temperature (APT) furent obtenus et la faisabilite de ces procede fut discute. Le comportement du systeme binaire fut aussi prevu por le HiSiv-3000 et le SBA-15 en utilisant des models extendus de Langmuir et d' adsorption ideal de solution.

Des courbes de percement du chlorure de methyl avec HiSiv-3000 et SBA-15 pour l'APV furent produites. Les effets des parametres de modelisation comme la temperature, concentration a l' entree, le debit et la longeur du lit furent etudie.

Il a ete conclu que, de tout les adsorbants etudie, les grain de carbone a pore moyen est le meilleur adsorbant en ce qui concerne l'enlevement du chlorure de methyl de l'air. Le tissus de carbon a le plus basse adsorption de la chaleur pour ce meme produit. La prediction du comportement de systeme binaire a demontre que l'adsorption de l'azote est negligible. Le carbone a pore moyen de montre la plus haute capacite de travail (adsorption et desorption) prevu pour les procede APP, APV et APT etudie. Finallement, APV et APT sont deux procede promettant pour la separation du chlorure de methyl de l'air.

Statement of Contributions of Collaborators

I hereby declare that I am the sole author of this thesis. I have performed all experiments, the associated data analysis and modeling.

My supervisor, Dr. Handan Tezel, provided continual guidance throughout this work and made editorial comments and corrections to my written work.

Dr. Abdelhamid Sayari and his student Dr. Yang Yong contributed by providing the mesoporous SBA-15 adsorbent and characterization of SBA-15 and as well as HiSiv-3000. They are coauthors of the first paper.

Signature: Date: Nov 27, 2003

To My Family

ACKNOWLEDGEMENTS

I would like to thank Dr. Tezel for her supervision and guidance through out my research. Without her support, advice and encouragement this thesis could not be done.

I would like to thank Dr. Sayari from Chemistry Department for providing me SBA-15 adsorbent, which was produced in his laboratory.

I am very grateful to our department's technicians, Louis Tremblay, Franco Ziroldo and Gerard Nina. I had been able to perform my experiments successfully with their technical help in solving equipment related problems. I would also like to thank all the professors and my colleagues at the Department of Chemical Engineering. I would like to thank Nilesh Patel for his friendship and help whenever I needed the most.

Last but not least, I would like to thank my family and my friends in Turkey and here in Canada. I appreciate very much their support and companionship throughout my studies.

TABLE OF CONTENTS

LIST OF TABLES

LIST OF FIGURES

CHAPTER 1

INTRODUCTION

Although the history of adsorption is dated back to ancient times, its industrial use started in 18th century. Adsorption of gases on charcoal was first discovered by Scheel in 1773 (Rouquerol et. al., 1999). The emission of heat during adsorption was discovered by Saussuare in 1814 (Saussure, 1814). During 19th century, calorimetric measurements of heat of adsorption and studies on adsorption forces were started (Dabrowski, 1999). Freundlich was the first theory about the interpretation of adsorption isotherms which was proposed by Boedecker in 1895 (Boedecker, 1985). In 1903, Tswett discovered selective adsorption. He also proposed chromatographic technique for adsorption experiments (Sakodynskii, 1972). During World War I and II, different types of adsorbents were found and used widely, especially activated carbon. After World War II, synthetic zeolite production gained importance.

Applications of adsorption such as separation and purification of gases and liquids, play very important role in environment protection, control of ozone depletion and prevention of global warming. In air treatment, volatile organic compounds are one of the most important gases that need to be focused on.

Controlling the emission of volatile organic compounds (VOCs) is a very crucial problem for human life and for environmental aspects. There are thousands of different VOCs emitted from many different industries, as well as from vehicles everyday. Emission of VOCs makes the earth suffer more and more and gives less chance to the future generations to have the opportunity of living on clean earth. In order to be in the category of

VOCs, the chemicals should contain carbon atom in their molecular structure and be able to vaporize easily in room temperature. Their contribution to global warming and to ground level ozone formation is very high. Most of the VOCs are also very harmful to human and animal health (Thornton, 2000).

1.1 OBJECTIVES

In separation of trace components from air, adsorption processes show better results than other separation processes. Being a clean process with no by-products and being able to recover the adsorbed components reduce the cost of the operation and make the adsorption process more desirable than other processes. As a result, adsorption processes have been used significantly in many industrial applications to control emission of many different gases.

Recent developments on production of new adsorbents lead to the need of experimental data to evaluate the capacities of these adsorbents for specific gases that need to be treated.

The objective of this thesis is to investigate the adsorption capacities of several adsorbents for methyl chloride. Methyl chloride is one of the volatile organic compounds and is emitted by several industries. The adsorbent screening was done and it was found that adsorbents having homogeneous surfaces would have higher capacities for VOC adsorption because organic compounds have a tendency to have higher attraction to homogeneous surfaces than heterogeneous surfaces. In the literature the only one adsorbent that was studied for methyl chloride adsorption was Takeda 5A carbon (Mariwala and Foley, 1994). The adsorbents that are investigated in this study are ZSM-5, activated carbon cloth and mesoporous activated carbon which are commercial adsorbents and SBA-15 which is an in-house adsorbent. Starting from the experimental data of pure adsorption isotherms of methyl chloride and nitrogen, several adsorption isotherm models were fitted to the data in order to have better understanding of the adsorption behavior of the adsorbents with these adsorbates. The binary system behavior of these gases with different adsorbents was predicted by two different methods by using the pure adsorption isotherm model fits. Heat of adsorption for

methyl chloride and nitrogen with the adsorbents that are used in this project were determined. Several adsorption processes such as pressure swing adsorption (PSA), vacuum swing adsorption (VSA) and temperature swing adsorption (TSA) were compared for the separation of methyl chloride from air by comparing the expected working capacities of these processes at different adsorption and desorption conditions. And finally, the modeling of the breakthrough curve for vacuum swing adsorption process was done and effects of several important parameters for the process were investigated to have a better overall view for the separation of methyl chloride by adsorption.

The ultimate goal of this study is to find the best adsorption process with the best adsorbent for the separation of methyl chloride from air.

1.2 STRUCTURE OF THIS THESIS

This thesis is composed of two papers that are going to be submitted shortly and a chapter about modeling of methyl chloride adsorption.

The second chapter contains the first paper to be submitted and is on the subject of methyl chloride and nitrogen adsorption on ZSM-5 zeolite and SBA-15 molecular sieve carbon. The pure adsorption isotherms at different temperatures were determined experimentally and several adsorption isotherm models were fitted to these isotherms. Heat of adsorption of methyl chloride and nitrogen were determined by using these two adsorbents. By using Toth isotherm parameters, adsorption isosteres of both adsorbates were determined. Binary adsorption isotherms were predicted. Expected working capacities for three adsorption processes, pressure swing adsorption (PSA), vacuum swing adsorption (VSA) and temperature swing adsorption (TSA) were determined for both adsorbent. Dr. Sayari and his student Dr. Yong contributed to this paper by providing mesoporous SBA-15 and characterizing both HiSiv-3000 and SBA-15.

The second paper is given in the third chapter. Methyl chloride adsorption on activated carbon cloth and mesocarbon were discussed in this chapter. Pure adsorption model parameters were determined for isotherms obtained at different temperatures. Pure methyl chloride isosteres were determined by using Toth isotherm parameters. Heats of adsorption

of methyl chloride were calculated by using Van't Hoff plot for both adsorbents. Expected working capacities for methyl chloride adsorption for PSA, VSA and TSA processes were determined and compared for adsorbents ZSM-5, SBA-15, carbon cloth and mesocarbon.

In the fourth chapter, adsorption of methyl chloride was modeled. The effects of temperature, inlet concentration, flow rate, bed length as well as different adsorbent type on the separation process were predicted.

In the final chapter, the summary of all conclusions were presented. Recommendations for future studies are also included in this chapter. Nomenclature and references were included at the end of each chapter. At the end of the thesis appendix was included. In appendices A and B, all graphs were presented related to chapters 2 and 3, respectively.

2.3 REFERENCES

Boedecker, C., J. Landw., 7 (1985) 48

Dabrowski, A., "Adsorption and Its Applications in Industry and Environmental Protection; Studies in Surface Science and Catalysis", Vol. 120A, Elsevier, Poland (1999)

Mariwala, R. K. and H. C. Foley, "Calculation of Micropore Sizes in Carbogenic Materials from the Methyl Chloride Adsorption Isotherm", Ind. Eng. Chem. Res., 33, 2314-2321 (1994)

Rouquerol, F., J. Rouquerol and K. Sing, "Adsorption by Powders and Porous Solids: Principles, Methodology and Applications", Academic Press, San Diego (1999)

Sakodynskii, K., "The Life and Scientific Works of Michael Tswett", J. Chromatogr., 73 (1972)

Saussure, T.de, Gilbert's Ann der Physik, 47 (1814).

Thornton, J., "Pandora's Poison: Chlorine, Health, and a new Environmental Strategy", MIT Press, Massachusetts (2000)

CHAPTER 2

ADSORPTION SEPARATION OF METHYL CHLORIDE FROM NITROGEN BY USING ZSM-5 AND MESOPOROUS SBA-15

Isil Toreci*, F. Handan Tezel*, Yang Yong** and Abdelhamid Sayari**

*Department of Chemical Engineering, University of Ottawa, 161 Louis Pasteur, Ottawa, Ontario K1N 6N5, Canada

**Department of Chemistry, and Centre for Catalysis Research and Innovation, University of Ottawa, 10 Marie Curie, Ottawa, Ontario, K1N 6N5, Canada

The adsorption capacities of zeolite ZSM-5 and periodic mesoporous molecular sieve SBA-15 were examined for methyl chloride (chloromethane) and nitrogen for separation of these gases. Adsorption isotherms were obtained by using constant volume technique up to 1.6 atm in the temperature range of 40 and 80°C. Langmuir, Freundlich, Sips and Toth were fitted to the isotherms and validations of these models were discussed. Adsorption isosteres were obtained by using Toth equation parameters. Binary adsorption isotherm predictions were done by using Extended Langmuir (EL) and Ideal Adsorbed Solution Theory (IAST) in order to have a better understanding of the separation of methyl chloride from air. Henry's Law constants and heat of adsorption for both adsorbents were also obtained. Expected working capacities of pressure swing adsorption (PSA), vacuum swing adsorption (VSA)

and temperature swing adsorption (TSA) were obtained at different adsorption and desorption conditions and feasibility of these processes were discussed.

2.1 INTRODUCTION AND LITERATURE REVIEW

Volatile Organic Compounds (VOCs) are produced extensively in many industries especially in high-tech industries. Control of emission of these gases is a very important issue due to the environmental problems and negative effects to human health. Some of them have great impact on ozone depletion and some others have a very high green house effect. Their photochemical reactions with nitrogen oxides produce ground level ozone, often referred to as urban smog. This smog is harmful to human health (Koh et. al., 2002). Due to the great impact of the presence of VOCs on environment and human health even at very low concentrations, they need to be removed from air.

Compared to other processes, such as incineration, condensation and absorption, adsorption separation processes are cleaner and more effective techniques in removing trace pollutants (Zhao et. al., 1998 and Huang et. al., 1999). Having no by-products and being able to recover the adsorbed species reduce the cost and make the adsorption more preferable one (Jennings et. al., 1985).

In this study, methyl chloride was examined as a representative volatile organic compound. It is used in the production of silicone (Bloemen and Burn, 1993) as well as in the manufacturing of synthetic rubber and in the production of higher hydrocarbons. Some of the health problems occurring in the exposure to high concentrations of methyl chloride are serious effects on nervous system, heart rate, blood pressure, liver and kidneys. Long term exposures studied in animals have shown effects on liver, kidney, spleen and central nervous system. EPA classifies it as a Group D carcinogen. The Occupational Safety and Health Administration (OSHA) has set the permissible exposure limit for methyl chloride as 100 ppm for an 8-hour workday in a 40-hour workweek (ATSDR, 1998).

In this study, SBA-15 and ZSM-5 zeolites were considered as potential adsorbents to be used to control the methyl chloride emissions. Their adsorption capacities for methyl chloride and nitrogen were examined. As the representative of air, nitrogen was used since

79% of air is composed of this gas. The adsorption properties of nitrogen and oxygen are similar to each other compared to volatile organic compounds therefore nitrogen is representing air. Binary mixture adsorption behavior was predicted to better understand the separation of methyl chloride from air. Heat of adsorption, which is a very important parameter in analysis of the regeneration process, was calculated for both of these adsorbents, as well. Expected working capacities for pressure swing adsorption (PSA), vacuum swing adsorption (VSA) and temperature swing adsorption (TSA) were obtained at different adsorption and desorption conditions and the feasibility of these processes was discussed.

HiSiv-3000 is essentially a pure silica ZSM-5 zeolite with Si/Al ratio in the order of thousands. ZSM-5 zeolites are porous crystalline aluminosilicates which are constructed from five member rings to create two intersecting channel systems with elliptical 10-member ring pore openings. The pore diameter of ZSM-5 zeolites is ca. 5Å (Thomas and Critenden, 1998). ZSM-5 zeolite is prepared under hydrothermal conditions using tetrapropyl ammonium hydroxide (TPAOH) as template. The SiO_2/Al_2O_3 ratio varies from 15 to infinity for the pure silica polymorph silicalite. Crystallization gets easier as the SiO_2/Al_2O_3 ratio increases (Szostak, 1992).

SBA-15 silica's pore system is comprised of a 2 dimensional hexagonally packed cylindrical pores (Zhao, D. et. al., 1998). Contrary to zeolites, the pore walls of SBA-15 consist of microporous amorphous silica. It is prepared using a poly(ethylene oxide)-poly(propylene oxide)-poly(ethylene oxide triblock copolymer as supramolecular template. This polymer denoted $EO_{20}PO_{70}EO_{20}$ is manufactured by BASF and commercially known as P123. Its molecular weight is 5800. The pore sizes of SBA-15 silica may be varied from 7 to 30 nm using organic additives such as trimethylbenzene.

2.2 THEORETICAL BACKGROUND

2.2.1 Pure Component Adsorption Models

For pure component adsorption isotherms, Langmuir, Freundlich, Sips and Toth models were used.

Langmuir: This model is based on dynamic equilibrium between adsorption and desorption. The surface is considered to be homogeneous and the adsorption is limited to a single monolayer. Adsorption of species is localized at definite sites (Langmuir, 1918). The surface coverage is given by following equation:

$$\theta = \frac{n}{n_s} = \frac{bP}{1+bP} \tag{2.1}$$

where n and ns are the number of adsorbed species and adsorption sites, respectively. P is the adsorbate pressure, and b is an empirical parameter.

Freundlich: This empirical model usually fits to nonlinear isotherms better (Zeldowitsh, 1935). It is a good model to explain the behavior of organic compounds adsorption from liquid systems on activated carbon or gas adsorption on heterogeneous surfaces. The parameter t is usually larger than 1 and depends on the heterogeneity of the adsorbent surface. The larger the parameter t is, the greater the heterogeneity of the system (Do, 1998).

$$\theta = \frac{n}{n_s} = KP^{1/t} \tag{2.2}$$

Sips: This model, known as Langmuir isotherm for non uniform surfaces is also empirical. It is basically the combination of Langmuir and Freundlich models as follows:

$$\theta = \frac{n}{n_s} = \frac{(bP)^{1/t}}{1+(bP)^{1/t}} \tag{2.3}$$

Toth: Toth equation, which is also an empirical model, describes many adsorption isotherms well. It usually fits to Henry's Law region better than Sips and Freundlich models.

$$\theta = \frac{n}{n_s} = \frac{bP}{\left[1+(bP)^t\right]^{1/t}} \tag{2.4}$$

All the parameters in Toth equation can be expressed as a function of temperature. This property enables us to extrapolate or interpolate isotherms at different temperatures. The temperature dependencies of parameters are given in equations 2.5 to 2.7 below:

$$b = b_0 \exp\left[\frac{\Delta H}{RT_0}\left(\frac{T_0}{T}-1\right)\right] \tag{2.5}$$

$$t = t_0 + \alpha\left(1-\frac{T_0}{T}\right) \tag{2.6}$$

$$n_s = n_{s,0} \exp\left[\chi\left(1-\frac{T}{T_0}\right)\right] \tag{2.7}$$

2.2.2 Binary adsorption Models

Extended Langmuir (EL): The assumptions for Langmuir isotherm for pure components are valid for binary systems as well. Parameters that are obtained from pure adsorption isotherms of individual components are used to predict the binary adsorption behavior. This model assumes that different components do not have any effect on the adsorption of other components and do not interact with each other (Markham and Benton, 1931).

$$\theta_i = \frac{n_i}{n_s} = \frac{b_i P_i}{1 + \sum_{j=1}^{2} B_j P_j} \tag{2.8}$$

Ideal Adsorbed Solution Theory (IAST): This theory has similarities with Raoult's Law for vapor-liquid equilibrium. Both the gas phase and the adsorbed phase are assumed to be ideal solutions. More details for this model were presented by Myers and Prausnitz (1965). The reduced spreading pressure, z, can be calculated by using the following equation (Eqn. 2.9). In order to find reduced spreading pressure, parameters of pure component adsorption isotherms, mole fraction of molecules in the mixture and the total pressure must be known.

$$z = \frac{A\pi}{RT} = \int_0^{P_1^0} \frac{n_1}{P_1} dP_1 = \int_0^{P_2^0} \frac{n_2}{P_2} dP_2 = \ldots \tag{2.9}$$

2.3 EXPERIMENTAL

Single component adsorption isotherms were obtained by using constant volume technique. Experiments were performed by constant volume system Micromeritics Model: Accusorb 2100E. Ultra pure nitrogen and methyl chloride were purchased from Praxair (Ottawa, Canada). The two adsorbents used, namely HiSiv-3000 and SBA-15 were described earlier. Pure silica ZSM-5 zeolite HiSiv-3000 was purchased from UOP (Mount Laurel, NJ, USA), whereas Periodic mesoporous silica SBA-15 was prepared in our laboratory as described hereafter.

The SBA-15 silica used in this study was prepared via a supramolecular templating technique as follows: 14 g of triblock copolymer Pluronic P123 (BASF) was added to a solution containing 105 g of distilled water and 420 g of 2 M HCl in a Teflon lined autoclave. The mixture was magnetically stirred at 35 °C for 1.5 h, during which complete dissolution of the template P123 was achieved. Then, 29.75 g of tetraethylorthosilicate was added and stirring was maintained for 5 min. The mixture was then kept under stirring at 35 °C for 18 h then at 80 °C for 24 h without stirring. The product was obtained by filtration

followed by washing by water and air-drying. The polymer was removed by calcination at 540 °C in flowing air for 5 h.

Samples of adsorbents were weighed and regenerated under vacuum at 350 °C for more than 14 hours inside the constant volume system. The adsorbate was then introduced into a manifold and the initial pressure was recorded. By opening the sample valve, the adsorbate was introduced to the adsorbent and the pressure drop due to adsorption was monitored as a function of time. After the equilibrium was reached, the final pressure was recorded. The difference between the initial and the final pressure was used in the calculations of the amount adsorbed for the amount of adsorbent present in the system at that equilibrium pressure by applying the Ideal Gas Law. At different equilibrium pressures, the procedure was repeated to obtain the complete adsorption isotherm at the temperature of the experiments performed.

2.4 RESULTS AND DISCUSSION

2.4.1 Characterization of Adsorbents

2.4.1.1 HiSiv-3000

The nitrogen adsorption experiment was performed at 77K using a Coulter Omnisorp 100 gas analyzer. The specific surface area (BET surface area) was determined from the linear part of the BET plot (P/P_0 = 0.05-0.15) and found to be 251 m^2/g (Figure 2.1). The pore size was determined by Harvath-Kawazoe method as 5Å. It was found from XRD analysis that HiSiv-3000 exhibits almost the same diffraction pattern as for standard ZSM-5.

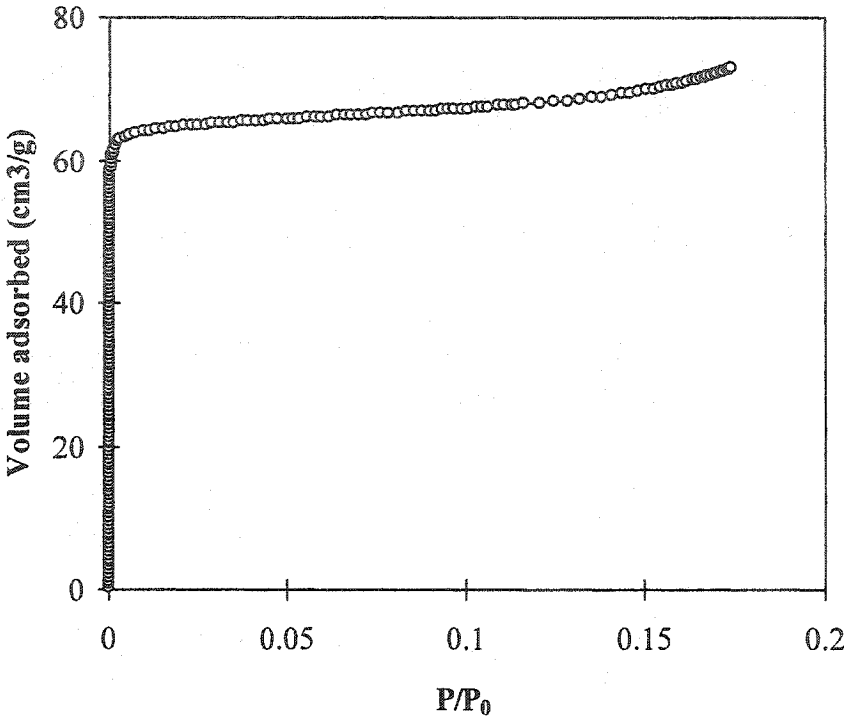

Figure 2.1: Nitrogen adsorption and desorption isotherm of HiSiv-3000 at 77 K.

2.4.1.2 SBA-15

X-ray powder diffraction (XRD) patterns were collected on a Scintag X_2 Advanced Diffraction System using CuKα radiation with 0.15418 nm wavelength. Nitrogen adsorption-desorption experiment was performed at 77 K using a Coulter Omnisorp 100 gas analyzer. Before measurements, samples were outgassed at 473 K in the degas port of the adsorption apparatus. The specific surface area was determined from the linear part of the BET plot (P/P_0 = 0.05–0.15). The pore size distribution was calculated from the adsorption branch using the KJS (Kruk, Jaroniec, Sayari) method (Kruk et. al., 1997).

The XDR pattern shown in Figure 2.2, is dominated by a peak at 2θ = 1.08°, corresponding to a distance of 8.18 nm. In addition, two weak, but well-resolved peaks appeared at 2θ = ca. 2°. Consistent with the occurrence of a 2D hexagonal mesophase, these peaks were attributed to (100), (110) and (200) diffractions. The cell parameter $a = 2d_{100}/\sqrt{3}$ was found to be 9.4 nm.

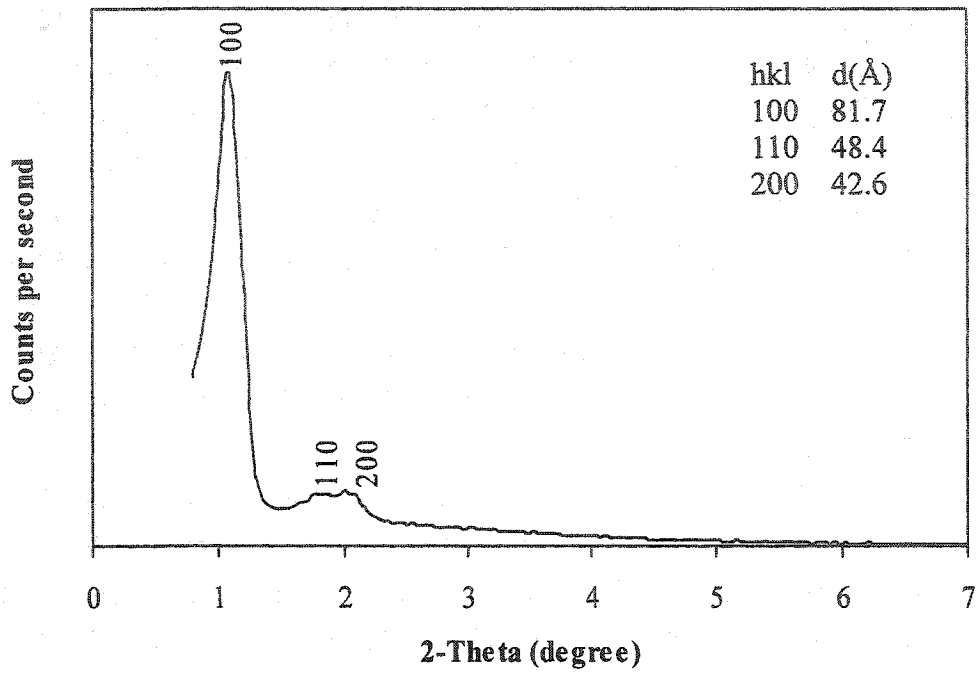

Figure 2.2: XRD pattern of SBA-15.

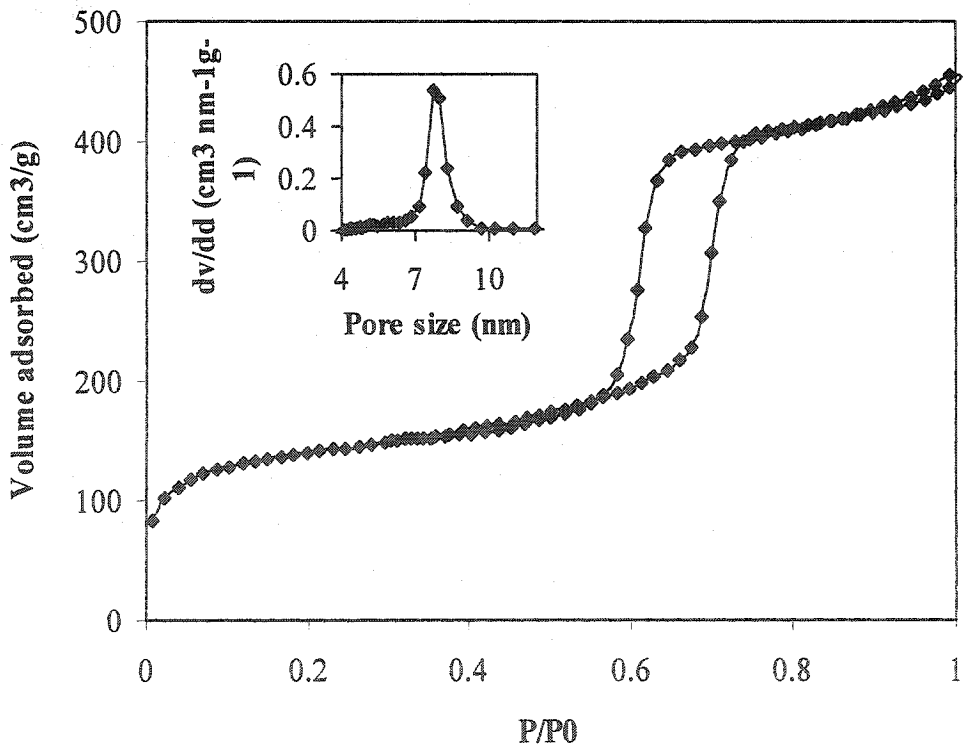

Figure 2.3: Nitrogen adsorption and desorption isotherm of SBA-15 at 77K.

The nitrogen adsorption desorption isotherm is shown in Figure 2.3. It exhibits the characteristic sharp steps corresponding to the condensation and evaporation of nitrogen from mesopores with narrow size distribution. The pore size distribution, calculated using the KJS model (Figure 2.3, inset) exhibits a maximum at w = 7.7 nm. Combining XRD and nitrogen adsorption data, the pore wall thickness can be calculated using the following equation: b = a – w = 1.7 nm. The surface area calculated based on the BET model was found to be 645 m^2/g, and the pore volume was 0.72 cm^3/g.

2.4.2 Pure Component Adsorption isotherms

Pure component adsorption isotherms of methyl chloride were obtained on HiSiv-3000 and SBA-15 at three different temperatures ranging between 40 and 80 °C as shown in Figures 2.4 and 2.5 respectively. For HiSiv-3000 Langmuir model and for SBA-15 Freundlich model were shown as best fit adsorption models to demonstrate the trends of adsorption isotherms. Compared to SBA-15, adsorption of methyl chloride on HiSiv-3000 is much greater at low pressures. However, at high pressures SBA-15 adsorbs more methyl chloride than HiSiv-3000 since surface area of SBA-15 is much higher than that of HiSiv-3000. Another observation obtained from pure component adsorption isotherms of methyl chloride is that, HiSiv-3000 adsorption isotherms behave more rectangular, whereas, methyl chloride adsorption isotherms for SBA-15 are more linear. Since SBA-15 has wider pore size distribution and has mesopores, as the pressure increases more adsorbate molecules are forced to be adsorbed on to the surface of the pores until all the pores are saturated with the adsorbate. On the other side, HiSiv-3000 has very narrow pore size distribution and once the pores are filled pressure increase do not increase the amount adsorbed. For both adsorbents, it was observed that as the temperature increases, the amount adsorbed decreases indicating that these adsorption processes are exothermic.

Another notable observation about the methyl chloride adsorption isotherm data is that with both adsorbents the isotherm data points show a slight bent at around 55 kPa pressure. This could be caused by instrumental error or could be characteristic of the methyl chloride itself.

For nitrogen adsorption, HiSiv-3000 also has higher adsorption capacity than SBA-15 as it can be seen from Figures 2.6 and 2.7, respectively. Nitrogen adsorption isotherms for SBA-15 show interesting behavior. They first increase linearly and then flatten above 80 kPa. This behavior made it difficult to fit the models to the isotherms. The capacities of both adsorbents for nitrogen are much less than their capacities for methyl chloride since the attraction between methyl chloride and adsorbents is much greater than attraction between nitrogen and the adsorbents. This is caused by the difference of the molecular weight.

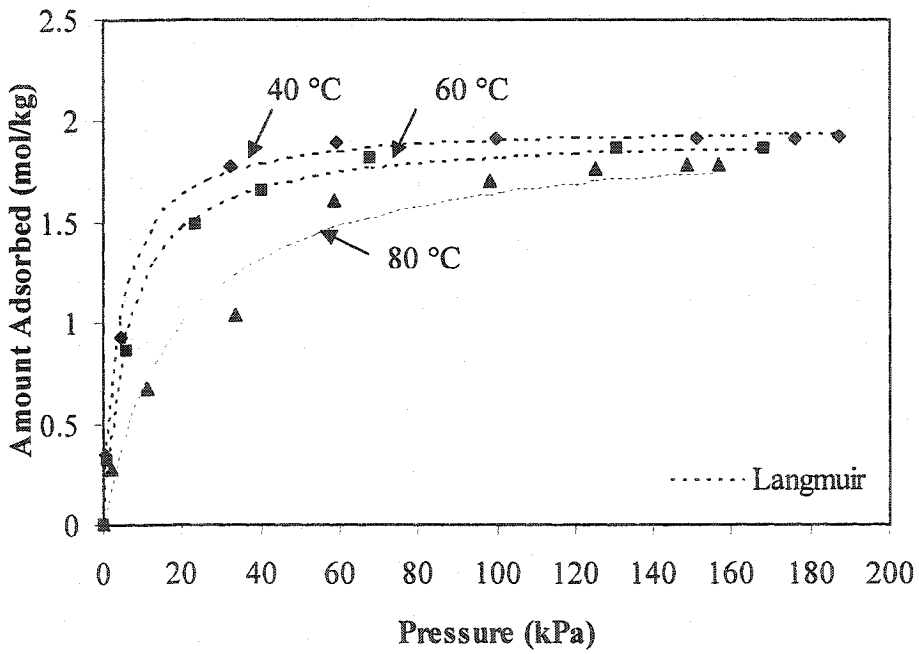

Figure 2.4: Methyl chloride adsorption isotherms for HiSiv-3000 at different temperatures and the corresponding Langmuir model fits.

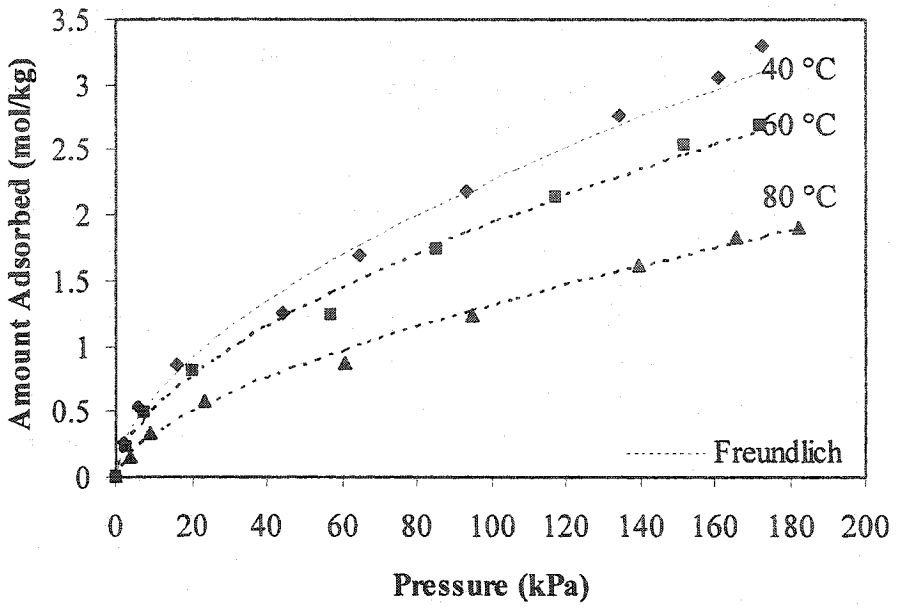

Figure 2.5: Methyl chloride adsorption isotherms for SBA-15 at different temperatures and the corresponding Freundlich model fits.

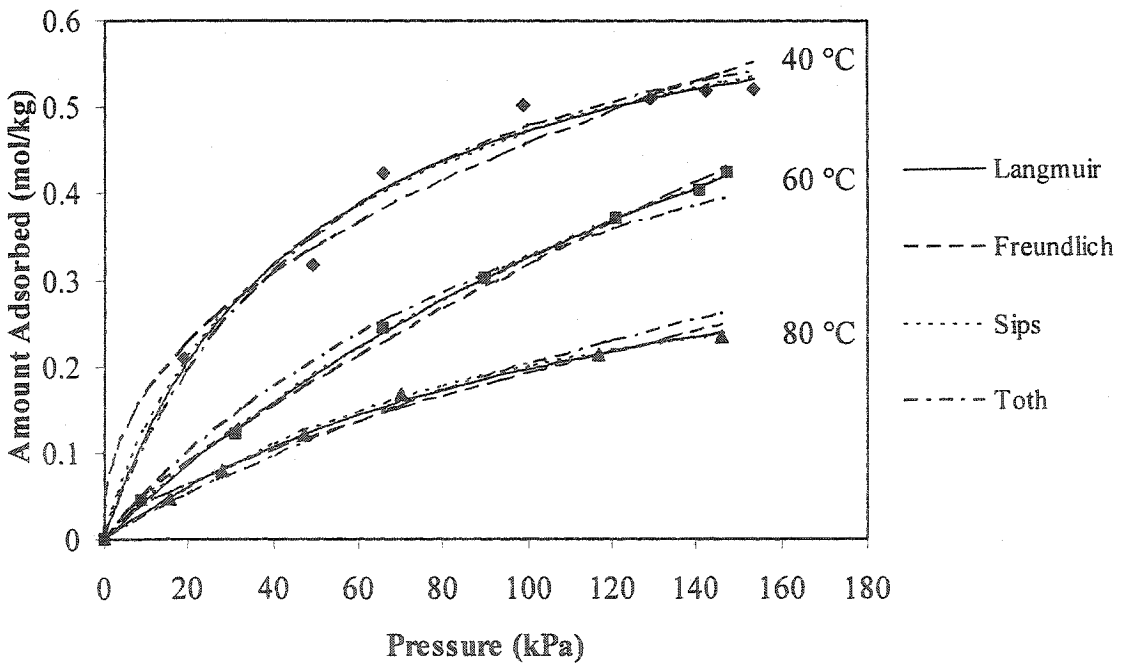

Figure 2.6: Nitrogen adsorption isotherms with HiSiv-3000 and pure adsorption isotherm model fits at different temperatures.

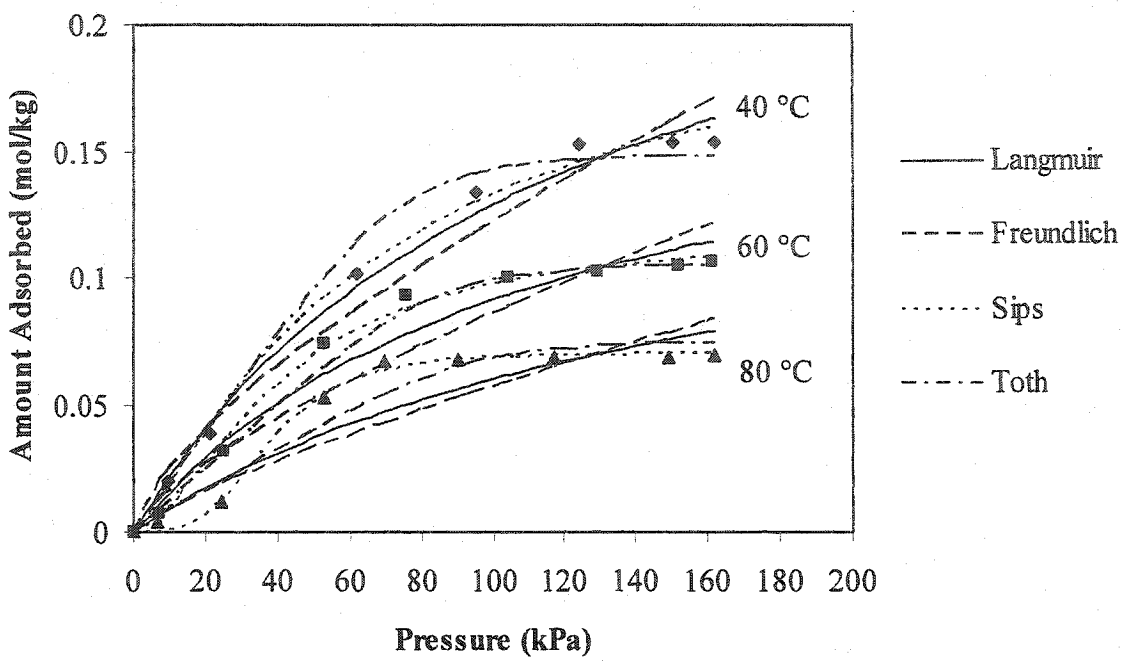

Figure 2.7: Nitrogen adsorption isotherms with SBA-15 and pure adsorption isotherm model fits at different temperatures.

2.4.3 Pure Component Adsorption Models

The model parameters found for all pure components adsorption data for all the models used for HiSiv-3000 and SBA-15 are shown in Tables 2.1 and 2.2, respectively. The precisions of the models to the actual data were compared by using the weighted sum of squared residual (WSSR) values, which are also shown in Tables 2.1 and 2.2 and as well as residual plots and % error plots. The examples of residual and % error plots can be found in Appendix A. The quantitative lack of fit test could not be performed because of the nature of the experimental procedure; the replicates of the experimental data could not be performed at the same x values. Without having the replicates at the same x values the quantitative lack of fit test can not be performed.

The weighted sum of squared residual (WSSR) values are defined by using the following equation:

$$WSSR = \frac{\sum (y - \hat{y})^2}{y} \tag{2.10}$$

where y is the experimental value

$\hat{y}$ is the predicted value

Among the pure component adsorption isotherm models, over all, it was observed that Toth and Sips agree well with all the experimental data for both adsorbents and adsorbates studied (Figures 2.6 – 2.9). Sips model shows slightly better fit to data than Toth, since Sips fits were done for individual temperatures separately, whereas the Toth fits were done to all data for different temperatures together, to give more practical fit over-all. The trends of all models were similar for all temperatures. Figures 2.8 and 2.9 show the best fits of all models for methyl chloride adsorption on HiSiv-3000 and SBA-15, respectively, at 40 °C. For methyl chloride isotherms, Langmuir fits better to HiSiv-3000 data, but it does not fit the data obtained for SBA-15 as well as other models. Freundlich fits better than Langmuir model for SBA-15. For nitrogen isotherm data with HiSiv-3000, Langmuir gave good fit similar to Toth and Sips; however, Langmuir was not a good fit for nitrogen isotherm with SBA-15, as can be seen from Figures 2.6 and 2.7.

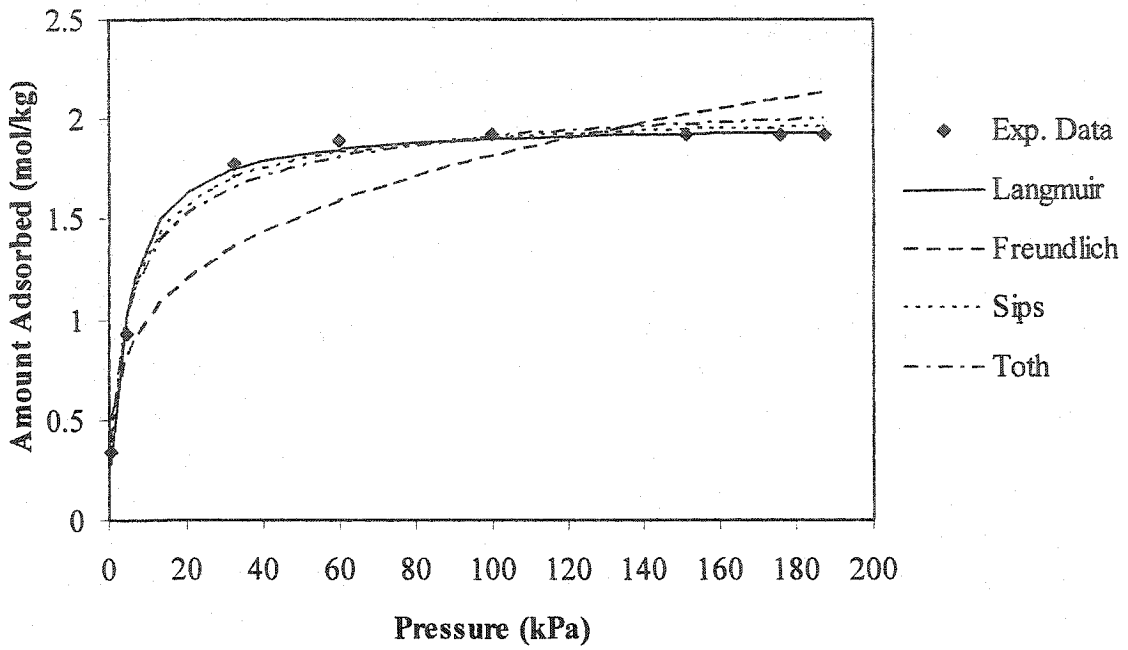

Figure 2.8: Methyl chloride adsorption isotherm with HiSiv-3000 and pure adsorption model fits at 40 °C.

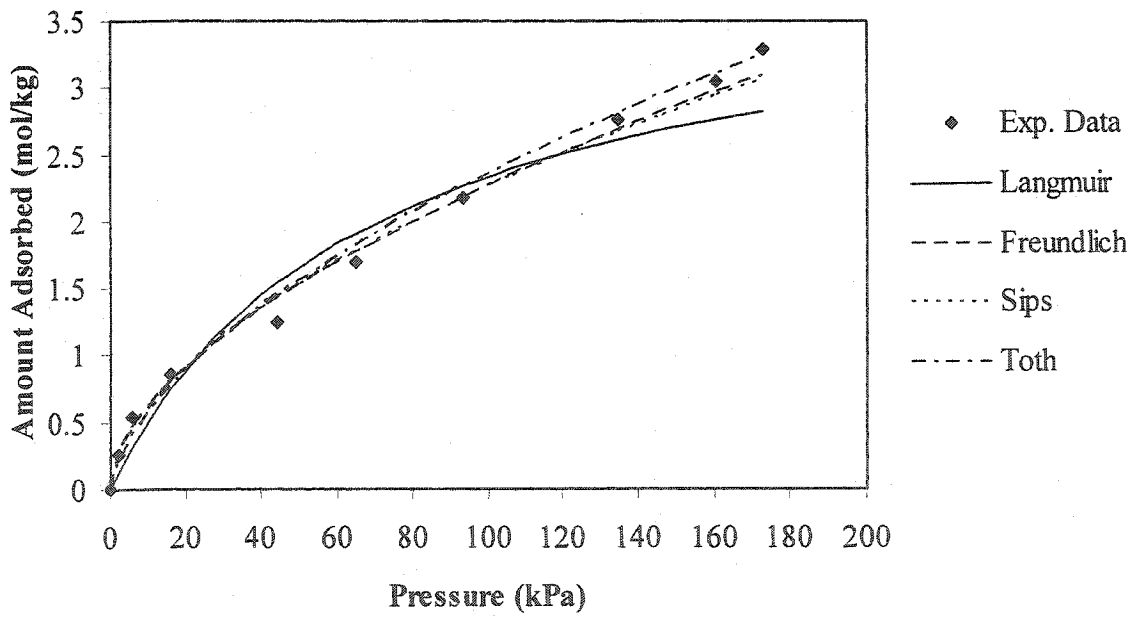

Figure 2.9: Methyl chloride adsorption isotherm with SBA-15 and pure adsorption model fits at 40 °C.

Table 2.1: Pure component adsorption model parameters for HiSiv-3000 and WSSR values for each model

Methyl Chloride	40°C		60°C		80°C	
	Parameters	**WSSR**	**Parameters**	**WSSR**	**Parameters**	**WSSR**
Langmuir	n_s = 1.9803 b = 0.0042	0.5051	n_s = 41.9317 b = 0.0028	0.5597	n_s = 1.9634 b = 0.0009	2.3980
Freundlich	K = 2.4296 1/t =0.2604	6.5378	K = 1.9379 1/t =0.2965	5.1151	K = 0.8844 1/t = 0.3956	1.9602
Sips	n_s = 2.0543 b = 0.0035 1/t = 0.8482	0.2566	n_s = 2.0836 b = 0.0021 1/t =0.8118	0.1622	n_s = 2.9081 b = 0.0003 1/t = 0.6449	1.0049
Toth	n_s = 2.2500 b = 0.0096 t = 0.5769	0.7191	n_s = 2.2500 b = 0.0032 t = 0.6583	0.7672	n_s = 2.2500 b = 0.0012 t = 0.7305	1.7814
Nitrogen						
Langmuir	n_s = 0.6970 b = 0.0004	0.1699	n_s = 1.0895 b = 0.0001	0.0151	n_s = 0.4461 b = 0.0001	0.0141
Freundlich	K = 0.1931 1/t = 0.4347	0.2740	K = 0.0124 1/t = 0.7942	0.0580	K = 0.0154 1/t = 0.6848	0.0882
Sips	n_s = 0.7577 b = 0.0003 1/t = 0.9000	0.1650	n_s = 1.1656 b = 0.0001 1/t = 0.9799	0.0147	n_s = 0.3517 b = 0.0002 1/t = 1.1637	0.0049
Toth	n_s = 0.7010 b = 0.0003 t =1.0896	0.1957	n_s = 0.6790 b = 0.0001 t =1.0896	0.1860	n_s = 0.6576 b = 0.0001 t =1.0896	0.1673

Table 2.2: Pure component adsorption model parameters for SBA-15 and WSSR values for each model

Methyl Chloride	40°C		60°C		80°C	
	Parameters	**WSSR**	**Parameters**	**WSSR**	**Parameters**	**WSSR**
Langmuir	n_s = 3.9291 b = 0.0003	6.8479	n_s = 3.4845 b = 0.0002	5.1956	n_s = 2.6717 b = 0.0002	2.6248
Freundlich	K = 0.3924 1/t = 0.5694	1.0786	K =0.3203 1/t = 0.5760	0.8163	K = 0.1718 1/t = 0.6111	0.4394
Sips	n_s = 50.3327 b = 9.11×10^{-7} 1/t = 0.5791	1.1926	n_s = 29.0184 b = 2.21×10^{-6} 1/t = 0.6006	0.9406	n_s = 15.8482 b = 4.33×10^{-6} 1/t = 0.6457	0.5199
Toth	n_s = 11883.11 b = 5.72×10^{-6} t = 0.1042	2.0511	n_s = 11883.105 b = 3.62×10^{-6} t = 0.1042	3.1147	n_s = 11883.11 b = 2.41×10^{-6} t = 0.1042	1.4172
Nitrogen						
Langmuir	n_s = 0.2822 b = 0.0002	0.0484	n_s = 0.1946 b = 0.0002	0.2064	n_s = 0.1599 b = 0.0001	0.4767
Freundlich	K = 0.0094 1/t =0.6921	0.1747	K = 0.0054 1/t = 0.7224	0.4535	K = 0.0023 1/t = 0.7875	0.6412
Sips	n_s = 0.2096 b = 0.0003 1/t =1.2454	0.0226	n_s = 0.1183 b = 0.0004 1/t =1.7210	0.0302	n_s = 0.0704 b = 0.0005 1/t = 3.6248	0.0962
Toth	n_s = 0.1486 b = 0.0002 t =5.4401	0.0631	n_s = 0.1056 b = 0.0002 t = 5.4401	0.0467	n_s = 0.0750 b = 0.0002 t = 5.4401	0.2563

2.4.4 Regeneration Conditions

The applicability of the adsorption process depends on the regeneration conditions of the adsorbent. In order to have a better understanding of the process, experiments were performed at different regeneration conditions. First, to check the repeatability of the experimental results, two experiments were performed at 40 °C by using two fresh adsorbents. It was observed that methyl chloride isotherms are very similar to each other. After checking the repeatability, the adsorbent used in the second experiment was regenerated at 350 °C and under vacuum for 15 hours and the adsorption isotherm of methyl chloride at 40 °C was determined again. Second regeneration was done only under vacuum at room temperature for again 15 hours and the same experiment was performed for the determination of the adsorption isotherm. The results of repeatability and the regeneration experiments are shown in Figure 2.10. These experiments were carried out using both adsorbents, HiSiv-3000 and SBA-15, separately. The results of regeneration experiments showed that both adsorbents can be regenerated by a combination of high temperature and vacuum or by vacuum only, without changing the capacity for methyl chloride. This makes both of these adsorbents good candidates for pressure swing adsorption (PSA) or vacuum swing adsorption (VSA) applications.

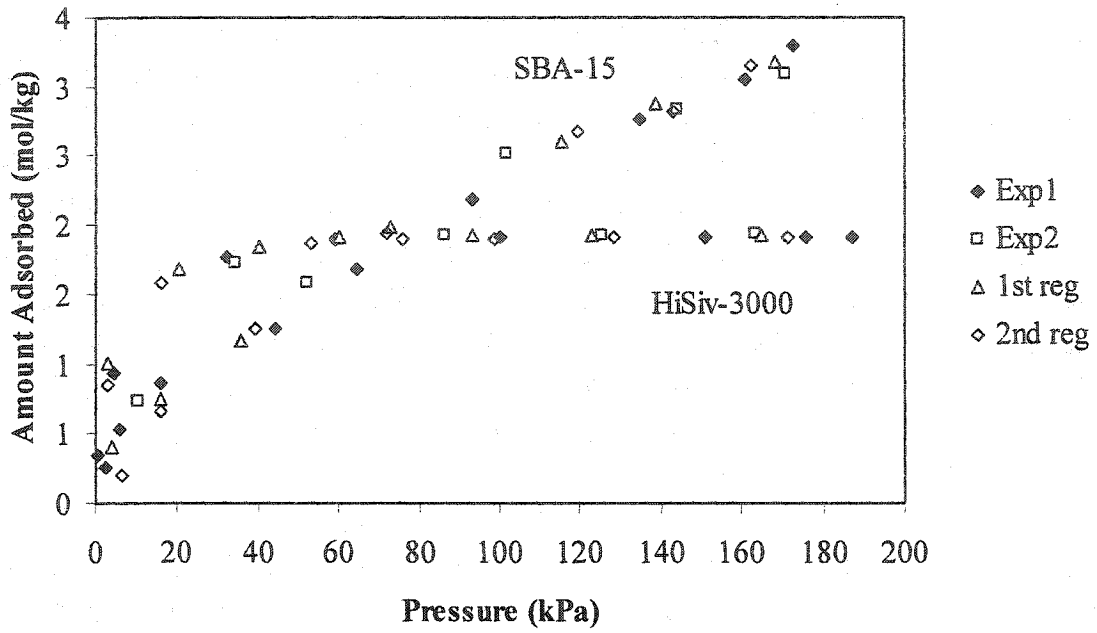

Figure 2.10: Methyl chloride adsorption isotherms at 40°C showing the repeatability, as well as the effect of different regeneration conditions. 1st regeneration is at 350°C with vacuum. 2nd and 3rd regenerations are at room temperature (21.5°C) with vacuum.

2.4.5 Adsorption Isosteres

The adsorption isosteres were obtained for methyl chloride and nitrogen by using the Toth isotherm parameters and are shown in Figures 2.11 – 2.14. From Figures 2.11 and 2.12 it was observed that the amount of methyl chloride adsorbed at higher pressures is higher for SBA-15 than that for HiSiv-3000. As it was observed from pure component adsorption isotherms at 40 °C shown in Figure 2.10, at lower pressures (less than 80 kPa) HiSiv-3000 has more adsorption capacity for methyl chloride than SBA-15. The amount adsorbed curves are more horizontal at lower pressures in Figures 2.11 and 2.12, which indicate that the effect of temperature on the amount adsorbed is less pronounced. As pressure increases it was observed that the curvature of contours increases indicating the increase in effect of temperature.

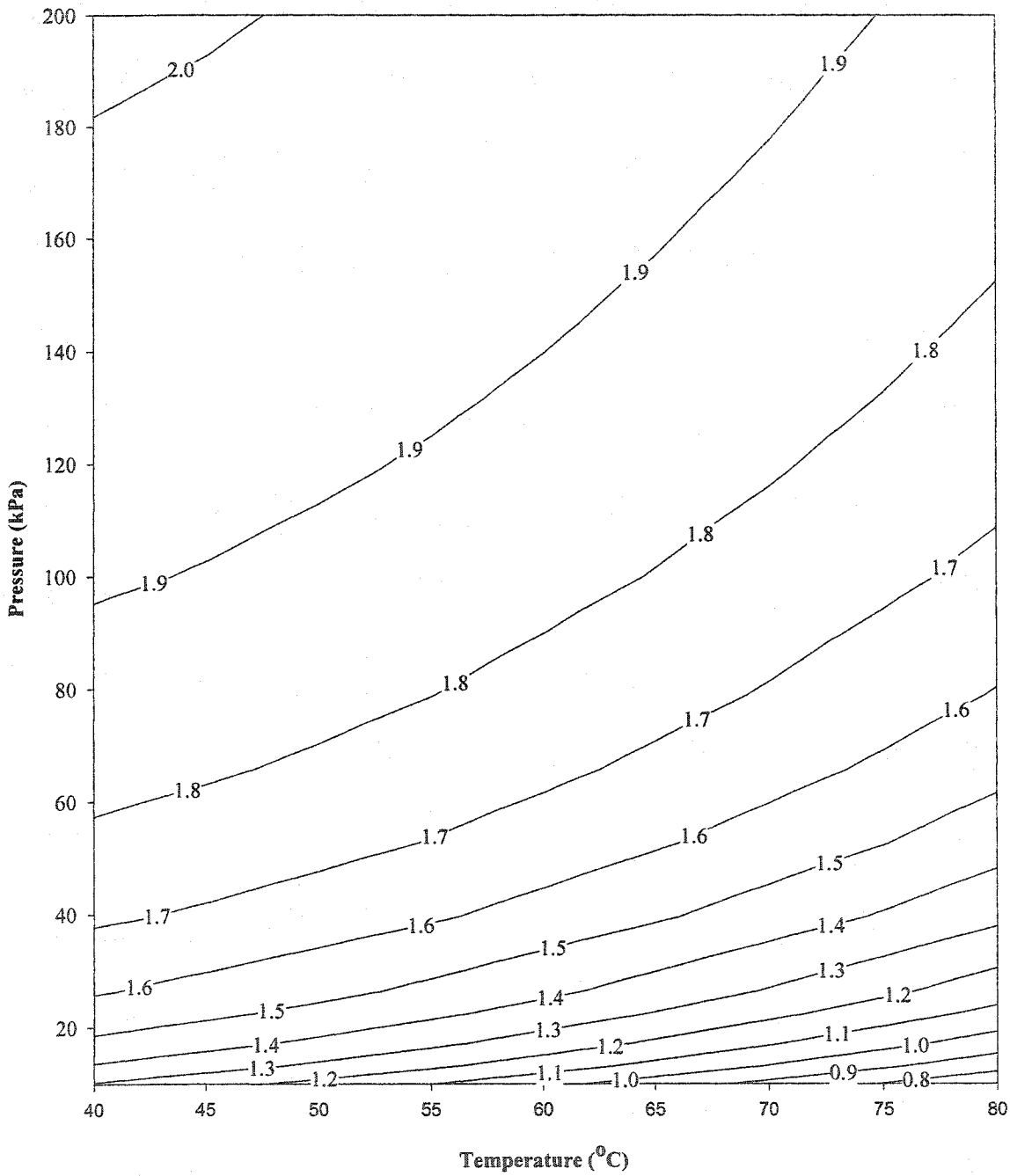

Figure 2.11: Adsorption isosteres of methyl chloride by using HiSiv-3000. Contours indicate amount adsorbed as mol/kg.

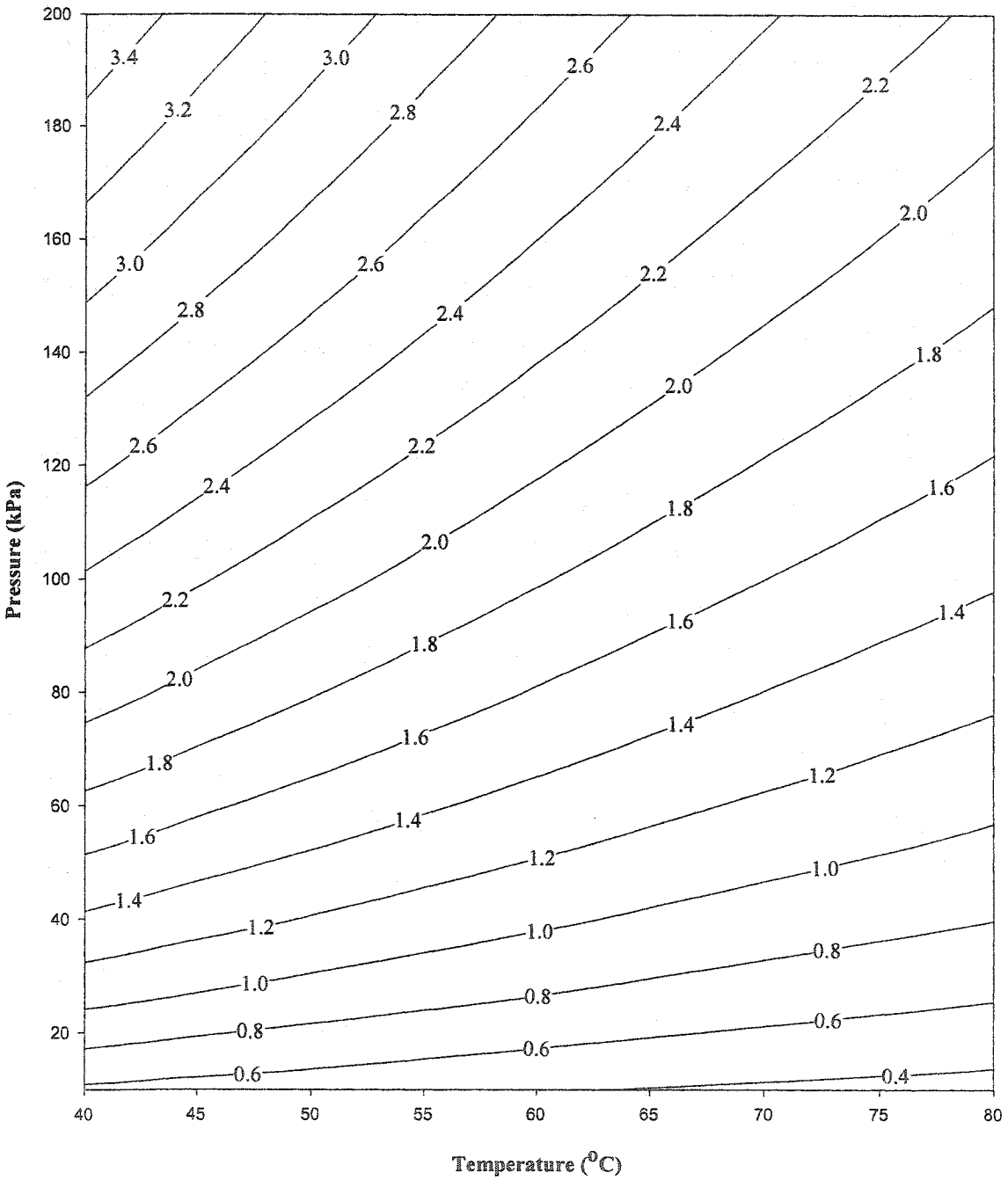

Figure 2.12: Adsorption isosteres of methyl chloride by using SBA-15. Contours indicate amount adsorbed as mol/kg.

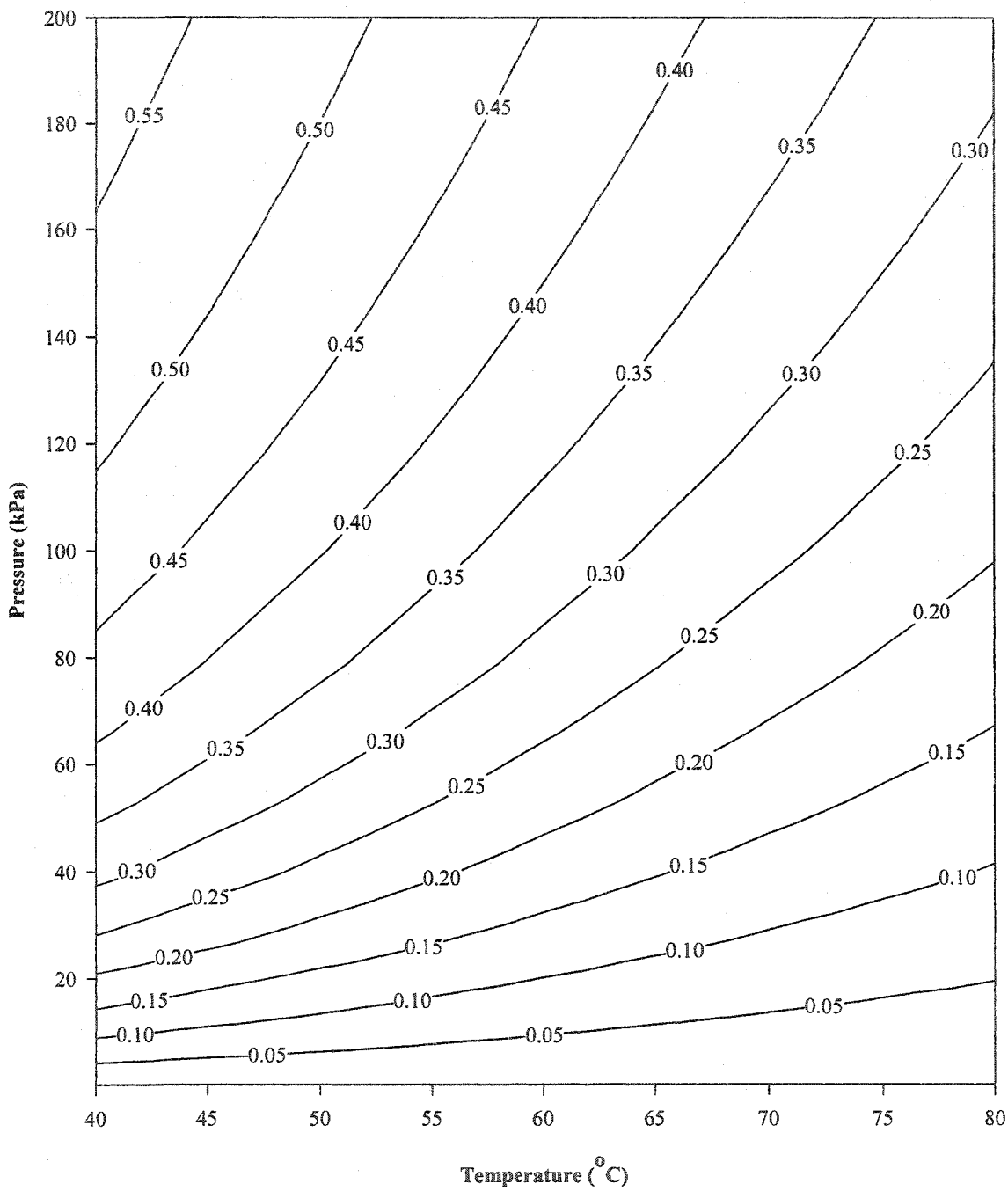

Figure 2.13: Adsorption isosteres of nitrogen by using HiSiv-3000. Contours indicate amount adsorbed as mol/kg.

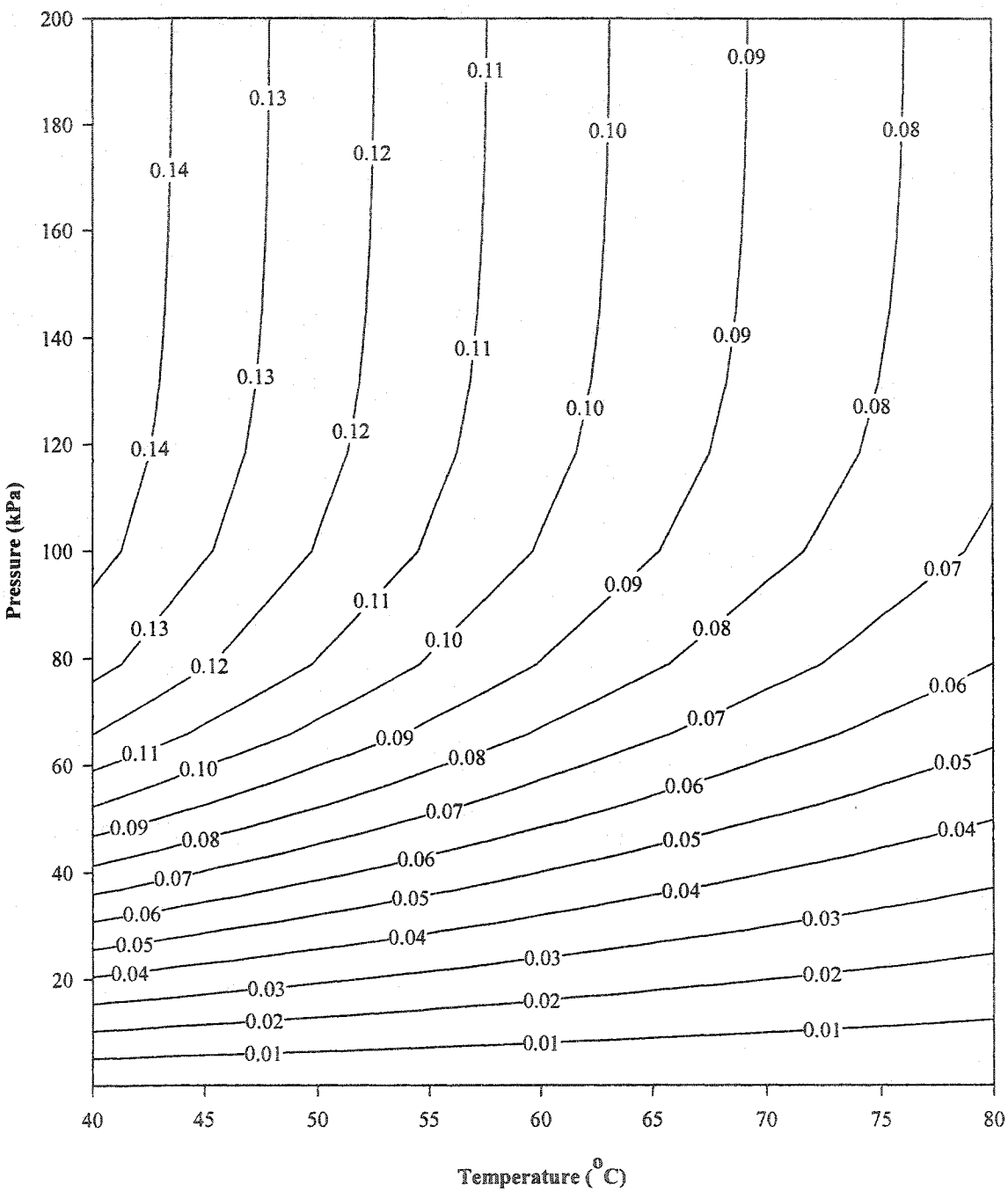

Figure 2.14: Adsorption isosteres of nitrogen by using SBA-15. Contours indicate amount adsorbed as mol/kg.

Figures 2.13 and 2.14 show that nitrogen adsorption by using HiSiv-3000 is higher than that obtained by using SBA-15 at all pressures and temperatures. For nitrogen isosteres with SBA-15, it is observed that above 100 kPa pressure, the amount adsorbed curves are almost vertical; indicating that pressure effect is practically negligible above this point.

2.4.6 Adsorption Isotherm Predictions for Binary System

The prediction of binary mixture adsorption of methyl chloride and nitrogen system were obtained by using Extended Langmuir Method and Ideal Adsorbed Solution Theory (IAST) at different temperatures for 101 kPa total pressure which are shown in Figures 2.15 – 2.18. From these predictions it was observed that the methyl chloride dominates the adsorption. The adsorption isotherm of this adsorbate in binary system is very similar to its pure adsorption isotherm. The total amount adsorbed curve is practically the methyl chloride isotherm in this system. The nitrogen adsorption in binary system is almost negligible. Although the binary isotherm predictions by using both methods are similar to each other, nitrogen adsorption decreases much faster in Ideal Adsorbed Solution Theory as the composition of methyl chloride in gas phase increases. For the binary adsorption isotherms it was observed that as temperature increases the amount adsorbed decreases which was also observed in pure component adsorption isotherms. The cross over of methyl chloride isotherm on binary system predicted by Extended Langmuir will be discussed later in this paper.

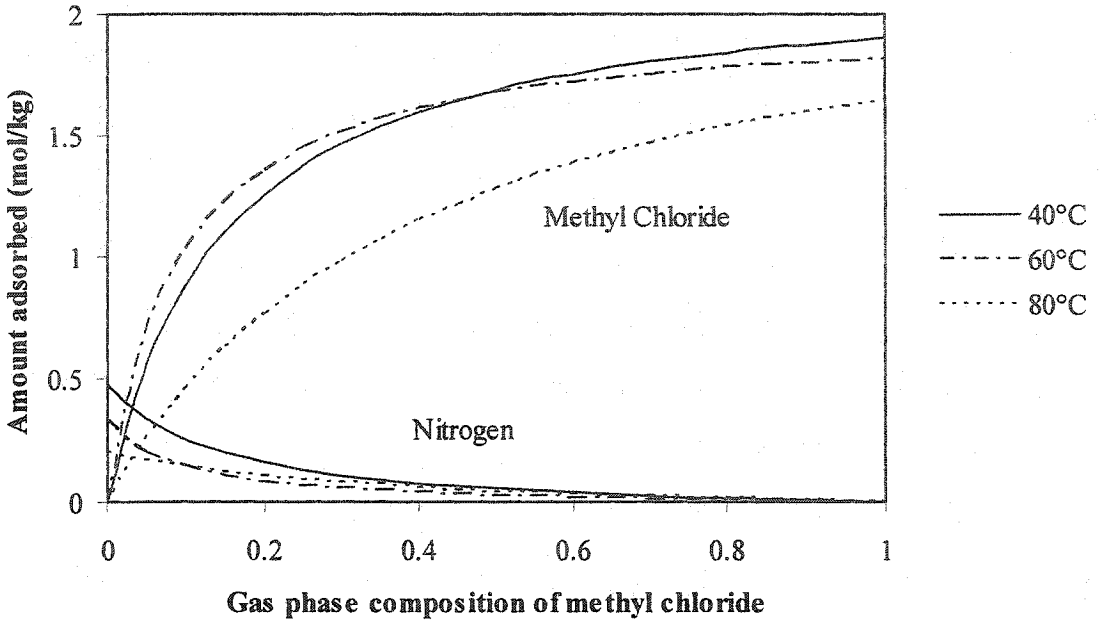

Figure 2.15: Extended Langmuir prediction for binary system of nitrogen and methyl chloride with HiSiv-3000 at different temperatures for 101 kPa total pressure.

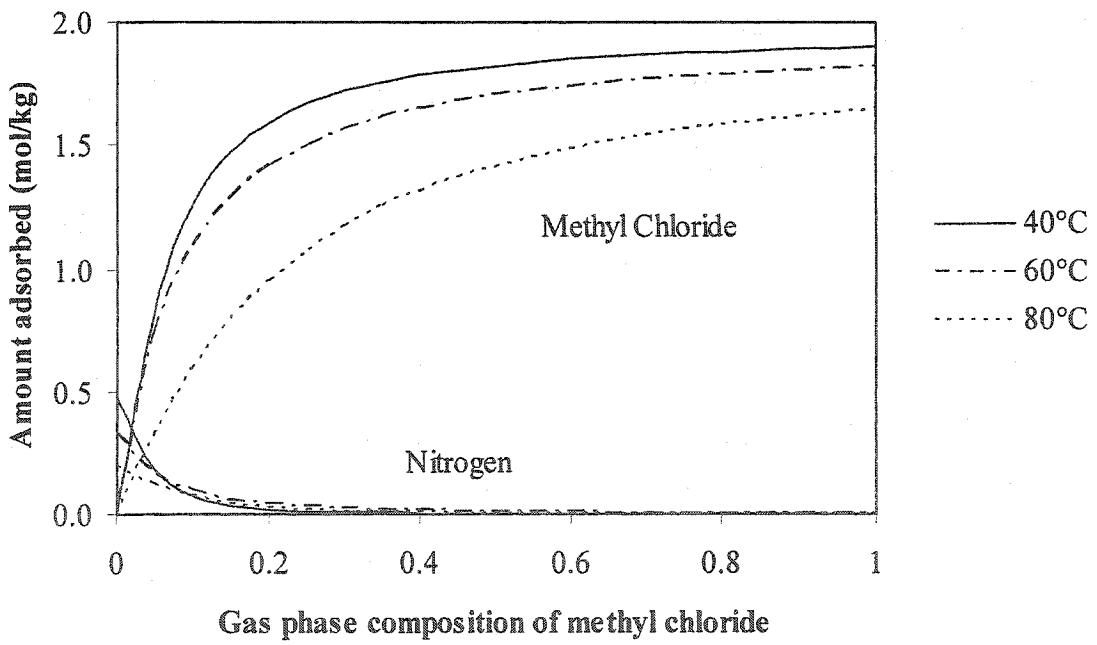

Figure 2.16: IAST prediction for binary system of nitrogen and methyl chloride with HiSiv-3000 at different temperatures for 101 kPa total pressure.

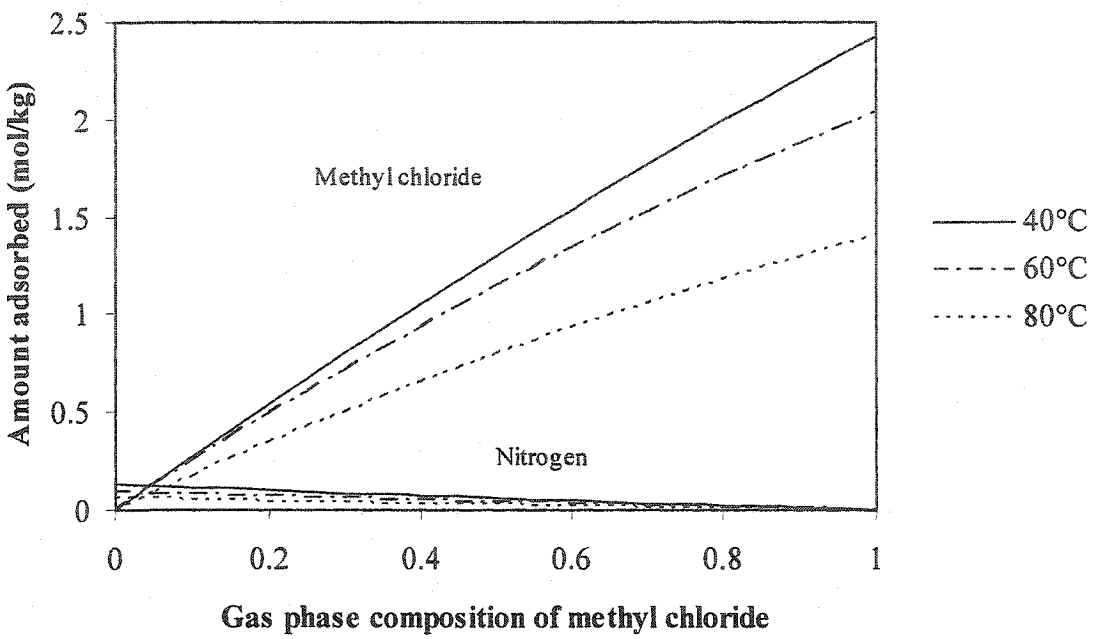

Figure 2.17: Extended Langmuir prediction for binary system of nitrogen and methyl chloride with SBA-15 adsorbent at different temperatures for 101 kPa total pressure.

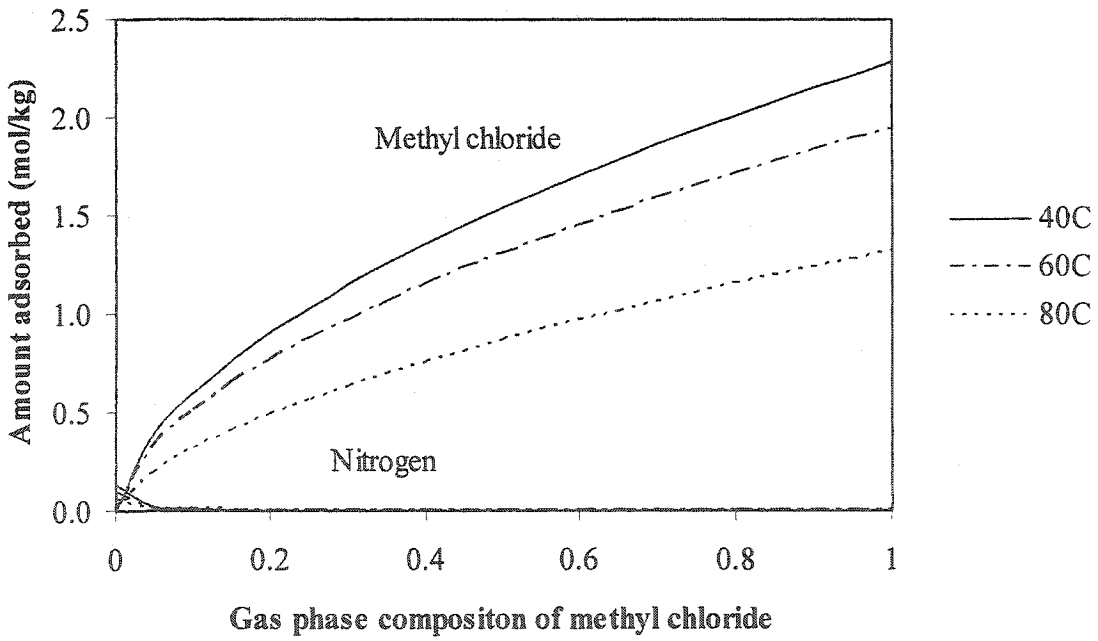

Figure 2.18: IAST prediction for binary system of nitrogen and methyl chloride with SBA-15 adsorbent at different temperatures for 101 kPa total pressure.

The phase diagram of binary mixture of methyl chloride and nitrogen at 40 °C by using both adsorbents with extended Langmuir and IAST are shown in Figures 2.19 and 2.20, respectively. These phase diagrams indicate that good separation can be obtained by using both adsorbents since the lines are very far apart from the 45° line.

Extended Langmuir model uses the Langmuir parameters obtained from the pure isotherms to predict the binary behavior. In this case, as it was discussed before, methyl chloride adsorption on SBA-15 does not fit Langmuir model well. Langmuir isotherm underestimates the adsorbed amount at higher pressures for all temperatures studied. Although, Extended Langmuir model is more accurate with HiSiv-3000 than with SBA-15, it is observed that fitted model parameters (given in Table 2.1) for adsorption of nitrogen with HiSiv-3000 at 60 °C are not consistent with the parameters obtained at 40 and 80 °C. This leads the curves for methyl chloride for 60 and 40 °C in Extended Langmuir prediction of binary system behavior by using HiSiv-3000 to cross each other, which is observed in Figure 2.15.

Also for the adsorption of nitrogen by using HiSiv-3000 at 60 °C, Langmuir parameters obtained are not consistent with the parameters obtained at the other temperatures. In other words, Langmuir fit to nitrogen adsorption by using HiSiv-3000 as adsorbent is not as precise as the other fits. Therefore, because of the parameters, the curves for methyl chloride for 60 and 40 °C in Extended Langmuir prediction of binary system behavior by using HiSiv-3000 cross each other, which are seen in Figure 2.15.

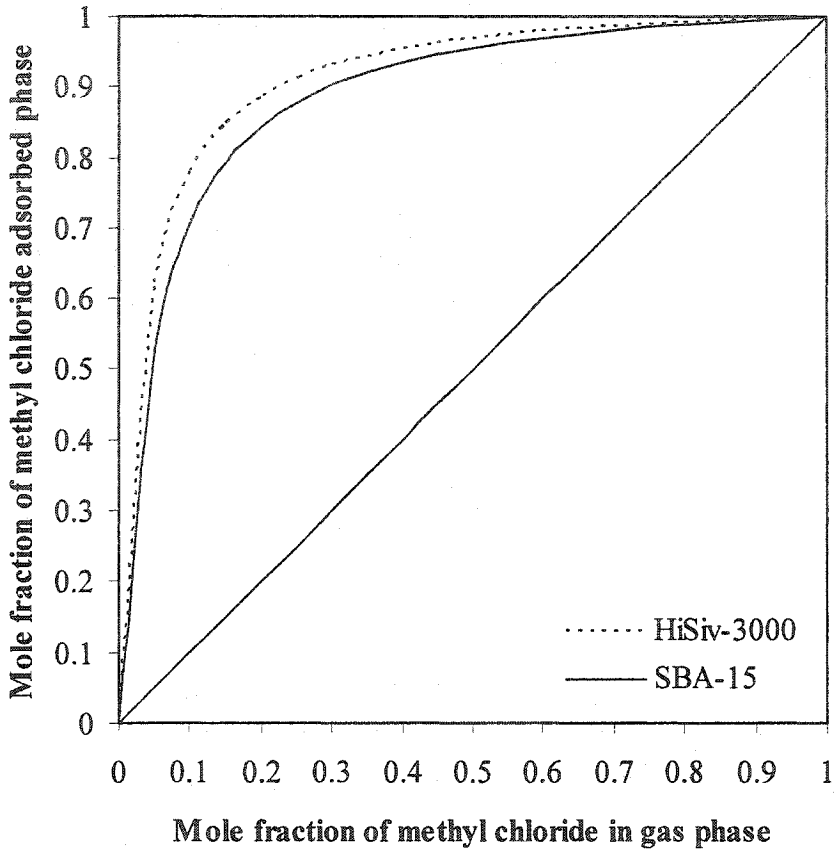

Figure 2.19: Phase diagram of binary system of methyl chloride and nitrogen by using Extended Langmuir method at 40°C for 101 kPa total pressure.

On the other hand, according to Ideal Adsorbed Solution Theory, the spreading pressure of nitrogen should be extrapolating in order to have the same area under the curve with methyl chloride in the calculations of IAST (Eqn. 2.9). For SBA-15, IAST is more dependable. From Figure 2.7, it can be seen that adsorption of nitrogen with SBA-15 reaches saturation at around 150 kPa at all temperatures studied which enables us to extrapolate the spreading pressure of nitrogen more precisely. However, in the case of nitrogen adsorption with HiSiv-3000, the isotherms shown in Figure 2.6 look more linear for all the temperatures studied. Therefore the precision of spreading pressure calculations for this case is less accurate.

Although both models have some limitations, the separations by using both adsorbents are very high since the nitrogen adsorption in binary system is very low.

IAST predictions show that (Figure 2.20) although pure methyl chloride adsorption capacity of HiSiv-3000 is greater than that of SBA-15, SBA-15 gives better separation in binary mixtures, which is expected, since it adsorbs much less nitrogen (Figures 2.6 and 2.7).

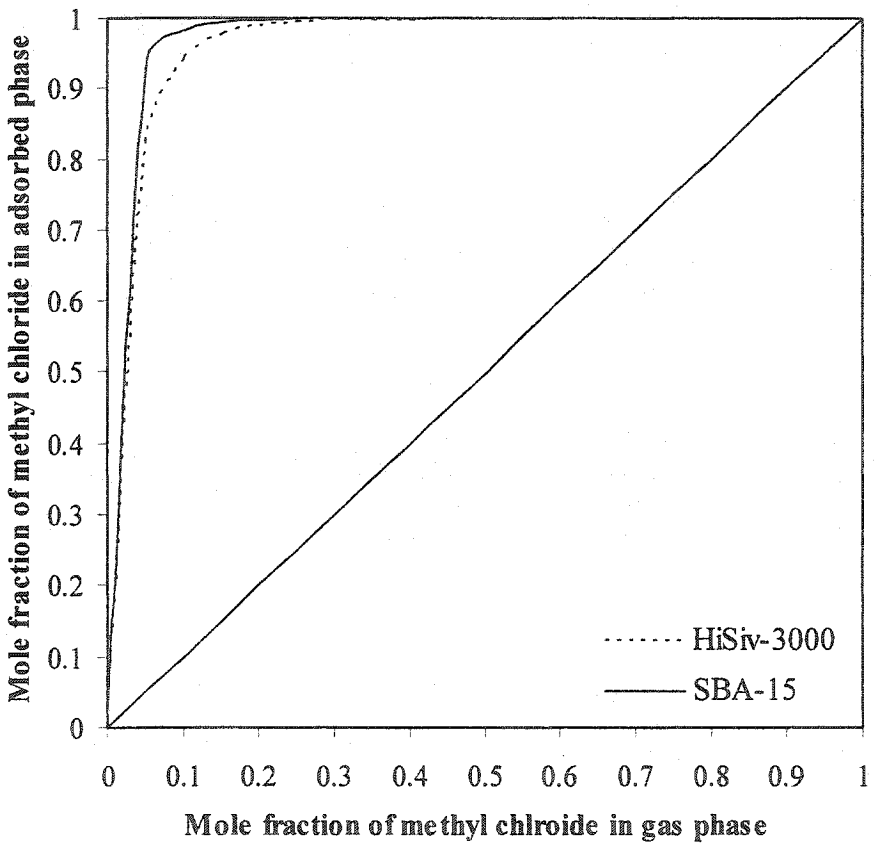

Figure 2.20: Phase diagram of binary system of methyl chloride and nitrogen by using IAST at 40°C for 101 kPa total pressure.

2.4.7 Heat of Adsorption

By using the Van't Hoff plot (equation 2.11) from Henry's law constants, heats of adsorption and pre-exponential constants of methyl chloride and nitrogen adsorptions on HiSiv-3000 and SBA-15 adsorbents can be determined and the results are shown in Table 2.3.

$$\ln K = \ln K_0 + \left(\frac{-\Delta H}{R}\right)\frac{1}{T} \tag{2.11}$$

Henry's law constants are also shown as a function of inverse temperature in Figure 2.21. It can be seen from the table that, methyl chloride has higher heat of adsorption than nitrogen for both adsorbents. This shows that methyl chloride has greater interaction with both adsorbents than nitrogen. Another important observation is that with SBA-15, the heat of adsorption of methyl chloride is much less than that of HiSiv-3000. It is even less than the heat of adsorption of nitrogen with HiSiv-3000. The lower the heat of adsorption, the easier the regeneration is. In other words, lesser the energy required for regeneration. Therefore, SBA-15 has great advantage in regeneration as well.

Table 2.3: Heats of Adsorption and Pre-exponential constants of Van't Hoff plots for methyl chloride and nitrogen with HiSiv-3000 and SBA-15.

Adsorbents	Methyl chloride		Nitrogen	
	$-\Delta H$ (kJ mol^{-1})	K_0 (mol kg^{-1} kPa^{-1})	$-\Delta H$ (kJ mol^{-1})	K_0 (mol kg^{-1} kPa^{-1})
HiSiv-3000	52.32	1.36×10^{-9}	25.96	5.09×10^{-7}
SBA-15	21.86	2.76×10^{-5}	9.65	5.04×10^{-5}

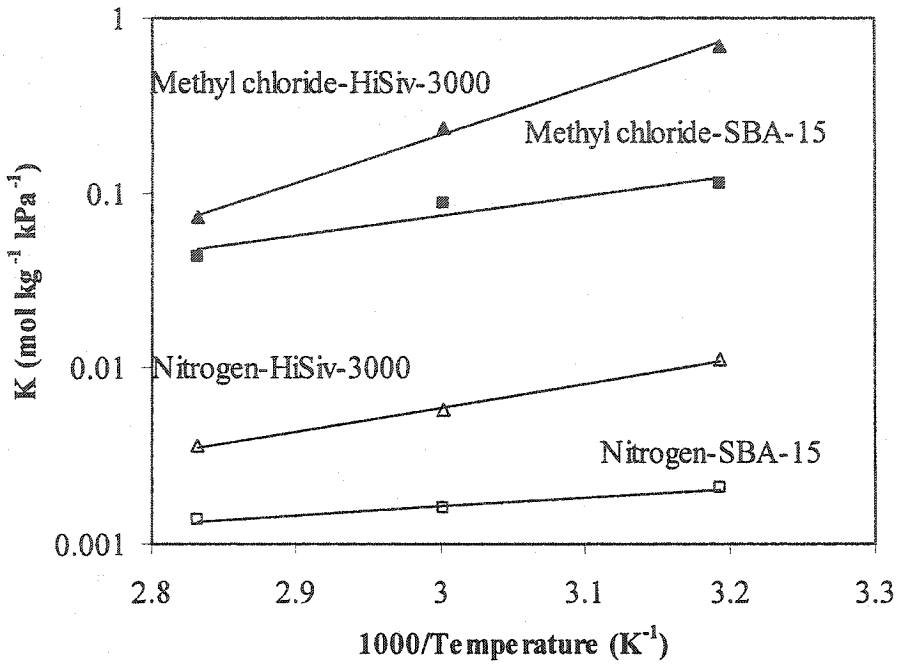

Figure 2.21: Henry's law constants for methyl chloride and nitrogen at different temperatures for adsorbents HiSiv-3000 and SBA-15.

2.4.8 Expected Working Capacities

One of the most important parameters in designing any process is the expected working capacity (EWC) of that unit. In adsorption separation processes, expected working capacity can be calculated by the difference in the adsorption capacities at adsorption and desorption steps shown in equation 2.12. Here, it is assumed that nitrogen adsorption is insignificant in this separation, which was observed in the binary adsorption isotherm predictions.

$$\text{Expected working capacity (EWC)} = n_{\text{adsorption}} - n_{\text{desorption}} \qquad (2.12)$$

In pressure swing adsorption (PSA) process, adsorption takes place at higher pressures where desorption is done at atmospheric pressure. Temperature is kept at 40 °C since it was the lowest temperature the experimental data was obtained. As adsorption

pressure increases, the amount adsorbed increases. Therefore, the difference between the capacities of adsorption and desorption (EWC) would increase, if desorption pressure is kept at atmospheric pressure. This behavior can be seen in Figure 2.22. In this figure, the expected working capacities of HiSiv-3000 and SBA-15 was compared for a PSA unit at 40 °C for desorption pressure of 101 kPa. It was observed that EWC of SBA-15 is much higher than that of HiSiv-3000.

An alternative adsorption process to PSA can be vacuum swing adsorption (VSA), where the adsorption takes place at atmospheric pressure and desorption is done under vacuum. Temperature was kept at 40 °C for VSA process as well for the calculation of the expected working capacities. In this case, as desorption pressure decreases, the effective working capacity increases if adsorption pressure is kept at atmospheric pressure. From the comparison of the two adsorbents in the case of VSA process shown in Figure 2.23, it can be seen that SBA-15 has better expected working capacity for this case, as well.

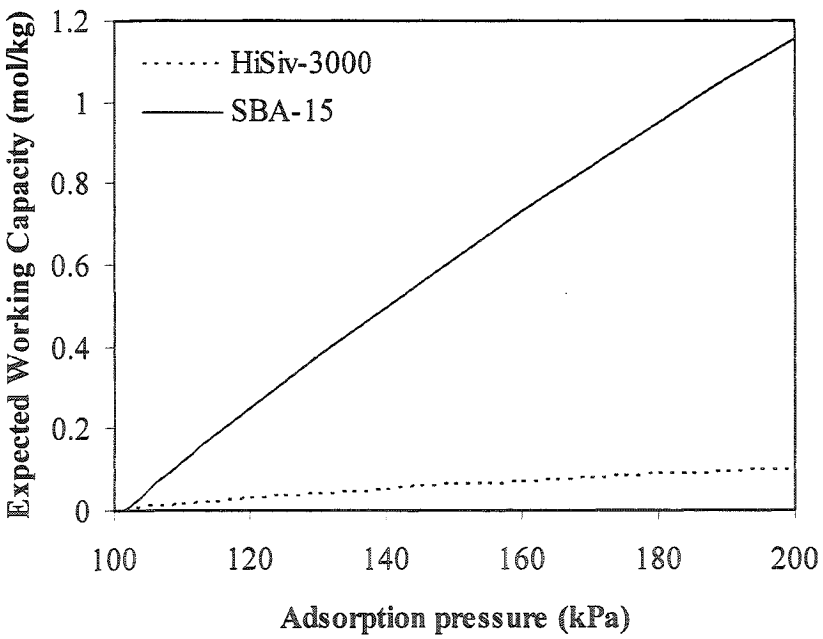

Figure 2.22: Expected working capacities for a pressure swing adsorption system for the adsorption of methyl chloride at 40°C, keeping desorption pressure at 101 kPa.

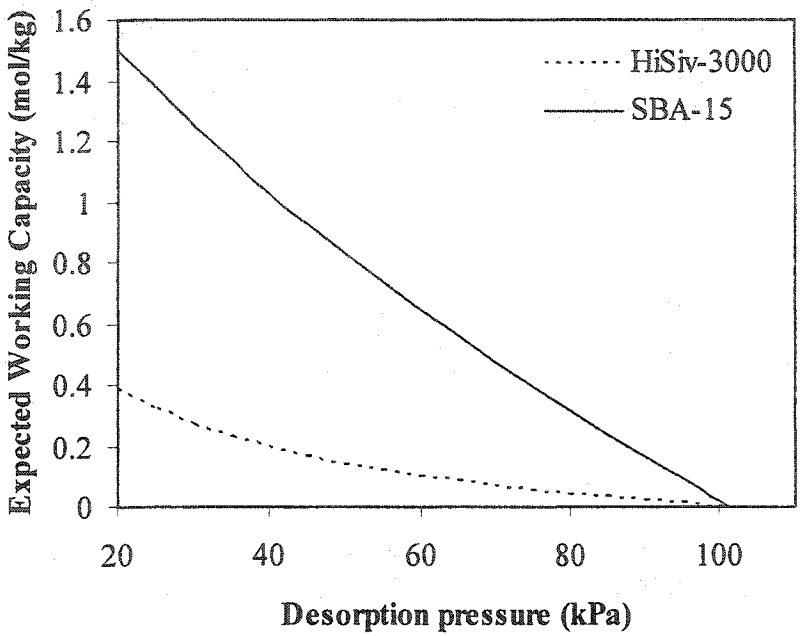

Figure 2.23: Expected working capacities for a vacuum swing adsorption system for the adsorption of methyl chloride at 40°C, keeping adsorption pressure at 101 kPa.

Another possible process for the adsorption of methyl chloride is temperature swing adsorption (TSA). In this process instead of changing pressure, temperature effect is used for changing the amount adsorbed during adsorption and desorption. As mentioned before, temperature increase results in decrease in adsorption capacity. In TSA, usually adsorption takes place at room temperature (25°C) and desorption is done at higher temperatures. In this case, pressure is kept at atmospheric pressure. In Figure 2.24, EWCs are given for this case as a function of desorption temperature keeping the adsorption temperature at 25°C. It can be seen that EWC of SBA-15 is much better than HiSiv-3000 in this case as well.

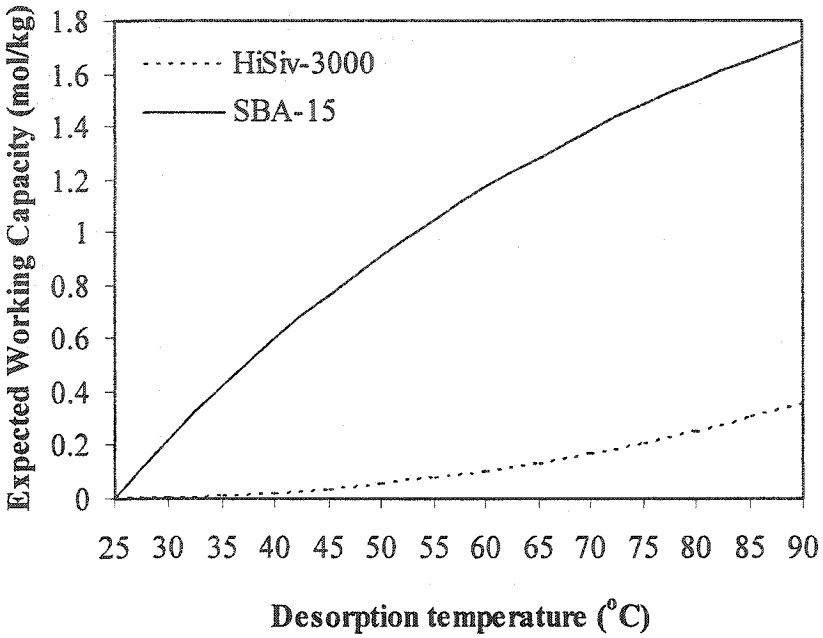

Figure 2.24: Expected working capacities for a temperature swing adsorption system for the adsorption of methyl chloride at atmospheric pressure, keeping adsorption temperature at 25°C.

When different adsorption processes were compared for both adsorbents, it was observed that temperature swing adsorption is the best option for this separation under these conditions since it produced the highest EWC values. It was also observed that vacuum swing adsorption gives much better efficiency than pressure swing adsorption. Since methyl chloride dominates the adsorption for the binary adsorption of methyl chloride and nitrogen, the shape of the methyl chloride isotherm with the adsorbents studied plays a very important role on the efficiency of the processes. As it was seen in Figure 2.5, pure methyl chloride adsorption isotherm with SBA-15 is more linear throughout the pressure range studied which indicates that any pressure change will have great impact on the amount adsorbed for both higher and lower pressures. On the other hand, the pure adsorption isotherm of methyl chloride with HiSiv-3000 has more rectangular shape (Figure 2.4). At higher pressures, the amount adsorbed does not change much. The pressure effect on the amount adsorbed is much higher at lower pressures. Therefore vacuum swing adsorption process is much effective than other processes for HiSiv-3000. The reason for SBA-15 showing higher EWC values for

temperature swing adsorption is that the temperature effect on pure methyl chloride adsorption isotherms with this adsorbent is much greater than that with HiSiv-3000 at atmospheric pressure.

It was observed that SBA-15 is a much better adsorbent than HiSiv-3000 when applicability to all the adsorption processes is considered.

2.5. CONCLUSIONS

Adsorption capacities of HiSiv-3000 and SBA-15 for methyl chloride and nitrogen were determined by using constant volume method in the temperature range from 40 and 80 °C. Several adsorption isotherm models were fitted to the experimental data and binary system behavior was predicted by using Extended Langmuir Model and Ideal Adsorbed Solution Theory. Henry's law constant and heat of adsorption for both adsorbates with both adsorbents were determined. Expected working capacities of PSA, VSA and TSA were determined. From this study several conclusions have been reached:

- At higher pressures SBA-15 adsorbs more methyl chloride; whereas, at lower pressures methyl chloride adsorption by using Hisiv-3000 is much greater due to the fact that SBA-15 has larger pore size and surface area.
- For nitrogen adsorption, Hisiv-3000 also has higher adsorption capacity than SBA-15.
- Toth and Sips models fit well to all the isotherm data.
- Langmuir fits well to HiSiv-3000 data for methyl chloride adsorption.
- Freundlich model fits better than Langmuir for methyl chloride adsorption isotherm by using SBA-15 as adsorbent.
- The effect of temperature on the methyl chloride adsorption at lower pressures is very low. As pressure increases the curvature of the contours in isosteres increases which indicates the increase of the temperature effect.
- The common conclusion obtained from both phase diagrams by using Extended Langmuir and Ideal Adsorbed Solution Theory is that the nitrogen adsorption in

binary system is negligible; therefore the separation of methyl chloride from nitrogen by using both adsorbents studied is very good.

- Heat of adsorption of methyl chloride by using SBA-15 is much lower than that of HiSiv-3000, even less than the heat of adsorption of nitrogen by using HiSiv-3000.
- Expected working capacities of SBA-15 for all adsorption processes are much larger than that of HiSiv-3000.
- Vacuum swing adsorption and temperature swing adsorption processes are two promising processes to be used for the separation of methyl chloride from air.
- Overall, SBA-15 gives better results than HiSiv-3000, indicating that SBA-15 is a more suitable adsorbent than HiSiv-3000 for the separation of methyl chloride from air.

2.6. NOMENCLATURE

A	area per mole, m^3 mol^{-1}
b	isotherm parameter, kPa^{-1}
b_i	empirical parameter for component *i*, kPa^{-1}
b_0	affinity at reference temperature, T_0, kPa^{-1}
K	Henry's Law constant, mol kg^{-1} $kPa^{-1/t}$
K_0	pre-exponential constant for Van't Hoff plot, mol kg^{-1} bar^{-1}
n	amount adsorbed, mol kg^{-1}
n_i	amount adsorbed for component *i*, mol kg^{-1}
n_s	amount adsorbed at monolayer saturation, mol kg^{-1}
$n_{s,0}$	empirical parameter, mol kg^{-1}
P	pressure, kPa
P_i	partial pressure of component *i*, kPa
R	Gas constant, m^3 kPa mol^{-1} K^{-1}
T	temperature, K
T_0	reference temperature, K
t	empirical parameter, dimensionless

t_0 empirical parameter, dimensionless

y experimental value, mol kg^{-1}

$\hat{y}$ predicted value, mol kg^{-1}

z reduced spreading pressure, kPa

Greek Letters

ΔH heat of adsorption, kJ mol^{-1}

θ fractional surface coverage, dimensionless

θ_i partial fractional surface coverage of component *i*, dimensionless

π spreading pressure, kPa

χ empirical parameter, dimensionless

Abbreviations

EL Extended Langmuir

EWC Expected Working Capacity

IAST Ideal Adsorbed Solution Theory

PSA Pressure Swing Adsorption

TSA Temperature Swing Adsorption

VOC Volatile Organic Compound

VSA Vacuum Swing Adsorption

WSSR Weighted sum of squared residual

Acknowledgements

Financial support received from Natural Sciences and Engineering Council (NSERC) of Canada and Chemical Engineering Department at University of Ottawa is gratefully acknowledged.

2.7. REFERENCES

Agency for Toxic Substances and Disease Registry (ATSDR): Toxicological Profile for Chloromethane (Update), U.S. Public Health Service, U.S. Department of Health and Human Services, Atlanta, 1998

Bloemen, H.J. and Burn, J., Chemistry and Analysis of Volatile Organic Compounds in the Environment, Blackie Academic & Professional, Glasgow, 1993

Cochran, T.W., Kabel, R.L. and Danner, R.P., Vacancy Solution Theory of Adsorption Using Flory-Higgins Activity Coefficient Equations, A.I.Ch.E. Journal, 1985, 31(2), 268-277.

Do, D.D., Adsorption Analysis Equilibria and Kinetics, Imperial College Press, Danvers, 1998.

Huang, C.C., Lin, Y.C. and Lu, F.C., Dynamic Adsorption of Organic Solvent Vapors onto a Packed Bed of Activated Carbon Cloth, Separation Science and Technology, 1999, 34, 555-570.

Jennings, M.S., Krohn, N.E., Berry, R.S., Palazzolo, M.A., Parks, R.M. and Fidler, K.K., Catalytic Incineration for Control of Volatile Organic Compound Emissions, Noyes Publications, New Jersey, 1985.

Koh, C.A., Westacott, R.E., Mooney, R.I., Boissel, V., Tahir, S.F. and Tricarico, V., Separation of Dichloromethane-Nitrogen Mixtures by Adsorption: Experimental and Molecular Simulation Studies, Molecular Physics, 2002, 100, 2087-2095.

Kruk, M., Jaroniec, M. and Sayari, A., Application of Large Pore MCM-41 Molecular Sieves to Improve Pore Size Analysis Using Nitrogen Adsorption Measurements, Langmuir, 1997, 13, 6267-6273.

Langmuir, I., Adsorption of Gases on Plane Surfaces of Glass, Mica and Platinum, Journal of American Chemical Society, 1918, 40, 1361-1403.

Markham, E.C. and Benton, A.F., The Adsorption of Gas Mixtures by Silica, Journal of American Chemical Society, 1931, 53, 497-507.

Myers, J.A. and Prausnitz, J.M., Thermodynamics of Mixed-Gas Adsorption, A.I.Ch.E. Journal, 1965, 11(1), 121-127.

Szostak, R., Handbook of Molecular Sieves, Van Nostrand Reinhold, New York, 1992.

Thomas, W.J. and Critenden, B., Adsorption Technology and Design, Butterworth-Heinemann, Oxford, 1998.

Zeldowish, J., On the Theory of the Freundlich Adsorption Isotherm, Acta Phsicochim, U.R.S.S., 1935, 1(6), 961-973.

Zhao, D., Huo, Q., Feng, J., Chmelka, B.F. and Stucky, G.D., Triblock Copolymer Syntheses of Mesoporous Silica with Periodic 50 to 300 Å Pores, Science, 1998, 279, 548-552.

Zhao, X.S., Ma, Q. and Lu, G.Q., VOC Removal: Comparison of MCM 41 with Hydrophobic Zeolites and Activated Carbon, Energy & Fuels, 1998, 12, 1051-1054.

CHAPTER 3

ADSORPTION OF METHYL CHLORIDE BY ACTIVATED CARBONS

I. Toreci and F.H. Tezel

Department of Chemical Engineering, University of Ottawa, 161 Louis Pasteur, Ottawa, Ontario K1N 6N5, Canada

Adsorption of methyl chloride has been studied by using activated carbon cloth and mesocarbon (from Spectracorp). The adsorption isotherms were obtained by using constant volume method at different temperatures ranging between 21.5 and 80 °C up to 1.6 atm pressure. Langmuir, Freundlich, Toth and Sips models were fitted to the experimental data and their validation were discussed. Repeatability was investigated and regeneration of the same adsorbent at different conditions was studied. The adsorption isosteres were obtained by using Toth parameters. Henry's law constants and heat of adsorption for methyl chloride by using both adsorbents were determined. Mesocarbon adsorbent had the highest capacity for methyl chloride. Feasibility of pressure swing adsorption (PSA), vacuum swing adsorption (VSA) and temperature swing adsorption (TSA) for separation of methyl chloride from air were discussed by determining the expected working capacities for these processes at different adsorption and desorption conditions. Mesocarbon gave the best expected working capacities for all these different scenarios.

3.1 INTRODUCTION

Volatile organic compounds exist extensively in everywhere. They have been used in many industries, especially in high-tech industries. Their existence has distorted the balance of ecosystems and is unfavorable to human health (Bloemen and Burn, 1993). Even at very low concentrations they can have big impact on environment; therefore they have to be separated from air before they are released to the atmosphere.

Adsorption is the most effective process among others such as incineration, condensation or absorption for removing trace pollutants from air (Zhao et. al., 1998 and Huang et. al., 1999). Adsorption produces no by-products. Recycling or recovery of the adsorbed species is possible which reduces the operating cost. It has low capital cost (Jennings et. al., 1985).

Chlorinated organic substances are one kind of volatile organic compounds. Chloromethane, which is the simplest chlorinated organic substance, is present in the environment at very high quantities. It is produced mostly by algae and fungi and by industrial activity, as well. The primary use of chloromethane is in the production of silicone. It is also used in manufacturing synthetic rubber and higher hydrocarbons. Chloromethane, as well as all chlorinated organic substance have impact on ozone depletion in stratosphere. Chlorine atom in the molecule reacts with ozone and degrades it to oxygen molecules. Although ozone keeps the ultraviolet radiation away from the surface of earth, oxygen molecules do not have that effect (Thornton, 2000).

Chloromethane has many destructive effects on human health. Exposures at high concentrations of chloromethane can lead to serious effects on nervous system, heat rate, liver and kidneys. Chloromethane is classified as a Group D carcinogen by EPA. The permissible exposure limit for this substance is set as 100 ppm for an 8-hour workday in a 40-hour workweek by the Occupational Safety and Health Administration (ATSDR, 1998).

In this study, methyl chloride adsorption by super activated mesocarbon and activated carbon cloth were studied. Pure adsorption data of methyl chloride were determined by using these adsorbents. The adsorption isosteres were attained to have a better view of the

temperature and pressure effect on adsorption. The heat of adsorptions and Henry's Law constants were also calculated.

3.2 THEORETICAL BACKGROUND

3.2.1 Activated Carbon Cloth

Activated carbons are used in different forms such as granular, palletized, powder and cloth. Activated carbon cloth (ACC) is a very promising form of activated carbon for separation and recovery of volatile organic compounds. Activated carbon cloths are usually prepared from polyacrylonitrile and phenolic based fibers which provide uniform pore structure. Usually they contain fewer amounts of inorganic impurities than other conventional activated carbons (Huang et. al., 1999).

ACC has many advantages over the conventional activated carbons used in industry. Due to the fact that it has stringy shape, it allows the intraparticle adsorption to take place faster than granular activated carbon (GAC) (Singh et. al., 2002). This property of ACC helps to reduce the contact time as well as allows higher velocity of inlet stream and also smaller bed depth of the adsorption unit. It has higher efficiency to provide higher product purity. It is found that ACC has higher adsorption capacity of VOCs than GAC which permits to handle high concentrations effectively by using smaller adsorption unit. In the presence of water vapor, destructive effect of humidity on the efficiency and the high capacity of ACC is less than that of GAC (Singh et. al., 2002). Another important property of ACCs is it has zero ash content (Lordgooei et. al., 1998). Ashes on the surface of the adsorbent can catalyze VOCs which causes the blockage of the pores, which reduces the surface area of the adsorbent leading to reduction of capacity (Zhao et. al, 1998). An additional property of ACCs is that, it has proper electric conductivity suitable for electro thermal regeneration (Lordgooei et. al., 1998).

3.2.2 Mesocarbon

Mesocarbon is also an activated carbon. The only difference between the conventional activated carbons and mesocarbon is the pore size. As the name implies, it has mesopores where as activated carbons usually have micropores.

According to IUPAC (International Union of Pure and Applied Chemistry) classification, if pore size is less than 20 Å, it is called micropore. For pore to be mesopore, its size should be between 20 and 500 Å. It is called macropore when pore size is larger than 500 Å. All molecules in micropores are considered as adsorbed phase since molecules can not escape from the solid surface force field, where as in mesopores and macropores, molecules can be either in the adsorbed phase or free gaseous phase (Ruthven et. al., 1994).

3.2.3 Pure Adsorption Models

Langmuir, Freundlich and Toth models were used as pure adsorption models.

Langmuir:
$$\theta = \frac{n}{n_s} = \frac{bP}{1+bP} \tag{3.1}$$

Freundlich:
$$n = KP^t \tag{3.2}$$

Toth:
$$\theta = \frac{n}{n_s} = \frac{bP}{\left[1+(bP)^t\right]^{1/t}} \tag{3.3}$$

The parameters of Toth equation can be found by using only one data set obtained at one temperature or this equation can be fitted to all the data obtained at different temperatures since all the parameters are temperature dependent. Multi temperature fit provides the extrapolation or interpolation of isotherms at different temperatures and allows us to calculate the heat of adsorption. Equations 3.4-3.6 show the temperature dependence of Toth parameters.

$$b = b_0 \exp\left[\frac{Q}{RT_0}\left(\frac{T_0}{T} - 1\right)\right] \tag{3.4}$$

$$t = t_0 + \alpha\left(1 - \frac{T_0}{T}\right) \tag{3.5}$$

$$n_s = n_{s,0} \exp\left[\chi\left(1 - \frac{T}{T_0}\right)\right] \tag{3.6}$$

3.3 EXPERIMENTAL

Constant volume technique was used to determine the pure adsorption isotherms. Experiments were performed by constant volume system Micromeritics Model: Accusorb 2100E. The adsorbate methyl chloride was purchased from Praxair (Ottawa, Canada). The adsorbents used in this study, carbon cloth Spectracarb 2225 and super activated mesocarbon microbeads M-30 were purchased from Spectracorp (MA, USA). The experiments were performed as explained in our previous study (Toreci et. al., 2003).

3.4 RESULTS AND DISCUSSION

Pure adsorption isotherms were obtained by using volumetric method at four different temperatures ranging from 21.5 to 80 °C. The results of experiments were very exciting and promising. Figure 3.1 shows methyl chloride adsorption isotherms by using carbon cloth, mesocarbon, HiSiv-3000, SBA-15 and Takeda 5A at 40 °C. HiSiv-3000 and SBA-15 data were taken from our previous work (Toreci et al., 2003); adsorption isotherm of methyl chloride with Takeda 5A carbon was obtained by Mariwala and Foley (1994) and compared to the activated carbon adsorbents. It can be seen from this figure that the capacities of both carbon cloth and mesocarbon were much more than other adsorbents' capacities that were studied in the literature. Mesocarbon adsorbent showed much higher methyl chloride adsorption capacity, almost twice as much as that obtained for carbon cloth. Methyl chloride adsorption capacity for carbon cloth was three times those for HiSiv-3000 and SBA-15.

Although at very low pressures Takeda 5A has higher adsorption capacity, since adsorption isotherm of methyl chloride with Takeda 5A is very rectangular desorption of methyl chloride is very difficult. For methyl chloride adsorption with Takeda 5A, pressure swing adsorption can not be used since above atmospheric pressure its isotherm is horizontal which makes it impossible to desorb methyl chloride by changing pressure above 3 kPa. This makes Takeda 5A a less feasible adsorbent for this separation.

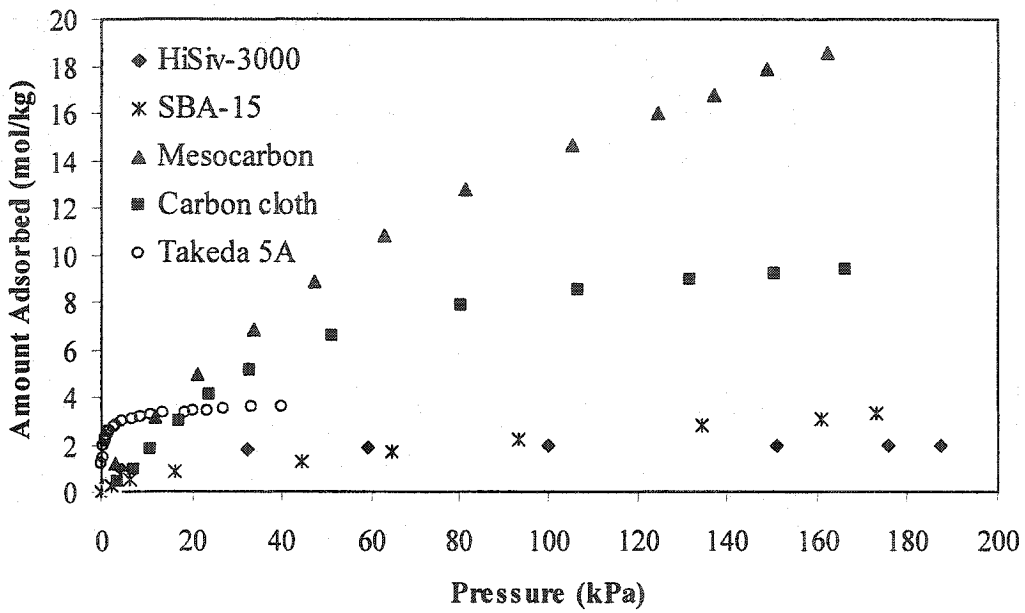

Figure 3.1: Adsorption isotherm of methyl chloride by using different adsorbents at 40 °C.

The methyl chloride adsorption isotherms obtained by carbon cloth and mesocarbon are shown in figures 3.2 and 3.3, respectively at different temperatures. In these figures Toth isotherm fitting by using single temperature data were also drawn to show the trend. Methyl chloride adsorption by using carbon cloth reached saturation within the pressure range studied, whereas adsorption isotherms obtained for mesocarbon show more linearity. It was observed that as temperature increases the amount adsorbed decreases for both adsorbents. This shows that adsorption by both adsorbents are exothermic.

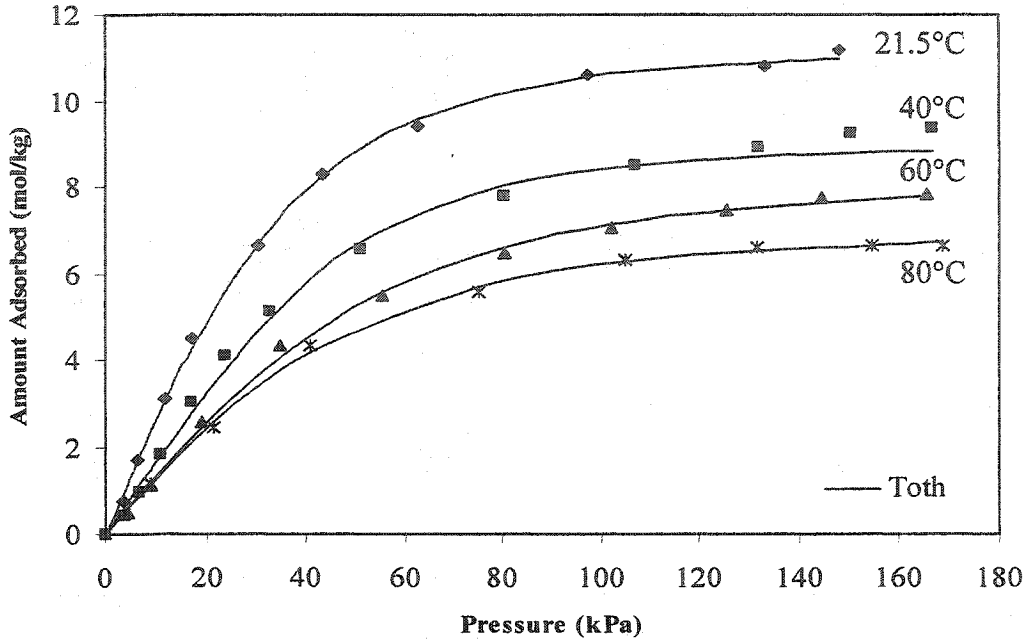

Figure 3.2: Methyl chloride adsorption isotherms by using carbon cloth and Toth fit at different temperatures

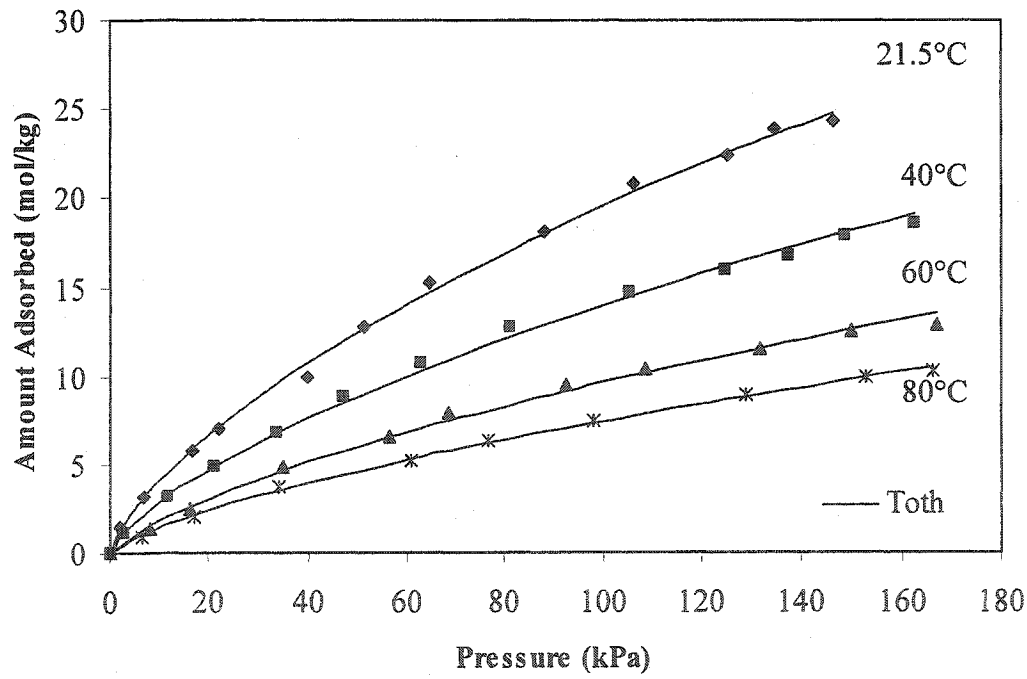

Figure 3.3: Methyl chloride adsorption isotherms by using mesocarbon and Toth fit at different temperatures

Langmuir, Freundlich and Toth adsorption models were fitted to pure methyl chloride isotherms. Sips model was also used and the results were found to be very similar to the single temperature Toth model. Therefore they are not shown in the figures. Figures 3.4 and 3.5 show different model fits for adsorption of methyl chloride at 21.5 °C. The shown fit for Toth model was obtained by multi temperature fit. Although the difference between single temperature fit and multiple temperatures fit is very small, single temperature fit gave slightly better results since it has more flexibility. However, multiple temperature Toth model is a better choice to use, since it can be used to obtain adsorption isosteres and expected working capacities of adsorption processes as well.

The model parameters that are found and weighted sum of squares of residual (WSSR) values for carbon cloth and mesocarbon are shown in Tables 3.1 and 3.2, respectively. The models are compared by WSSR values and as well as residual and % error plots. Some examples of residual and % error plots of methyl chloride adsorption with mesocarbon and carbon cloth are shown in Appendix B. Lack of fit test could not performed due to the nature of the experimental procedure. WSSR values are calculated by using the following equation:

$$WSSR = \frac{\sum (y - \hat{y})^2}{y} \tag{3.7}$$

where y is the experimental value

$\hat{y}$ is the predicted value

From Figures 3.4 and 3.5 it can be seen that Toth isotherm gave the best fit to experimental data. For carbon cloth, none of the other isotherm models described the data best. For methyl chloride adsorption with carbon cloth, although Langmuir fit's WSSR value is close to that of Toth fit, it was observed that Langmuir is under estimates the capacity of carbon cloth at pressures between 20 and 80 kPa (Figure 3.4). Langmuir fits better than Toth fit to the adsorption data only at 80 °C. From WSSR values (Table 3.1) it can easily be seen that Freundlich is not fitting the data at all.

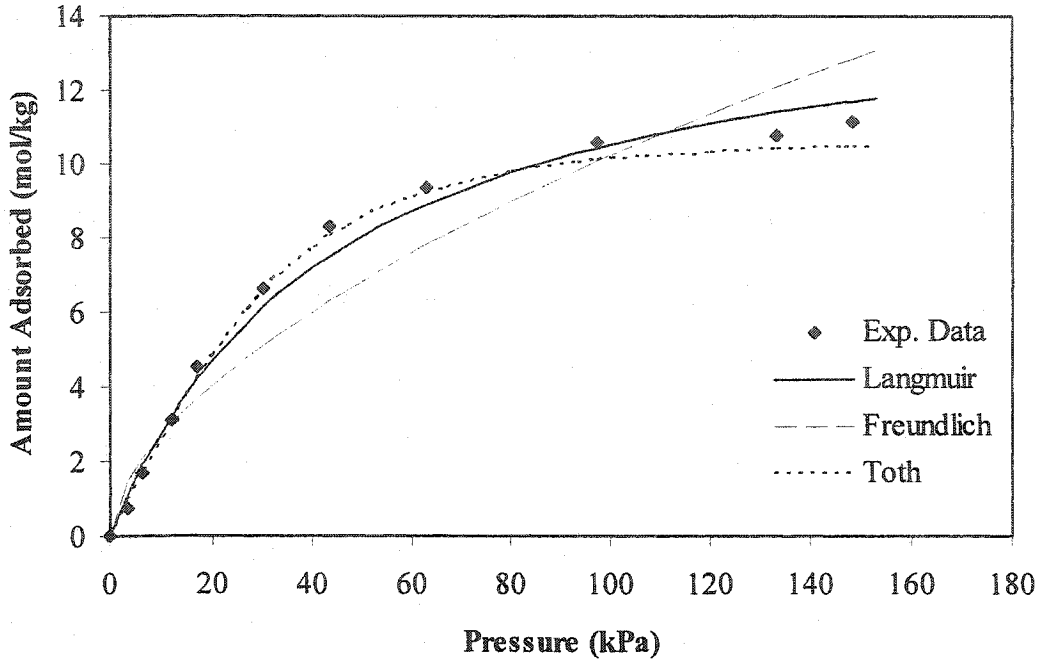

Figure 3.4: Methyl chloride adsorption isotherm by using carbon cloth and pure adsorption model fits at 21.5 °C

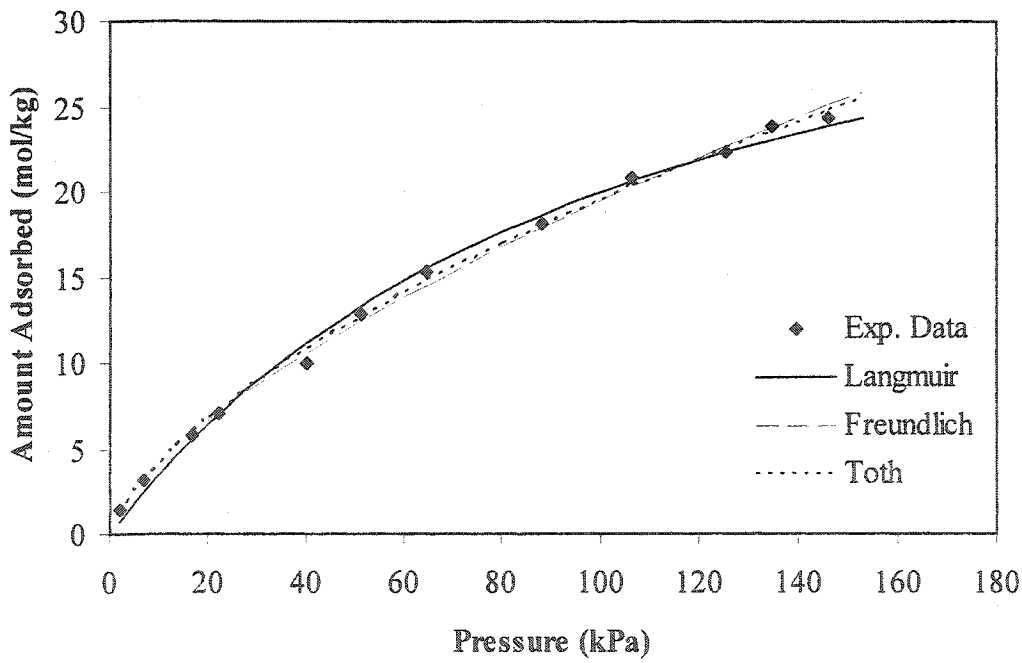

Figure 3.5: Methyl chloride adsorption isotherm by using mesocarbon and pure adsorption model fits at 21.5 °C

Table 3.1: Pure adsorption model parameters for carbon cloth and WSSR values for each model used for methyl chloride adsorption at different temperatures.

Methyl Chloride	Langmuir		Freundlich		Toth	
	Parameters	WSSR	Parameters	WSSR	Parameters	WSSR
21.5 °C	n_s = 15.1827 b = 0.0004	9.3302	K = 1.6617 1/t = 0.5791	54.7985	n_s = 10.8086 b = 0.0004 t = 2.1287	3.2620
40 °C	n_s = 14.7101 b = 0.0002	12.0139	K = 0.6130 1/t = 0.7024	38.7153	n_s = 9.6424 b = 0.0003 t = 2.1287	8.2379
60 °C	n_s = 11.8400 b = 0.0002	5.0415	K = 0.6753 1/t = 0.6469	26.3627	n_s = 8.5227 b = 0.0003 t = 2.1287	2.8850
80 °C	n_s = 9.4661 b = 0.0003	2.8850	K = 0.7737 1/t = 0.6020	19.9924	n_s = 7.5330 b = 0.0002 t = 2.1287	9.0309

For methyl chloride adsorption with mesocarbon, by looking the WSSR values in Table 3.2, it can be concluded that Freundlich fits as good as Toth. This can also be seen in Figure 3.5. Langmuir also fits well to all adsorption isotherms except the one at 21.5 °C. Toth fits very good to the experimental data but for the data at 60 °C, it is not as good fit as the others models but it is important to remember since it is a multiple temperature model overall it fits very well.

Table 3.2: Pure adsorption model parameters for mesocarbon and WSSR values for each model used for methyl chloride adsorption at different temperatures.

Methyl Chloride	Langmuir		Freundlich		Toth	
	Parameters	WSSR	Parameters	WSSR	Parameters	WSSR
21.5 °C	n_s = 41.7060 b = 0.0002	15.9707	K = 1.7658 1/t = 0.6672	2.7165	n_s = 9490.721 b = 6.69x10^{-6} t = 0.1600	2.8824
40 °C	n_s = 30.6177 b = 0.0002	3.9416	K = 1.2903 1/t = 0.6636	3.9548	n_s = 9490.721 b = 3.91x10^{-6} t = 0.1600	2.4342
60 °C	n_s = 23.6587 b = 0.0001	0.7401	K = 0.7048 1/t = 0.6986	4.2669	n_s = 9490.721 b = 2.34x10^{-6} t = 0.1600	4.1887
80 °C	n_s = 19.2351 b = 0.0001	1.5557	K = 0.5120 1/t = 0.7082	1.3325	n_s = 9490.721 b = 1.48 x10^{-6} t = 0.1600	1.3703

In order to better understand its behavior and applicability of these adsorbents, adsorption isotherms for methyl chloride were obtained after different regeneration conditions to see whether adsorption is reversible. Reversibility will play an important role in applicability off these adsorbents to cyclic adsorption processes. First, new adsorbent sample was regenerated at 350 °C with vacuum for 16 hours and adsorption isotherms were obtained at 40 °C with constant volume method. Then, the same adsorbent sample was regenerated at the same conditions again to see if the performance of the adsorbents stays the same after the first use. The isotherms obtained after second regeneration were the same as the isotherm data obtained after the first regeneration (Figure3. 6). Then in order to understand the effect of temperature on regeneration, two more experiments were carried out. In these experiments, regenerations were done only with vacuum at room temperature (21.5 °C). The results are given in Figure 3.6 and are consistent with previously obtained isotherm data. It

was concluded that there is no need to use higher temperature in regeneration since the performance of adsorbents without having high temperature regeneration is the same with the one in which high temperature is used for regeneration. This shows that these adsorbents will be excellent candidates for methyl chloride adsorption for Vacuum Swing Adsorption (VSA).

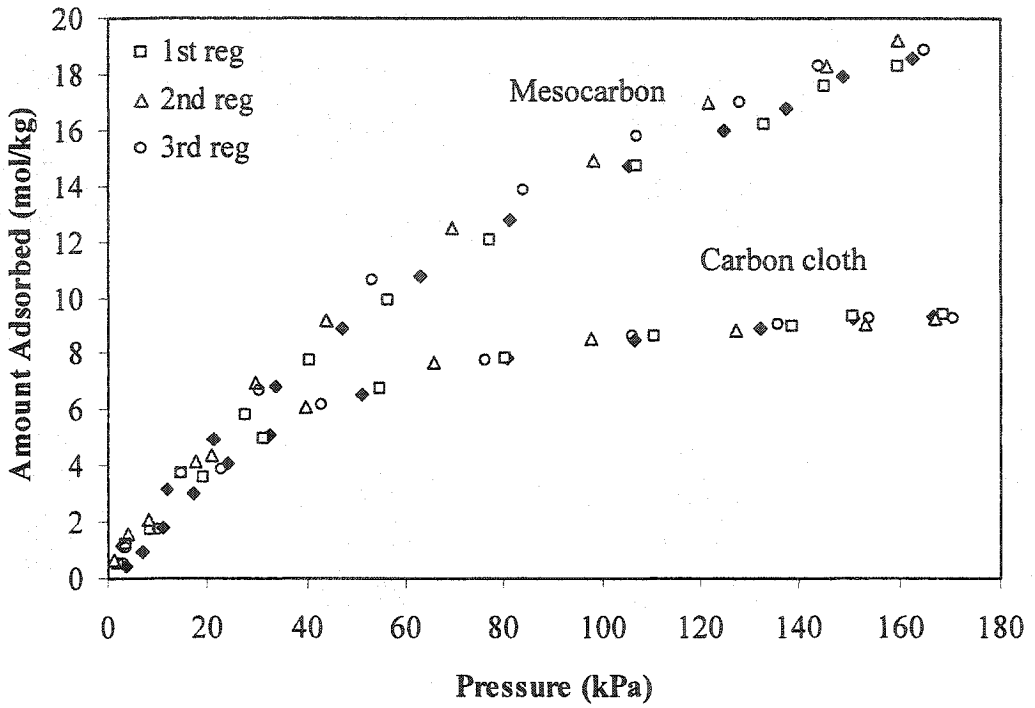

Figure 3.6: Adsorption isotherms at 40 °C. 1st regeneration is at 350 °C with vacuum. 2nd and 3rd regenerations are at room temperature (21.5 °C) with vacuum.

Adsorption isosteres of methyl chloride with carbon cloth and mesocarbon adsorbents were calculated by using Toth isotherm parameters and are shown in Figures 3.7 and 3.8, respectively. From these figures it can be seen that mesocarbon capacity for methyl chloride adsorption is much more than that of carbon cloth (under certain conditions, twice as much). Contours of carbon cloth are more horizontal at pressures lower than 40 kPa whereas, as the pressure increases the curvature of contours increases and eventually they became vertical. This indicates that at lower pressures temperature effect is less than that at higher pressures. On the other hand, in the isosteres obtained by using mesocarbon as adsorbent, it was

observed that the curvatures of contours are similar throughout the pressure and temperature range studied in this work.

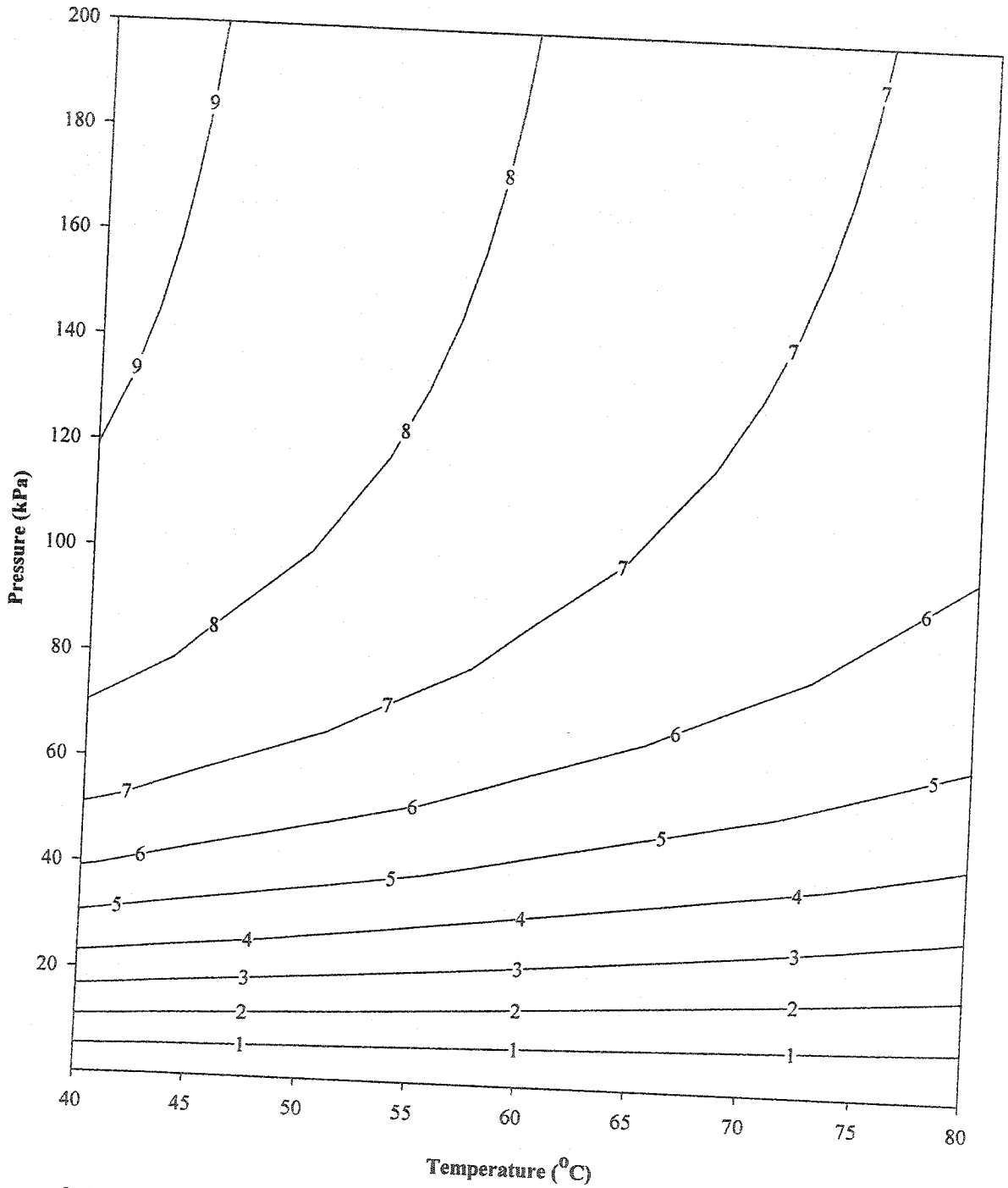

Figure 3.7: Adsorption isosteres of methyl chloride with carbon cloth. Contours indicate amount adsorbed as mol/kg.

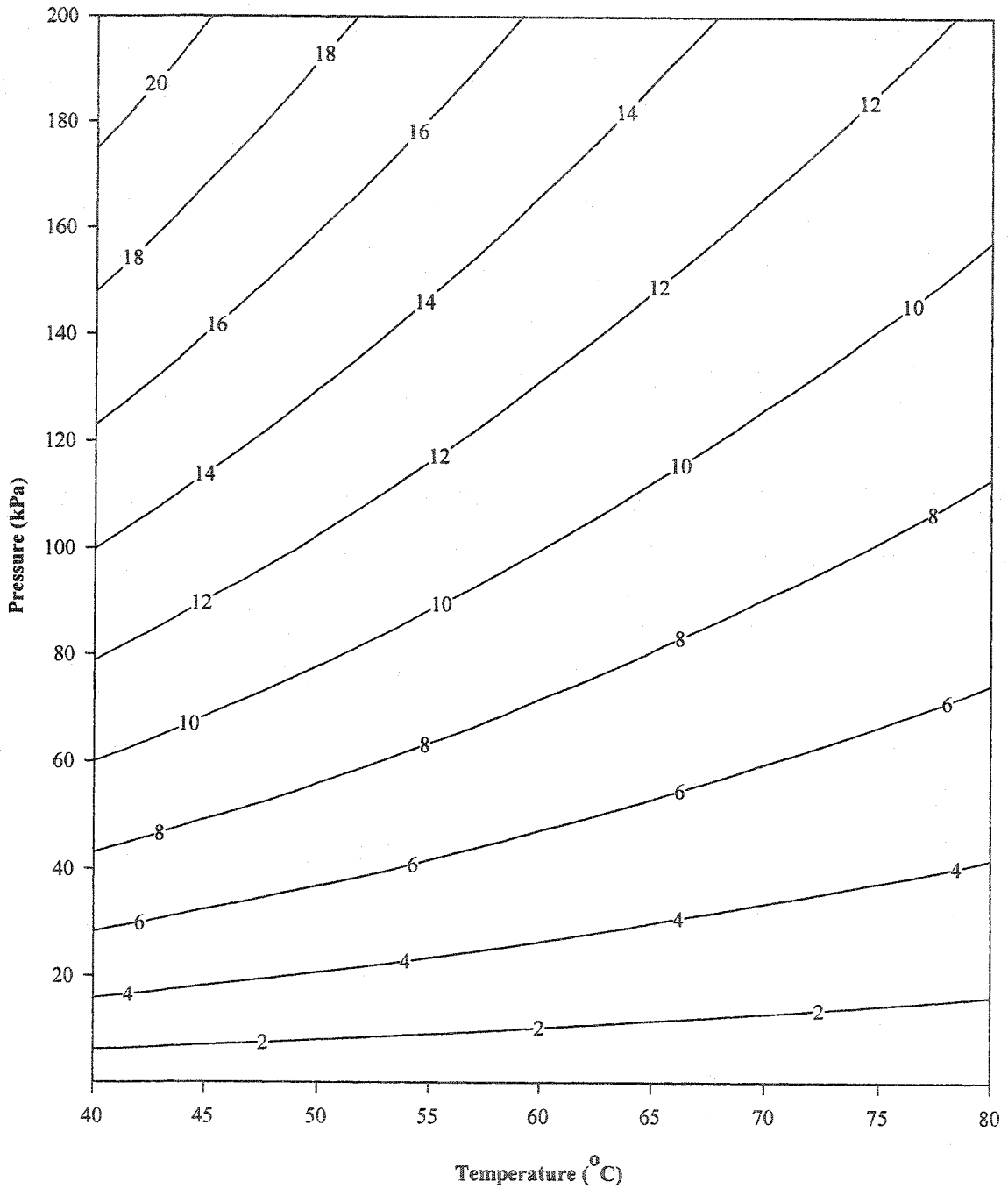

Figure 3.8: Adsorption isosteres of methyl chloride with mesocarbon. Contours indicate amount adsorbed as mol/kg.

Heat of adsorption is a very important parameter in understanding the separation and designing adsorption processes. Heats of adsorption and pre-exponential constants are obtained from Van't Hoff plots (Figure 3.9) and are given in Table 3.3 for carbon cloth and mesocarbon adsorbents. Van't Hoff equation is given in equation 3.8:

$$\ln K = \ln K_0 + \left(\frac{-\Delta H}{R}\right)\frac{1}{T} \tag{3.8}$$

Henry's Law constants for methyl chloride were plotted at different temperatures and shown in Figure 3.9. From these data it can be seen that, interaction of methyl chloride with carbon cloth is much less than that of mesocarbon since heat of adsorption of methyl chloride by using carbon cloth as the adsorbent is much less than that of mesocarbon. Since heat of adsorption is related to the energy required to regenerate the adsorbent, it can be concluded that regeneration of carbon cloth will need much less energy than mesocarbon.

Table 3.3: Heats of Adsorption and Pre-exponential constants from Van't Hoff plots for methyl chloride by using adsorbents carbon cloth and mesocarbon

Adsorbents	**Methyl chloride**	
	$-\Delta H$ (kJ mol^{-1})	**K_0 (mol kg^{-1} kPa^{-1})**
Carbon Cloth	12.21	1.47×10^{-3}
Mesocarbon	23.96	3.95×10^{-5}

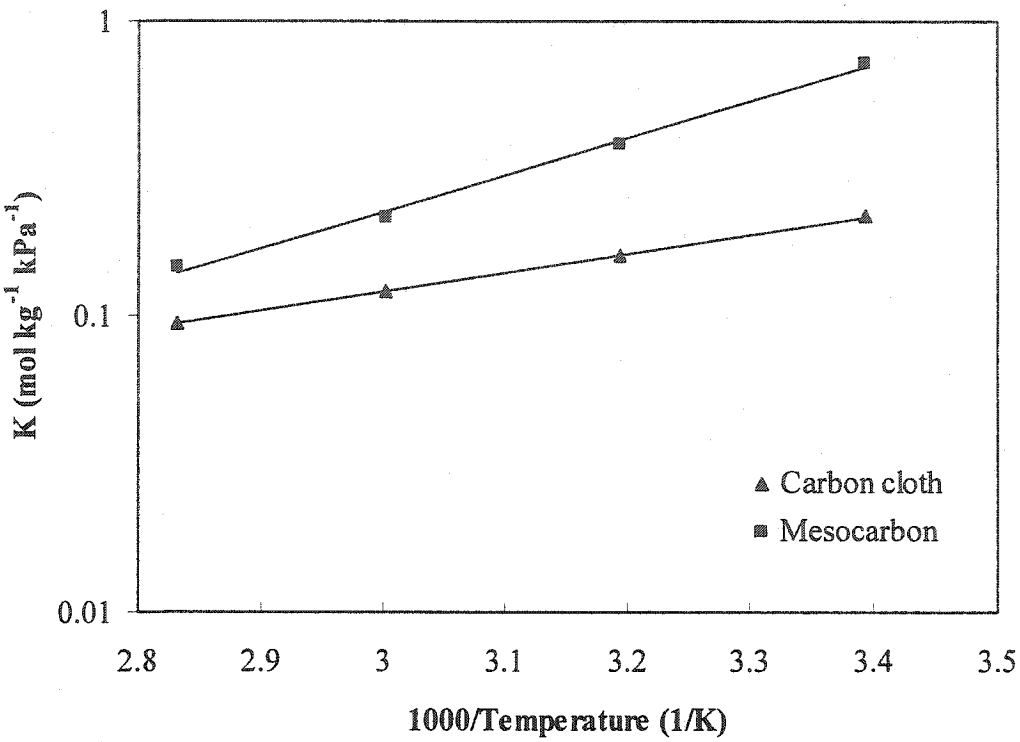

Figure 3.9: Henry's law constants for methyl chloride and nitrogen at different temperatures for carbon cloth and mesocarbon adsorbents.

From the pure adsorption isotherms and isosteres it was observed that activated carbon cloth and especially mesocarbon are two promising adsorbents in separation of low concentrations of volatile organic compounds from air. From the regeneration experiments it was also concluded that these adsorbents can be reused after regeneration without loosing their adsorption capacity. To determine which adsorption process is best for this separation, the expected working capacities (EWCs) were calculated at different adsorption and desorption conditions. For these calculations it is assumed that nitrogen adsorption is negligible. This is a reasonable assumption, since it was found in our earlier studies that binary adsorption behavior of methyl chloride and nitrogen mixture was dominated by methyl chloride (Toreci, et. al., 2003).

By using Toth parameters, amount adsorbed at different conditions were calculated and by using these data, expected working capacities for pressure swing adsorption (PSA),

vacuum swing adsorption (VSA) and temperature swing adsorption (TSA) processes were determined according to Equation 3.9:

$$\text{Expected working capacity (EWC)} = n_{\text{adsorption}} - n_{\text{desorption}} \quad (3.9)$$

The expected working capacities obtained by other adsorbents (HiSiv-3000 and SBA-15) given in the literature by Toreci et. al. (2003) are also shown and compared to the results in this study.

For pressure swing adsorption (PSA) process, pressure was kept at atmospheric pressure for desorption, whereas, pressure was increased for adsorption. The temperature was kept at room temperature (21.5 °C) both for adsorption and desorption. The results for expected working capacities for PSA are shown in Figure 3.10. Mesocarbon shows the highest EWC values, which are more than seven times as much as other adsorbents. SBA-15 values are higher than those for carbon cloth and HiSiv-3000 for PSA process. EWC values are the lowest for HiSiv-3000.

In vacuum swing adsorption (VSA), the adsorption takes place at atmospheric pressure, whereas, desorption pressure is changed by a vacuum pump. Again, for this process the temperature was kept at room temperature. EWC values were obtained as a function of desorption pressure and are shown in Figure 3.11. For this process, again, mesocarbon gives the highest expected working capacity values. Mesocarbon's capacity is almost double the values for carbon cloth. Carbon cloth gives better EWC values for VSA than PSA.

The other adsorption process that can be used for separation of volatile organic compounds from air is the temperature swing adsorption (TSA) process. In this process pressure is kept at atmospheric pressure and while adsorption takes place at lower temperatures desorption is carried out by increasing the temperature. To calculate the EWC values the adsorption temperature was kept at 21.5 °C and desorption temperature was varied. The results are given for different adsorbents in Figure 3.12. For this process again mesocarbon gave the best results. The expected working capacity of mesocarbon is found to be three times better than that of carbon cloth. HiSiv-3000 has the lowest EWC values.

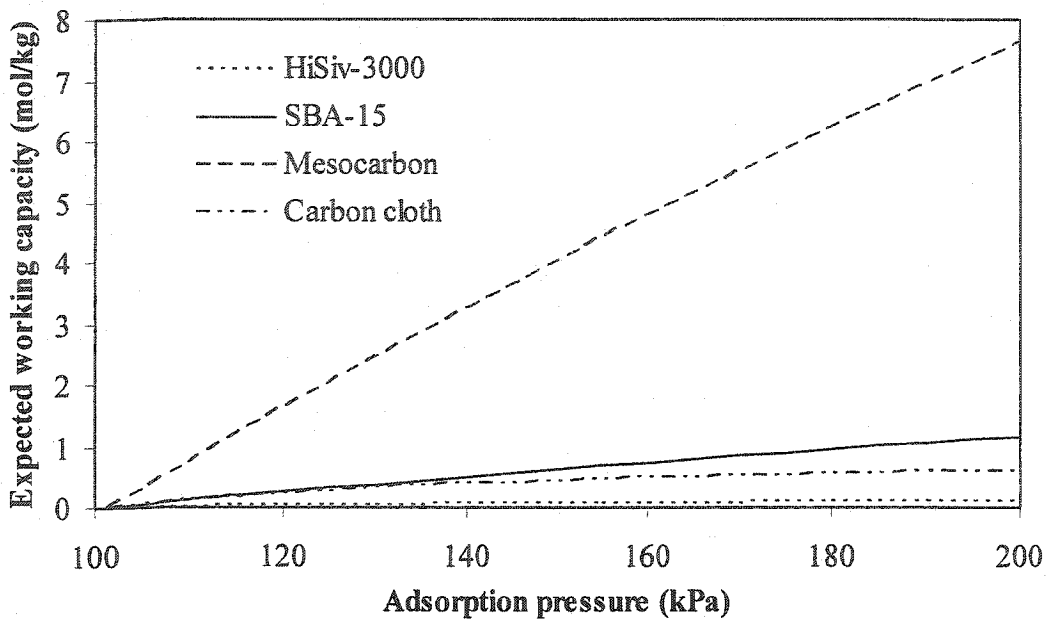

Figure 3.10: Expected working capacities for a pressure swing adsorption system for the adsorption of methyl chloride at 21.5 °C, keeping desorption pressure at 101 kPa.

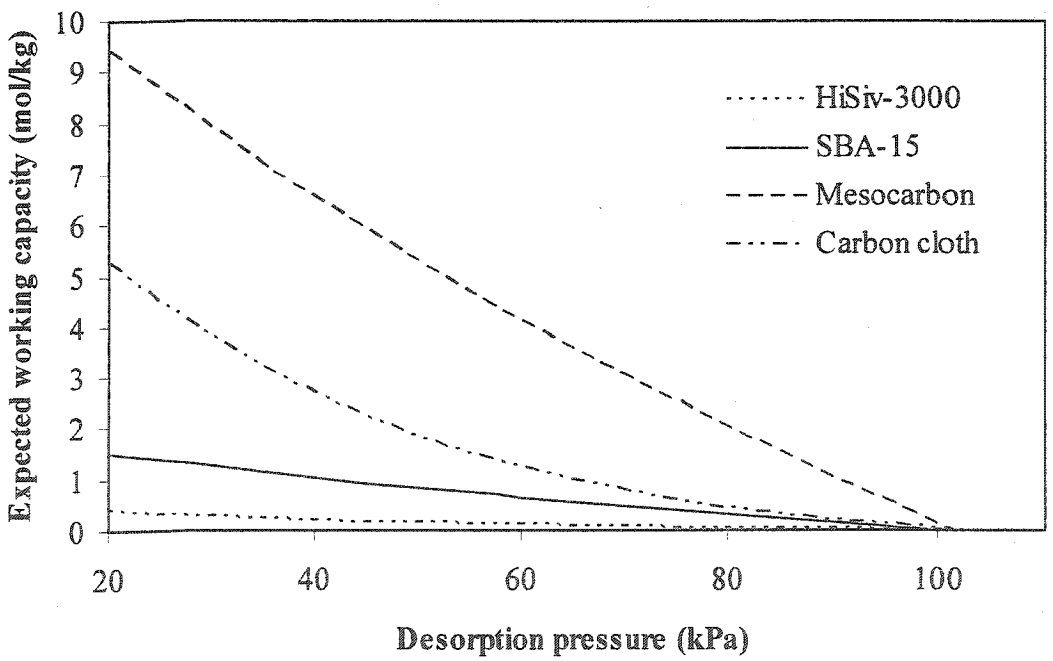

Figure 3.11: Expected working capacities for a vacuum swing adsorption system for the adsorption of methyl chloride at 21.5 °C, keeping adsorption pressure at 101 kPa.

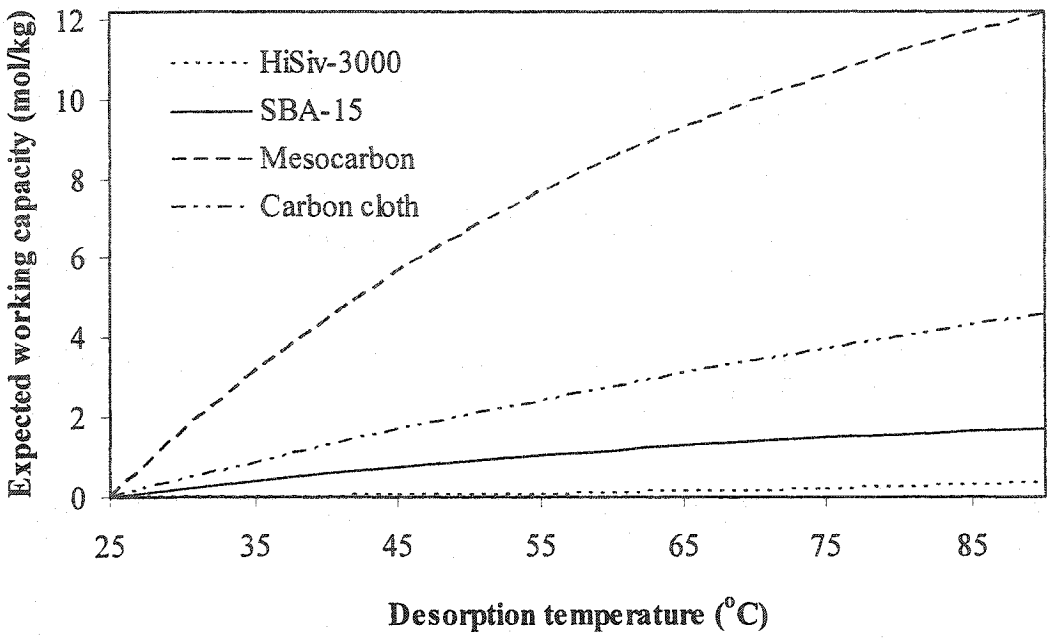

Figure 3.12: : Expected working capacities for a temperature swing adsorption system for the adsorption of methyl chloride at atmospheric pressure, keeping adsorption temperature at 21.5 °C

When all the three adsorption processes are compared, it was concluded that TSA is a promising process with adsorbents carbon cloth and mesocarbon, since it gave the best EWC values. VSA can also be considered as the second best effective process. The reason for PSA being the worse process for this separation is the shape of the isotherms of methyl chloride adsorption shown in Figures 3.2 and 3.3. The pressure effect on adsorption capacity is much less at higher pressures than at lower pressures with all the adsorbents. Therefore, as long as desorption pressure is fixed at atmospheric pressure, changing the adsorption pressure at higher values do not increase the EWC values much. In the VSA scenario, since the adsorption pressure is fixed at atmospheric pressure, and desorption pressure is changed at lower values, it is possible to get higher EWC values at lower pressures, even with small changes in pressure.

3.5 CONCLUSIONS

Several conclusions have been drawn from this study:

- Mesocarbon and carbon cloth have much higher adsorption capacities for methyl chloride than any other adsorbents studied in the literature.
- Mesocarbon has the highest methyl chloride adsorption capacity. Its capacity is twice as much as that of carbon cloth. Carbon cloth has the capacity almost triple the capacities of HiSiv-3000 and SBA-15.
- Toth fits best to all the isotherm data obtained by using both mesocarbon and carbon cloth.
- For the isotherm data of methyl chloride by using mesocarbon, Freundlich fits also gave good results.
- Regenerations of these adsorbents are possible with vacuum only. There is no need for high temperature regeneration.
- For carbon cloth, the effect of temperature on the amount adsorbed is less at lower pressures (less than 40 kPa) than at high pressures.
- The temperature effect on the amount adsorbed for mesocarbon is similar throughout the pressure range studied.
- Heat of adsorption of methyl chloride with carbon cloth as adsorbent is half of the heat of adsorption with mesocarbon.
- VSA and TSA are more feasible processes than PSA since the expected working capacities of both adsorbents are more for these processes than those for PSA.
- Mesocarbon is the best adsorbent compared to the ones studied in the literature. Being easily regenerated by only vacuum, very high capacity of adsorption and having very high expected working capacity with VSA and TSA are several advantages of mesocarbon making it the most preferable adsorbent for the separation of methyl chloride from air.

3.6 NOMENCLATURE

b	empirical parameter, kPa^{-1}
b_0	affinity at reference temperature, T_0, kPa^{-1}
K	empirical parameter, mol kg^{-1} $kPa^{-1/t}$
K_0	pre-exponential constant for Van't Hoff plot, mol kg^{-1} kPa^{-1}
n	amount adsorbed, mol kg^{-1}
n_s	amount adsorbed at monolayer saturation, mol kg^{-1}
$n_{s,0}$	empirical parameter, mol kg^{-1}
P	pressure, kPa
R	universal gas constant, kJ mol^{-1} K^{-1}
T	temperature, K
T_0	reference temperature, K
t	empirical parameter, dimensionless
t_0	empirical parameter, dimensionless
y	experimental value, mol kg^{-1}
$\hat{y}$	predicted value, mol kg^{-1}

Greek Letters

ΔH	heat of adsorption, kJ mol^{-1}
θ	fractional surface coverage, dimensionless
χ	empirical parameter, dimensionless

Abbreviations

ACC	Activated Carbon Cloth
EWC	Expected Working Capacity
GAC	Granular Activated Carbon
IUPAC	International Union of Pure and Applied Chemistry
PSA	Pressure Swing Adsorption
TSA	Temperature Swing Adsorption

VOC Volatile Organic Compound

VSA Vacuum Swing Adsorption

WSSR Weighted sum of squared residual

Acknowledgements

Financial support received from Natural Sciences and Engineering Council (NSERC) of Canada and Chemical Engineering Department at University of Ottawa is gratefully acknowledged.

3.7 REFERENCES

Agency for Toxic Substances and Disease Registry (ATSDR). *Toxicological Profile for Chloromethane (Update)*, U.S. Public Health Service, U.S. Department of Health and Human Services, Atlanta, GA. (1998)

Bloemen, H. J and J. Burn, "Chemistry and Analysis of Volatile Organic Compounds in the Environment", Blackie Academic & Professional, Glasgow, the Netherlands, (1993)

Do, D.D., "Adsorption Analysis Equilibria and Kinetics", Imperial College Press, Danvers, MA (1998) pp 49-76 and 156-168.

Huang, C. C., Y. C. Lin and F. C. Lu, "Dynamic Adsorption of Organic Solvent Vapors onto a Packed Bed of Activated Carbon Cloth", Separation Science and Technology, 34, 55-570 (1999)

Jennings, M.S., N.E. Krohn, R.s. Berry, M.A. Palazzolo, R.M. Parks, K.K. Fidler, "Catalytic Incineration for Control of Volatile Organic Compound Emissions", Noyes Publications, New Jersey 61-75 (1985)

Lordgooei, M., J. Sager, M. J. Rood and M. Rostam-Abadi, "Sorption and Modelling of Mass Transfer of Toxic Chemical Vapors in Activated-Carbon-Fiber-Cloth Adsorbers", Energy & Fuels, **12**, 1079-1088 (1998)

Mariwala, R. K. and H. C. Foley, "Calculation of Micropore Sizes in Carbogenic Materials from the Methyl Chloride Adsorption Isotherm", Ind. Eng. Chem. Res., 33, 2314-2321 (1994)

Ruthven, D. M., S. Farooq and K. S. Knabel, "Pressure Swing Adsorption", VCH Publishers, Inc., NY (1994)

Singh, K. P., D. Mohan, G. S. Tandon and G. S. D. Gupta, "Vapor-Phase Adsorption of Hexane and Benzene on Activated Carbon Fabric Cloth: Equilibria and Rate Studies", Ind. Eng. Chem. Res., **41**, 2480-2486 (2002).

Thornton, J., "Pandora's Poison: Chlorine, Health, and a new Environmental Strategy", MIT Press, Massachusetts (2000).

Toreci, I., F.H. Tezel, Y. Yong and A. Sayari, "Adsorption of Methyl Chloride from Nitrogen by Using Zeolite and Mesoporous Molecular Sieve", to be submitted to the Journal of Adsorption Science and Technology (2003)

Zhao, X.S., Q. Ma and G.Q. Lu, "VOC Removal: Comparison of MCM-41 with Hydrophobic Zeolites and Activated Carbon", Energy & Fuels, **12**, 1051-1054 (1998)

CHAPTER 4

MODELING OF METHYL CHLORIDE SEPARATION BY ADSORPTION

The separation of volatile organic compounds from air is a very important issue for related industries due to the fact that even small amount of VOCs can cause serious environmental and health problems. Adsorption is found to be the most effective technique to separate VOCs especially when they are present in small concentrations in air. Among different adsorption processes, vacuum swing adsorption (VSA) is frequently used in industry to separate trace components from air. Its simplicity, high separation efficiency and low operating cost are the main advantages of VSA. Beside these advantages, the design flexibility of this process causes the incremental growth of the development of this technology.

For modeling, many studies have been performed in recent years. Modeling for trace component separation by using activated carbon was studied by Ritter and Yang (1991), Lavanchy et.al. (1993) and Chenu et.al. (1998). For multicomponent breakthrough modeling Malek and Farooq (1997) worked on. They (1997) also worked on separation modeling of non-isothermal modeling on activated carbon and silica gel. Modeling by using zeolites performed for trace components by Farooq et.al. (1988), Hassan et. al. (1985), Pigorini and Le Van (1998) and Ruthven and Farooq (1994).

The modeling of this process is a vital task. In order to do this, adsorption equilibrium and kinetic parameters should be determined. Modeling provides the effect of all

parameters onto the process. Therefore, without actually carrying out any experiments, optimum values for these parameters can be determined.

In this chapter, the effects of temperature, inlet concentration, flow rate, bed length as well as different adsorbents on the separation of methyl chloride, which represents volatile organic compounds, from air, were discussed. Nitrogen was used as a representative of air since 79% of air is composed of nitrogen and adsorption of oxygen is very similar to the adsorption of nitrogen compared to VOCs. From our previous studies, nitrogen adsorption was shown to be negligible relative to methyl chloride. Therefore, only methyl chloride was assumed to be adsorbed in modeling studies. The pressure for this study was kept at 1 atmosphere and the inlet concentration of methyl chloride in air was kept as 1 %. For the applicability of the model, partial pressure of methyl chloride should be less than 10 kPa because only less than 10 kPa the isotherm of methyl chloride is linear. In order to be in the linear region, if total pressure is high, the concentration should be kept low.

As adsorbents only HiSiv-3000 and SBA-15 are used. Although the expected capacity of mesocarbon for vacuum swing adsorption is much higher than the other adsorbents studied, the necessary data of mesocarbon for modeling is not available currently. Carbon cloth also could not be modeled due to its cloth shape the model used in this study is not proper for this adsorbent.

4.1 THEORY

To model the adsorption of a trace component in vacuum swing adsorption column, isothermal and equilibrium controlled mathematical model was used. The adsorption column is packed with adsorbent, so the column acts like a packed bed reactor. The column is assumed to be isothermal since the inlet concentration of methyl chloride is very low. This causes very little amount of heat to be released due to adsorption. Adsorption in the column is equilibrium controlled since the adsorption equilibrium is reached slower than convective mass transfer in the column. This model includes the gas phase film transfer in the bed and diffusion in macropores of the adsorbent.

The flow rate was assumed to be constant. Decrease of the amount of gas passing through the column caused by the adsorption is negligible since the composition of the methyl chloride in the air is very low. The pressure drop in the bed is also negligible. The adsorption equilibrium is expressed as linear isotherm. Having very low inlet concentration leads the equilibrium to be reached at very low pressures. In low pressure range it is determined from experimental results that the isotherm is linear. It is assumed that ideal gas law is applicable. The fluid flow pattern is taken as plug flow with axial dispersion. Axial dispersion also is calculated but its effect is found to be negligible, therefore axial dispersion is assumed to be zero. These assumptions lead to the Rosen Model.

4.1.1 Mass Balance

Figure 4.1 shows the schematic diagram of a pressure swing adsorption. Adsorbent pellets are packed in a cylindrical column. Adsorption starts at the beginning of the column and continues through out the column as diffusion takes place. The resistances that are taking place during adsorption are external fluid film, intercrystalline macropore and microporous crystal mass transfer resistances, which are shown in Figure 4.2.

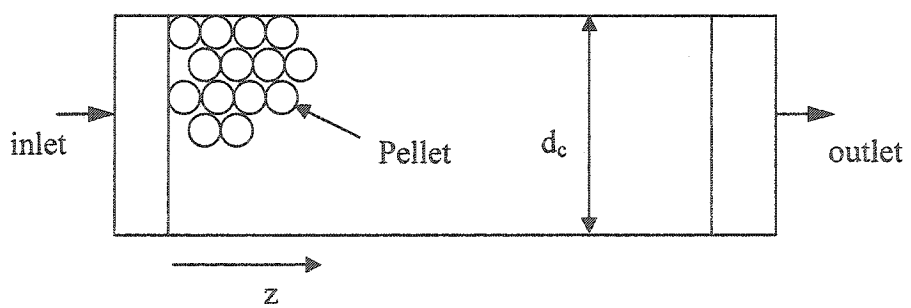

Figure 4.1: Schematic diagram of a pressure swing adsorption column

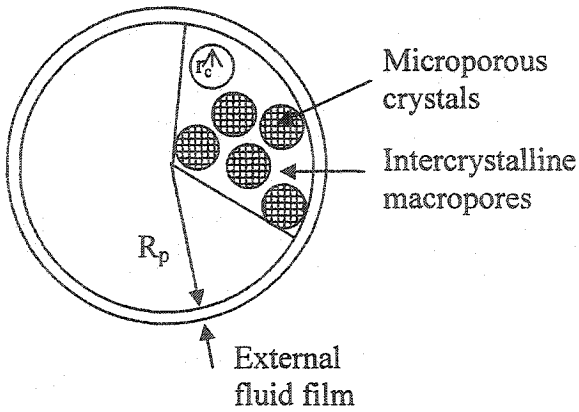

Figure 4.2: Schematic diagram of mass transfer resistances in the adsorbent pellet.

Mass balance in the packed bed reactor is expressed as the following equation (Yang, 1987):

$$-D_L \frac{\partial^2 C}{\partial z^2} + \frac{\partial (uC)}{\partial z} + \frac{\partial C}{\partial t} + \frac{(1-\varepsilon)}{\varepsilon} \frac{\partial \overline{q}}{\partial t} = 0 \tag{4.1}$$

(Axial dispersion) + (mass flux) + (mass accumulation in the gas phase) + (mass accumulation in the pellet) = 0

The open form of this equation is as follows:

$$-D_L \frac{\partial^2 C}{\partial z^2} + u\frac{\partial C}{\partial z} + C\frac{\partial u}{\partial z} + \frac{\partial C}{\partial t} + \frac{(1-\varepsilon)}{\varepsilon} \frac{\partial \overline{q}}{\partial t} = 0 \tag{4.2}$$

Since the inlet concentration of the adsorbate is very low, the decrease in flow rate due to adsorption is negligible. This leads no change in the flow rate in the column; therefore the mass balance equation in the column can be simplified as:

$$-D_L \frac{\partial^2 C}{\partial z^2} + u\frac{\partial C}{\partial z} + \frac{\partial C}{\partial t} + \frac{(1-\varepsilon)}{\varepsilon} \frac{\partial \overline{q}}{\partial t} = 0 \tag{4.3}$$

The volume-average adsorbate concentration, $\overline{q}$, can be expressed as:

$$\overline{q} = \frac{3}{R_p^3} \int_0^{R_p} KC^P r^2 dr \tag{4.4}$$

Therefore

$$\frac{\partial \overline{q}}{\partial t} = \frac{3}{R_p^3} \frac{\partial \left[\int_0^{R_p} KC^P r^2 dr \right]}{\partial t} \tag{4.5}$$

In linear driving force model, the pore diffusion is the limiting step for the mass transfer. Since there is the film mass transfer resistance, for the adsorption rate in the particle term at the boundary can be written as:

$$\frac{\partial q}{\partial t} = \frac{3k}{R_p} (C - C^P_{r=R_p}) \tag{4.6}$$

For the diffusion rate in a spherical particle the following equation is used:

$$\frac{\partial C^P}{\partial t} = D_e \left(\frac{\partial^2 C^P}{\partial r^2} + \frac{2}{r} \frac{\partial C^P}{\partial r} \right) \tag{4.7}$$

The initial and boundary conditions are

$$C^p = 0 \text{ at } t = 0, \qquad 0 < r < R_p, \qquad z > 0$$

$$C = C_o H(t) \text{ at } z = 0, \quad t > 0$$

Rosen model has asymptotic solution for long bed lengths and no film diffusion resistance (Yang, 1987):

$$\frac{C}{C_0} = \frac{1}{2}\left[1 + erf\frac{(3U/2V)-1}{2\left(\frac{1+5\upsilon}{5V}\right)^{1/2}}\right] \tag{4.8}$$

$$U = \frac{2D_e(t - L/u)}{R_p^2} \tag{4.9}$$

$$V = \frac{3D_e KL}{uR_p^2}\left(\frac{\varepsilon}{1-\varepsilon}\right) \tag{4.10}$$

$$\upsilon = \frac{D_e K}{kR_p} \tag{4.11}$$

where U is the dimensionless contact time parameter, V is the dimensionless bed length parameter and υ is the dimensionless film resistance parameter. Equation 4.8 gives exact solution within 1% error range when V values are larger than 50 (Yang, 1987). The parameters used in this study give V values to be much greater than 50 so that Equation 4.8 is used in order to predict the breakthrough curves at the outlet of the column.

4.1.2 Axial Dispersion

Axial dispersion coefficient was expressed in terms of Peclet number and the following equations were used to determine the axial dispersion (Yang, 1987):

$$D_L = \frac{2R_p\mu}{(Pe)\rho} \tag{4.12}$$

Peclet number was found from the correlation of Reynolds and Schmidt numbers:

$$\frac{1}{Pe} = \frac{0.3}{(\mathrm{Re})(Sc)} + \frac{0.5}{1+3.8/(\mathrm{Re})(Sc)} \tag{4.13}$$

when $0.008 < \mathrm{Re} < 400$,

$0.28 < \mathrm{Sc} < 2.2$,

$0.4 < \varepsilon < 0.5$

Reynolds number (Re) and Schmidt number (Sc) can be calculated by using the following equations:

$$\mathrm{Re} = \frac{D_p u \rho}{\mu} \tag{4.14}$$

$$Sc = \frac{\mu}{\rho D_m} \tag{4.15}$$

Molecular diffusivity (D_m) can be calculated for methyl chloride and nitrogen at a specified temperature and interstitial velocity (u) can also be calculated from the specified volumetric flow rate and bed porosity. Density (ρ) and viscosity (μ) of air is also found from literature at 1 atmosphere.

4.1.3 Effective Diffusivity

There are four types of macropore diffusion mechanisms: Molecular, Knudsen, Surface and Poiseuille. The type of diffusion changes depending on the pore diameter and the mean free path. When the pore diameter is relatively smaller than the mean free path, Knudsen diffusion occurs. In this type of diffusion, the collision between molecules to the pore wall is more frequently than the collision between the molecules. This occurs when

adsorbents have small pore sizes or at low pressures. Pore size and the mean molecular velocity are important factors in diffusion.

On the other hand, when the intermolecular collision is more frequently than collision between the molecules and the pore wall, Molecular diffusion occurs. For molecular diffusion temperature has more effect on the diffusion than for Knudsen diffusion.

Surface diffusion occurs when adsorption on to the pore wall is significantly large. The effect of surface diffusion increases when the adsorbates are larger and heavier.

Poiseuille occurs when there is a pressure difference between the two ends of the pores. At higher pressures and at larger pore sizes the importance of Poiseuille flow increases. For the case of modeling trace components' adsorption, the pressure at macropores is very low; therefore, Poiseuille flow has a negligible effect on effective diffusivity. Therefore, the effective diffusivity can be written as:

$$\frac{1}{D_e} = \frac{\tau_p}{D_m} + \frac{1}{\frac{D_k}{\tau_p} + \frac{1-\varepsilon_p}{\varepsilon_p}\frac{D_s}{\tau_s}K} \tag{4.16}$$

Effective diffusivity was determined by combining molecular, Knudsen and surface diffusivities. Tortuosity coefficient for surface and pellet was assumed to be equal to each other and they are taken as 4. For molecular diffusivity equation 4.13 (Kauzmann, 1966) and for Knudsen equation 4.14 (Bird et.al., 1960) were used. For surface diffusivity was found by using graph for the empirical correlation between surface diffusivity and heat of adsorption found by Sladek et al.

$$D_m = \frac{0.0018583 * T^{3/2}\sqrt{\frac{1}{M_A} + \frac{1}{M_B}}}{\sigma_{AB} * \Omega} \tag{4.17}$$

$$D_k = 9700 r_o \sqrt{\frac{T}{M}} \tag{4.18}$$

4.1.4 Mass transfer Coefficient

Interparticle mass transfer coefficient k can be calculated from Sherwood number (Yang, 1987).

$$Sh = \frac{kD_p}{D_m} = 2.0 + 1.1(Sc)^{0.33}(\mathrm{Re})^{0.6} \tag{4.19}$$

4.2 RESULTS

The parameters that were used for modeling adsorption of methyl chloride are shown in Table 4.1. For this study, the adsorbents that were considered were HiSiv-3000 and SBA-15. The Henry's Law constants that were used in the calculations were taken from Toreci et. al. (2003). Macropore radius of HiSiv-3000 was calculated by taking the crystal size as 0.074 mm. It is assumed that crystals are closely packed. For SBA-15, mesopore size was taken because of its characterization.

In the calculations of effective diffusivity it was observed that surface diffusion has negligible effect on overall diffusion. The same effect was also found for axial dispersion. Axial dispersion constant was found to be very low therefore axial dispersion term was neglected.

Table 4.1: Parameter values that are used in the modeling

Parameters	**HiSiv-3000**	**SBA-15**
Bed length, L (cm)	50	50
Bed diameter, d_c (cm)	5	5
Void fraction, ε	0.39	0.39
Pellet radius, R_p (cm)	0.1049	0.1049
Macropore radius, r_0 (cm)	0.0015	0.000425

4.2.1 EFFECT OF TEMPERATURE

It was observed that as temperature increases the adsorption capacity of both HiSiv-3000 and SBA-15 decreases. Figures 4.3 and 4.4 show the breakthrough curves of HiSiv-3000 and SBA-15, respectively at different temperatures for 0.5 m long column at 10 lt/min flow rate. As it can be seen from these figures, the increase in temperature causes a decrease in the breakthrough time. At temperature 40°C, bed gets saturated with the adsorbate at much longer time than at 60°C and 80°C; because of larger adsorption capacity at that temperature. When HiSiv-3000 results are compared to SBA-15 results, it can be seen that under the same conditions, HiSiv-3000 breaks through much earlier because of its lower adsorption capacity.

As temperature decreases the diffusion coefficient decreases which cause the tailing in the curvature. Since the breakthrough curves are in S-shape, the curvature in S-shape increases as tailing occurs.

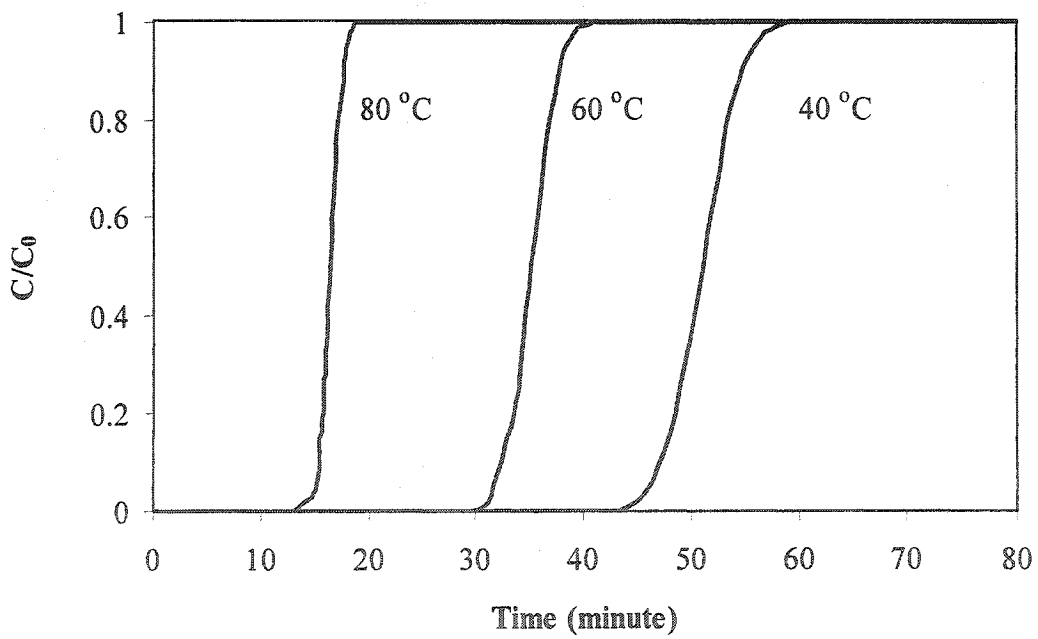

Figure 4.3: Breakthrough curves for methyl chloride adsorption with HiSiv-3000 at different temperatures when bed length is 0.5 m and inlet flow rate is 10 lt/min

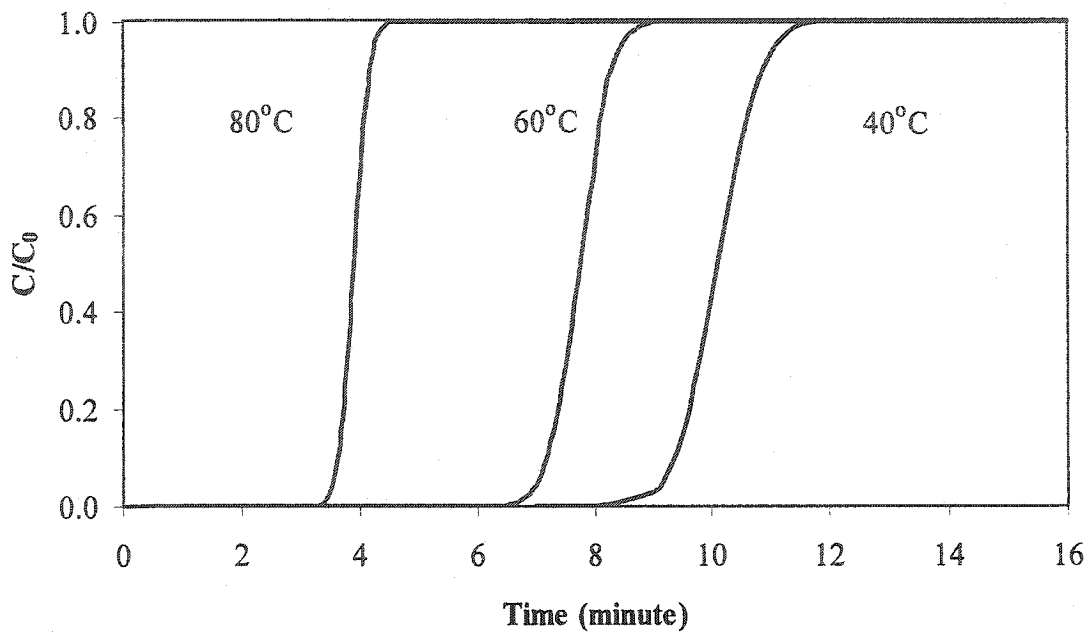

Figure 4.4: Breakthrough curves for methyl chloride adsorption with SBA-15 at different temperatures when bed length is 0.5 m and inlet flow rate is 10 lt/min

4.2.2 EFFECT OF BED LENGTH

From Figure 4.5 shows breakthrough curves with HiSiv-3000 for different bed lengths at 40 °C and 10 lt/min, it is observed that as the length of the bed increases the breakthrough time increases. This was expected since the amount of adsorbent in the column increases as the bed length increases. Breakthrough time of 1 meter long bed is twice as much as that of 0.5 meter long bed as breakthrough time of 2 meter long bed is as twice as that of 1 meter long bed. The same effect was also observed from the calculations of breakthrough curves of SBA-15 (Figure 4.6) with higher breakthrough timesx.

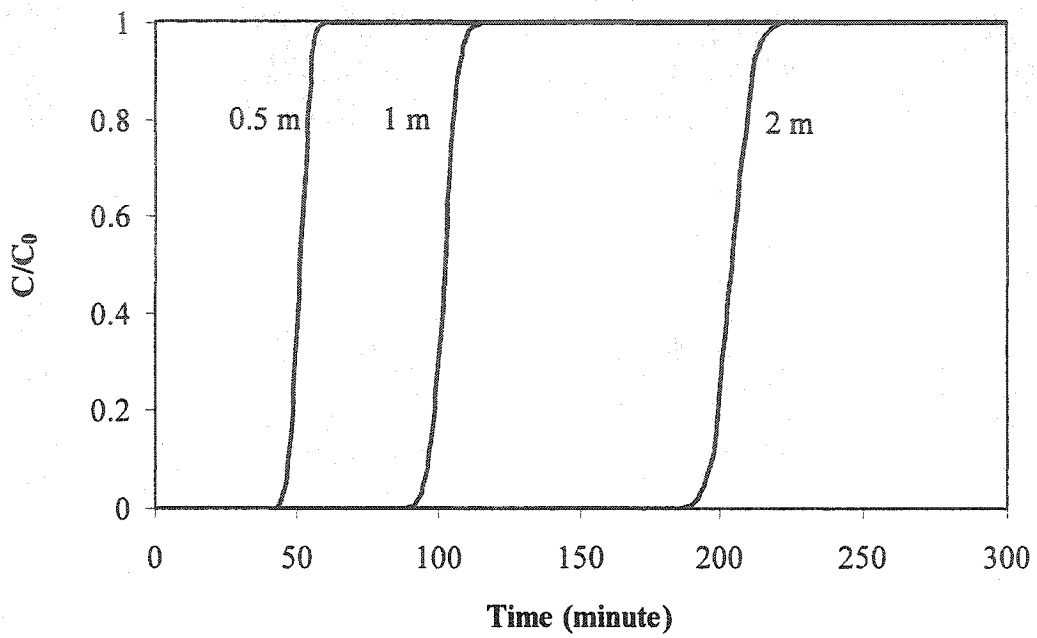

Figure 4.5: Breakthrough curves for methyl chloride adsorption with HiSiv-3000 at different bed lengths when temperature is 40°C and inlet flow rate is 10 lt/min

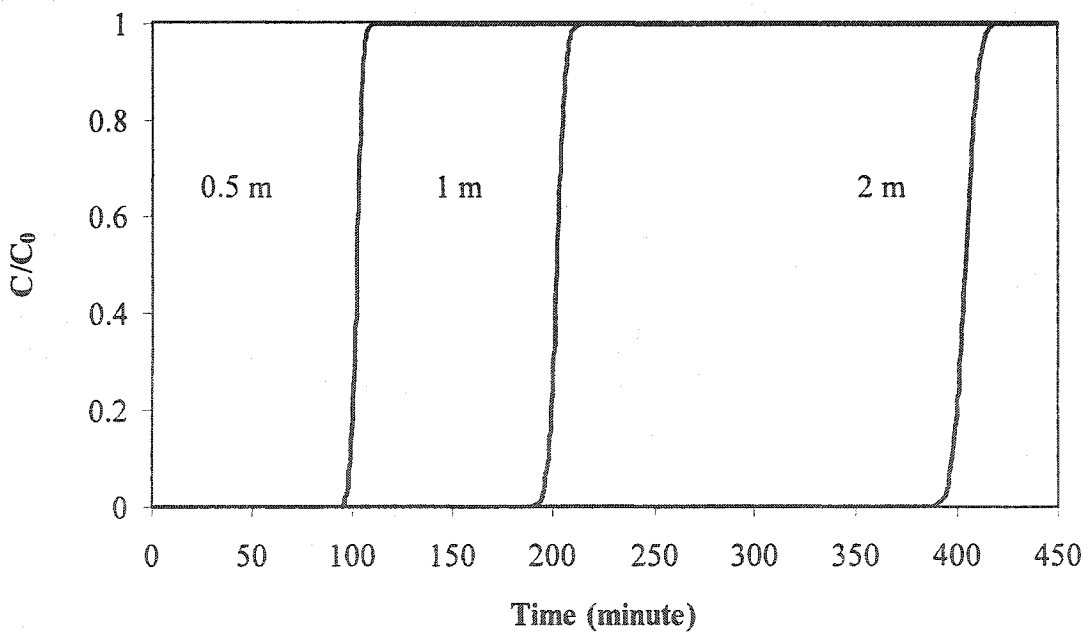

Figure 4.6: Breakthrough curves for methyl chloride adsorption with SBA-15 at different bed lengths when temperature is 40°C and inlet flow rate is 10 lt/min

4.2.3 EFFECT OF INLET FLOW RATE

The effect of inlet flow rate on breakthrough curve was shown in Figures 4.7 and 4.8 for HiSiv-3000 and SBA-15 respectively at 40 °C for 0.5 m column. It was observed that as inlet flow rate increases the breakthrough time decreases. The result is expected, since the amount of adsorbate going through the column per time increases with the increase in the inlet flow rate. As the flow rate decreases it was observed that the curvature increases. This is expected because as flow rate decreases overall mass transfer resistance increases; thus the system becomes more sluggish and more curvature in S-shape occurs in breakthrough curves.

Another observation is that, increasing the flow rate 3 times causes decrease of breakthrough time 3 times. Breakthrough time of 1lt/min is 3 times as longer as breakthrough time when the inlet flow rate is 3 lt/min. The same result is seen for 3 lt/min and 10 lt/min cases as well.

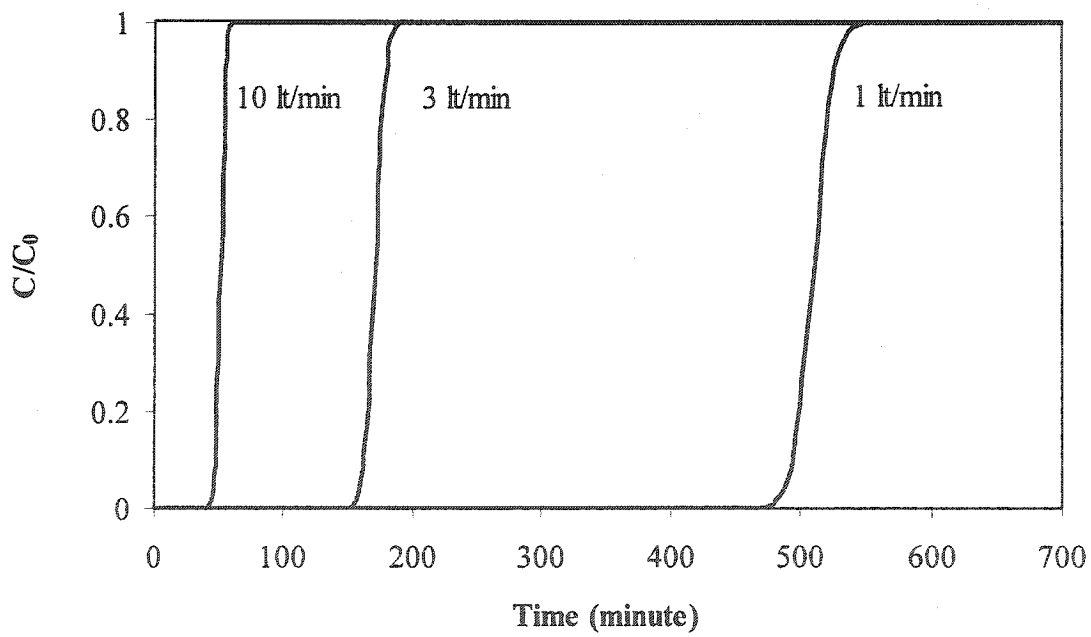

Figure 4.7: Breakthrough curves for methyl chloride adsorption with HiSiv-3000 at different inlet flow rates when temperature is 40°C and bed length is 0.5 m

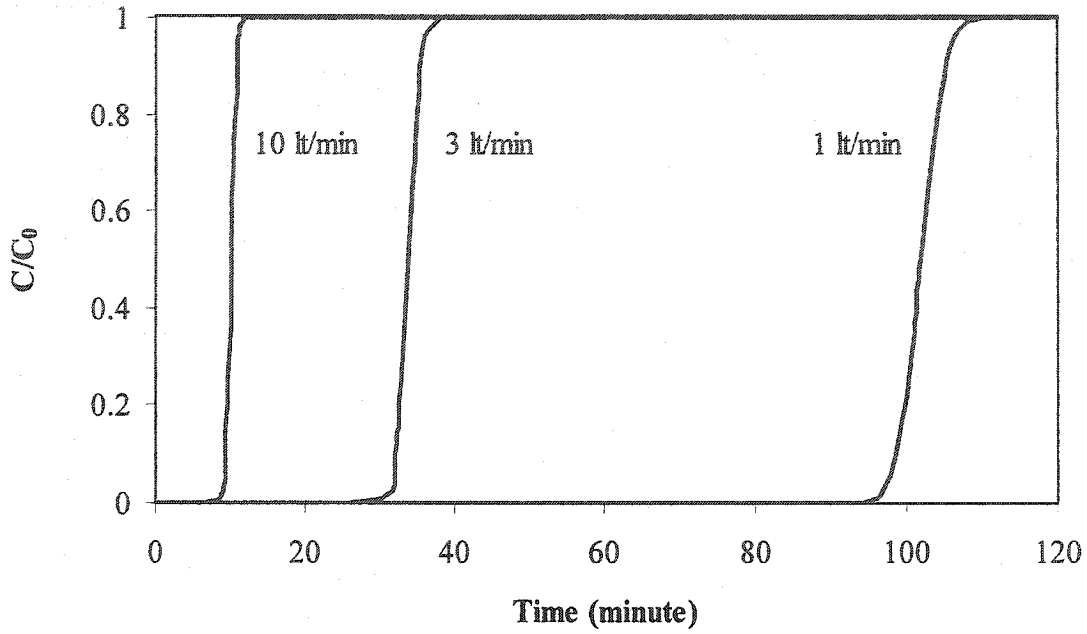

Figure 4.8: Breakthrough curves for methyl chloride adsorption with SBA-15 at different inlet flow rates when temperature is 40°C and bed length is 0.5 m

4.2.4 EFFECT OF ADSORBENT TYPE

Figure 4.9 shows the breakthrough curves of methyl chloride adsorption in a pressure swing adsorption column with HiSiv-3000 and SBA-15 at different temperatures with inlet flow rate of 10 lt/min and column length of 0.5 m. The effect of different adsorbent at different temperatures can be seen very clearly in this figure. Breakthrough times of SBA-15 are much longer than that of HiSiv-3000. Breakthrough time of SBA-15 at 80 °C is not only greater than that of HiSiv-3000 at 80 °C but also that of HiSiv-3000 at 60 °C. This is caused by the adsorption capacity difference of these adsorbents. SBA-15 has greater methyl chloride adsorption capacity than HiSiv-3000 has at all temperatures studied.

It is observed that increase in the capacity twice causes the breakthrough time to increase twice which is also expected.

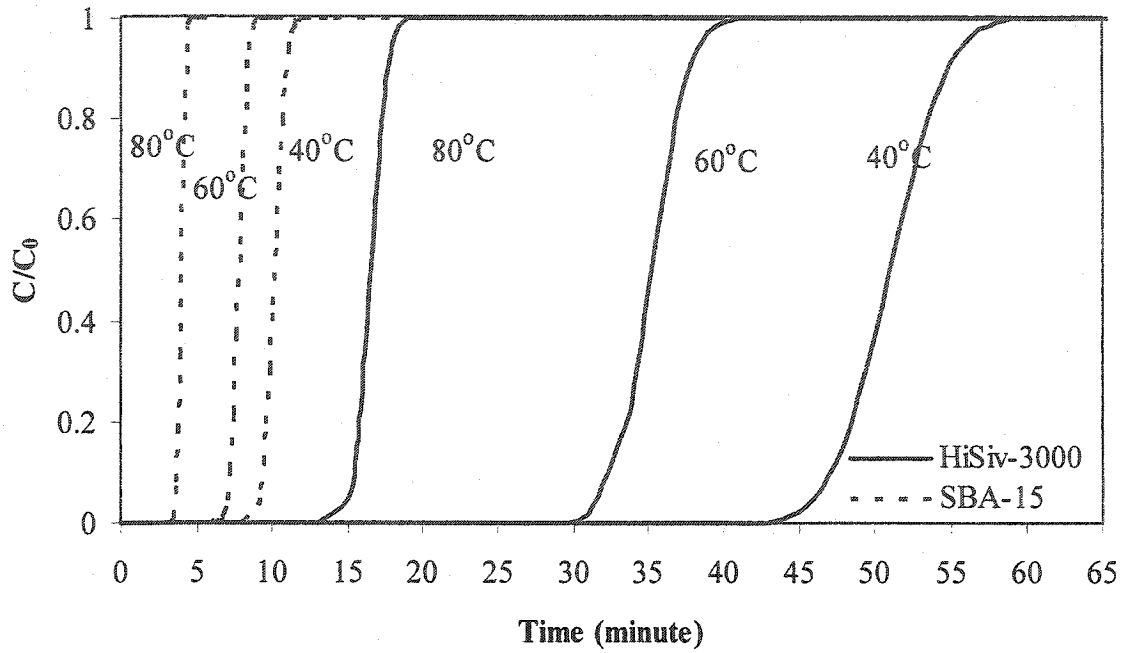

Figure 4.9: Breakthrough curves for methyl chloride adsorption with HiSiv-3000 and SBA-15 at different temperatures when bed length is 0.5 m and inlet flow rate is 10 lt/min

4.3 CONCLUSIONS

Several conclusions can be drawn from the modeling of methyl chloride adsorption:

- Increase in temperature causes decrease in breakthrough time since the capacities of adsorbents HiSiv-3000 and SBA-15 decrease as temperature increases.
- As bed length increases the breakthrough time increases because the amount of adsorbent in the bed increases as the bed length increases.
- The effect of increasing inlet flow rate is a decrease in the breakthrough time. More adsorbate per time passing through the column causes quick saturation of the adsorbent.
- Since the methyl chloride adsorption capacity of SBA-15 is greater than that of HiSiv-3000, the breakthrough times of SBA-15 are greater than those of HiSiv-3000.

4.4 NOMENCLATURE

C	Concentration of adsorbate in the column, mol cm^{-3}
C_o	Inlet concentration of adsorbate in the column, mol cm^{-3}
D_e	Effective diffusivity, $cm^2\ s^{-1}$
d_c	diameter of column, cm
D_k	Knudsen diffusivity, $cm^2\ s^{-1}$
D_L	Axial dispersion coefficient, $cm^2\ s^{-1}$
D_m	Molecular diffusivity, $cm^2\ s^{-1}$
D_p	Particle diameter, cm
D_s	Surface diffusivity, $cm^2\ s^{-1}$
K	Henry's Law constant, mol $kg^{-1}\ kPa^{-1}$
k	Mass transfer coefficient through gas film, m s^{-1}
L	length of the column, cm
M	Average of molecular weights of adsorbed components
M_A	Molecular weight of component A
M_B	Molecular weight of component B
Pe	Peclet number, dimensionless
q	Amount adsorbed, mol cm^{-3}
$\bar{q}$	Volume-average adsorbate concentration, mol cm^{-3}
Re	Reynolds number, dimensionless
R_p	Pellet radius, cm
r	Radius, cm
r_0	Pore radius, cm
Sh	Sherwood number, dimensionless
Sc	Schmidt number, dimensionless
T	Temperature, K
t	Time, s
U	Contact time parameter, dimensionless
u	Interstitial velocity, m s^{-1}

V Bed length parameter, dimensionless

z Distance in the bed from entrance, cm

Greek Letters

ε Intrapellet void fraction, dimensionless

ε_p Interpellet void fraction, dimensionless

μ Viscosity of air, kg $cm^{-1}s^{-1}$

ρ Density of air, kg cm^{-3}

σ_{AB} Constant in the Lennard-Jones potential-energy function for the pair AB

τ_p Tortuosity coefficient for particle

τ_s Tortuosity coefficient for surface

υ Film resistance parameter, dimensionless

Ω Constant in the Lennard-Jones potential-energy function for the pair AB, Å

4.5 REFERENCES

Bird, R. B., W.E. Steward and E.N. Lightfood, "Transport Phenomena", Wiley, New York (1960)

Chenu, M., A. Bouzaza, D. Wolbert and A. Laplanche, "Adsorption of Volatile Organic Compounds (VOC) Mixtures onto Activated Carbon. Experimental Study and Simulation of Multicomponent Adsorption", Environmental Technology, **19**, 1029-1038 (1998)

Kauzmann, W., "Kinetic Theory of Gases", Benjamin, New York (1966)

Lavanchy, A., R. Rebstein and F. Stoeckli, "Variable Pressure Adsorption and Desorption by Active Carbon Beds under PSA conditions: A Comparison of Models with Experimental Data", Pure & Appl. Chem., **65**, 2175-2179 (1993)

Ritter, J. A. and R. T. Yang, "Pressure Swing Adsorption: Experimental and Theoretical Study on Air Purification and Vapor Recovery", Ind. Eng. Chem. Res., **30**, 1023-1032 (1991)

Sladek, K. J., E. R. Gilliland and R. F. Baddour, Ind. Eng. Chem. Fundam., 13, 100 (1974)

Yang, R. T., "Gas Separation by Adsorption Processes", Butterworth, Massachusetts (1987)

Toreci, I., F. H. Tezel, Y. Yong and A. Sayari, "Adsorption of Methyl Chloride from Nitrogen by Using Zeolite and Mesoporous Molecular Sieve", to be submitted to the Journal of Adsorption Science and Technology (2003)

Pigorini G. and M. D. Le Van, "Equilibrium Theory for Pressure-Swing Adsorption. 4. Optimizations for trace Separation and Purification in Two-Component Adsorption", Ind. Eng. Chem. Res., 37, 2516-2528 (1998)

Malek A. and S. Farooq, "Effect of Velocity Variation on Equilibrium Calculations from Multicomponent Breakthrough Experiments", Chemical Engineering Science, **52**, 443-447 (1997)

Malek A. and S. Farooq, "Kinetics of Hydrocarbon Adsorption on Activated Carbon and Silica Gel", AIChE Journal, 43, 761-776 (1997)

Ruthven D. M. and S. Farooq, "Concentration of a trace Component by Pressure Swing Adsorption", Chemical Engineering Science, 49, 51-60 (1994)

Hasssan M. M., N. S. Raghavan, D. M. Ruthven and H. A. Boniface, AIChE Journal, 31, 2008 (1985)

CHAPTER 5

CONCLUSIONS

This thesis is composed of two papers given in chapter 2 and 3 and another chapter. The first paper is about adsorption of methyl chloride and nitrogen with HiSiv-3000 and SBA-15 and is given in the second chapter. The second paper is about the adsorption of methyl chloride with carbon cloth and mesocarbon and is given in the third chapter. The fourth chapter is about the modeling of breakthrough curves for vacuum swing adsorption process and the effect of some important parameters in modeling. At the end of each chapter the related conclusions are given. This chapter is the summary of thesis as a whole. The most important conclusions are summarized here.

In this study, experiments were performed to obtain adsorption isotherms of methyl chloride with HiSiv-3000, SBA-15, carbon cloth and mesocarbon and those of nitrogen with HiSiv-3000 and SBA-15 up to 1.6 kPa at temperatures between 40 and 80°C. Langmuir, Freundlich, Sips and Toth adsorption isotherm models were fitted to the experimental data. Adsorption isotheres were plotted by using pure component parameters of Toth isotherm model. Binary system predictions were made by using Extended Langmuir and Ideal Adsorbed Solution theories for HiSiv-3000 and SBA-15. Heats of adsorption, Henrys law constants and expected working capacities for PSA, VSA and TSA were calculated for all adsorbents studied. Methyl chloride adsorption for pressure swing adsorption was modeled by using the Rosen model for HiSiv-3000 and SBA-15 adsorbents. From this study several conclusions were drawn:

- Although it was observed that HiSiv-3000 has higher methyl chloride adsorption capacity at lower pressures than SBA-15, for nitrogen adsorption HiSiv-3000 has higher adsorption capacity.
- Mesocarbon's methyl chloride adsorption capacity was found to be the highest. The adsorbent which has second highest methyl chloride adsorption capacity was found to be carbon cloth.
- Toth and Sips models fit well to all the adsorption isotherm data. Langmuir gave better fit to HiSiv-3000 data for methyl chloride and nitrogen adsorption, and as well as for SBA-15 nitrogen adsorption data.
- On the other hand, Freundlich adsorption isotherm model fitted the adsorption isotherm data of methyl chloride with SBA-15 and mesocarbon.
- For all the adsorbents studied it was found that regeneration of these adsorbents is possible with vacuum only, there is no need for higher temperatures to degas the adsorbates from these adsorbents.
- From the adsorption isosteres it was observed that at lower pressures the temperature effect on adsorption is less than that at higher pressures for methyl chloride adsorption on HiSiv-3000, SBA-15 and carbon cloth whereas, temperature effect is similar for methyl chloride adsorption on mesocarbon in the pressure range studied.
- It was found from the prediction of binary system adsorption by Extended Langmuir and Ideal Adsorption Solution Theory that nitrogen adsorption is negligible in the binary system therefore separation of methyl chloride adsorption from nitrogen is possible by adsorption.
- Heat of adsorption of methyl chloride with carbon cloth is the lowest among all the adsorbents studied
- Heat of adsorption of methyl chloride with SBA-15, mesocarbon and carbon cloth are much less than that of HiSiv-3000, even less than the heat of adsorption of nitrogen with HiSiv-3000.

- Expected working capacities of mesocarbon for pressure swing adsorption, vacuum swing adsorption and temperature swing adsorption were found to be the highest among all the adsorbents studied.
- Vacuum swing adsorption and temperature swing adsorption were found to be two promising processes for separation of methyl chloride from air.
- It was found that mesocarbon is the best adsorbent in the literature to separate methyl chloride from air. It has several advantages: first of all, it has very high capacity of methyl chloride adsorption. Secondly, it can be regenerated easily by vacuum only. Finally, for vacuum swing adsorption and temperature swing adsorption it has very high expected working capacities. It is a better choice than using HiSiv-3000, SBA-15 and carbon cloth for methyl chloride adsorption and its separation from air.
- From the modeling of the breakthrough curves for vacuum swing adsorption process with Rosen model, it was found that breakthrough time increases as temperature decreases, or as the column length increases or as flow rate decreases.
- As final conclusion, it is found that since the adsorption capacity of SBA-15 for methyl chloride is greater than that of HiSiv-3000, the breakthrough time is greater for SBA-15 than for HiSiv-3000.

5.1 RECOMENDATIONS

For future studies several recommendations can be given:

- Adsorption of other volatile organic compounds should be performed with HiSiv-3000, SBA-15, carbon cloth and mesocarbon. Especially adsorption of other chlorinated compounds can give better understanding the of effect of chlorine in the compound on the capacity of adsorbents.
- Experimental binary isotherms should be performed to verify the precision of the predictions done by Extended Langmuir and Ideal Adsorbed Solution theories.

- Diffusion studies should be performed in order to understand adsorption process taking place in macropores and micropores of the adsorbents.
- Although some studies have been done with FEMLAB program for the simulation of adsorption in packed bed reactor, satisfactory results could not be reached. More detailed modeling and simulation should be done in order to understand the adsorption behavior of these adsorbents in packed bed reactors.
- Experiments on a pilot packed bed reactor can give the accuracy of the modeling of separation of methyl chloride from air.

APPENDICES

APPENDIX A: EXTRA FIGURES FOR ZSM-5 AND SBA-15 ADSORPTION

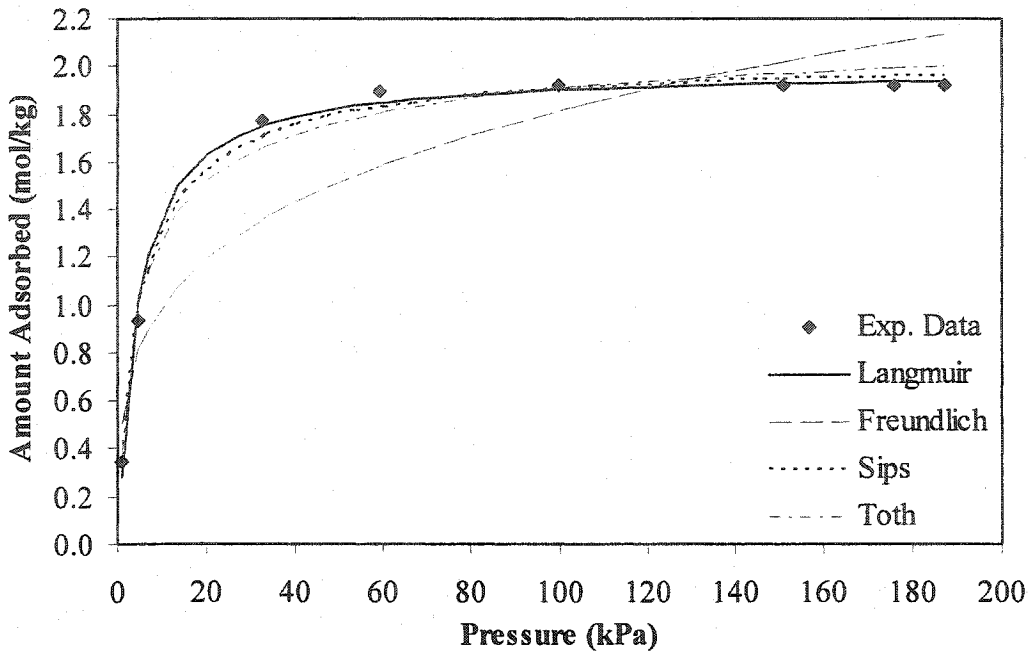

Figure A1: Adsorption isotherm of methyl chloride with HiSiv-3000 and fitted models at 40°C.

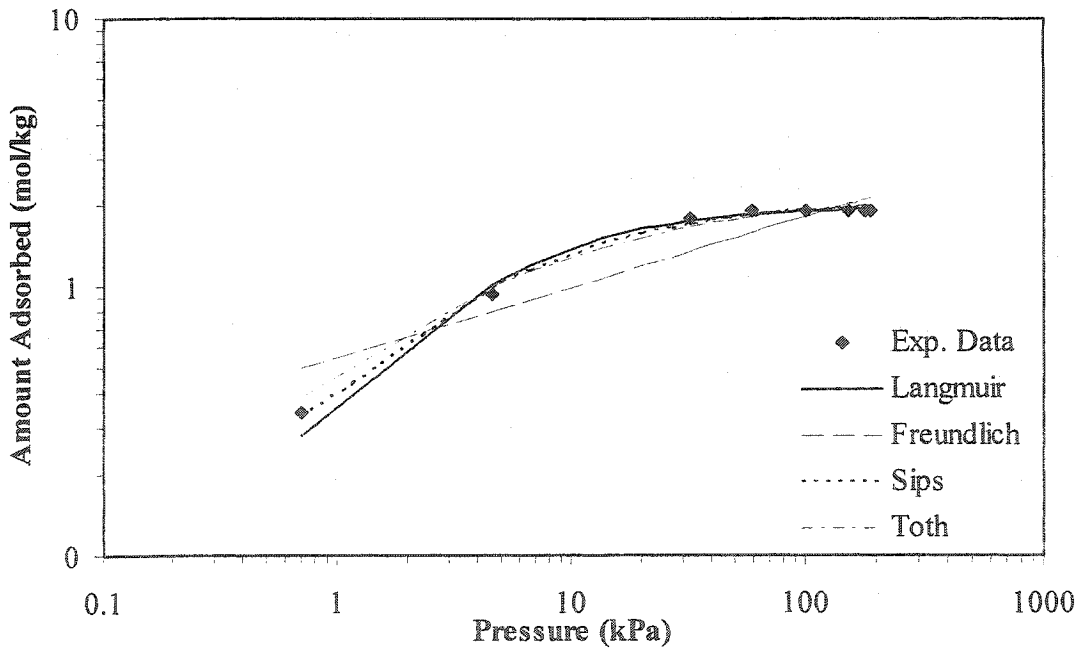

Figure A2: Adsorption isotherm of methyl chloride with HiSiv-3000 and fitted models at 40°C at logarithmic scale.

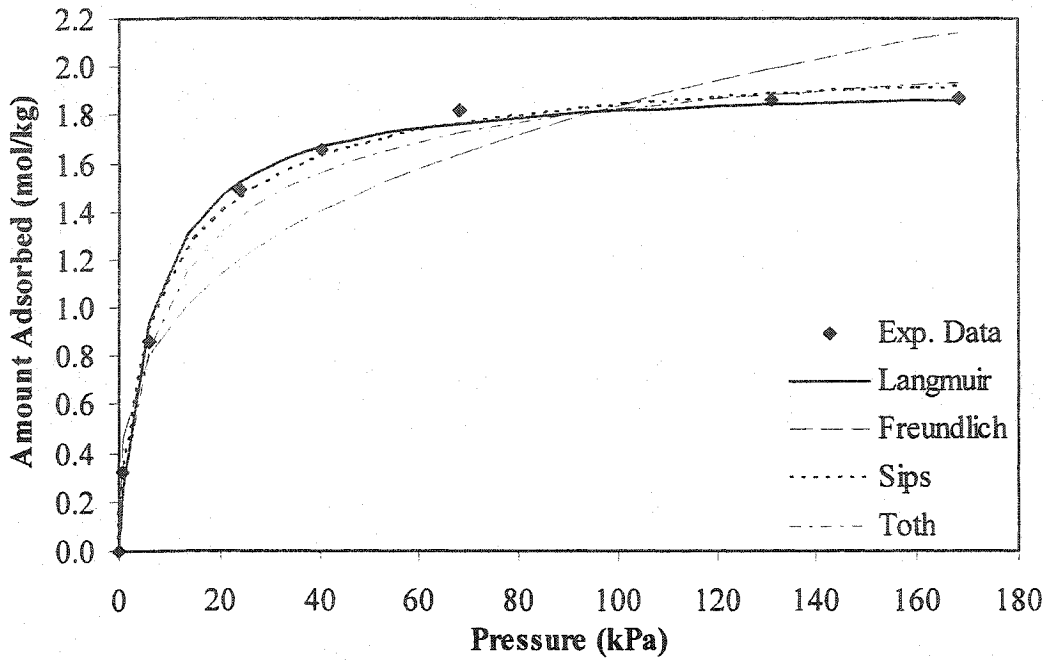

Figure A3: Adsorption isotherm of methyl chloride with HiSiv-3000 and fitted models at 60°C.

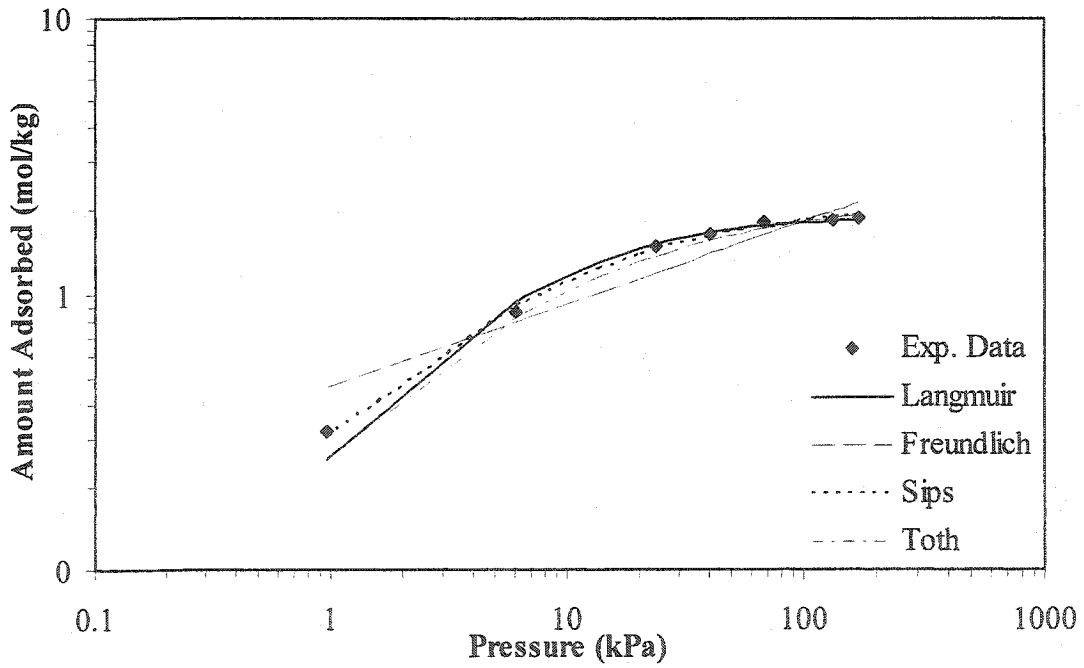

Figure A4: Adsorption isotherm of methyl chloride with HiSiv-3000 and fitted models at 60°C at logarithmic scale.

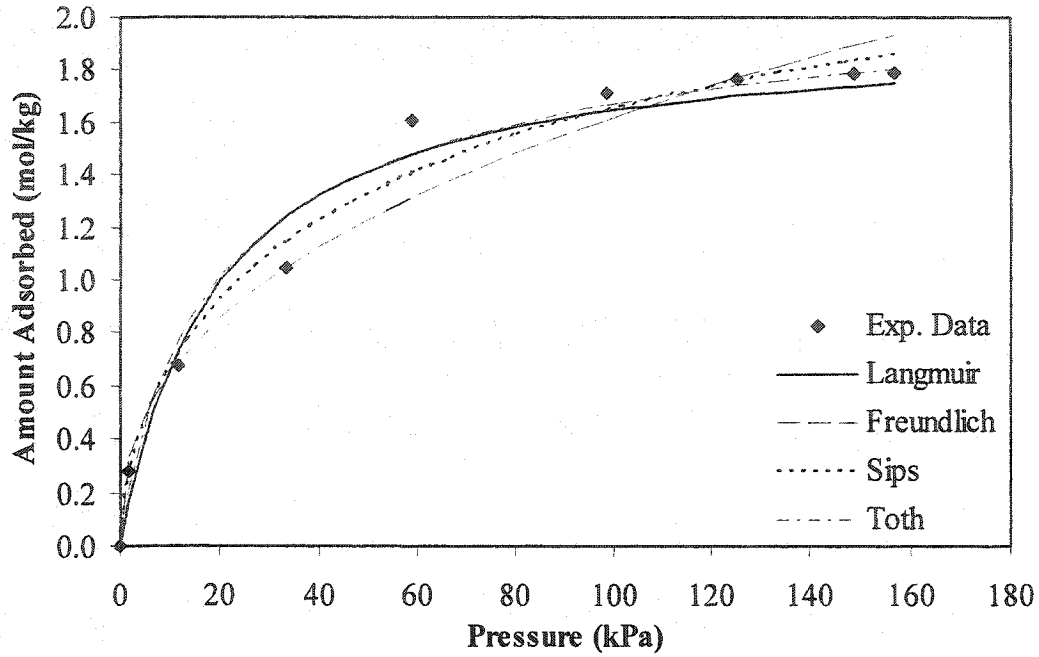

Figure A5: Adsorption isotherm of methyl chloride with HiSiv-3000 and fitted models at 80°C.

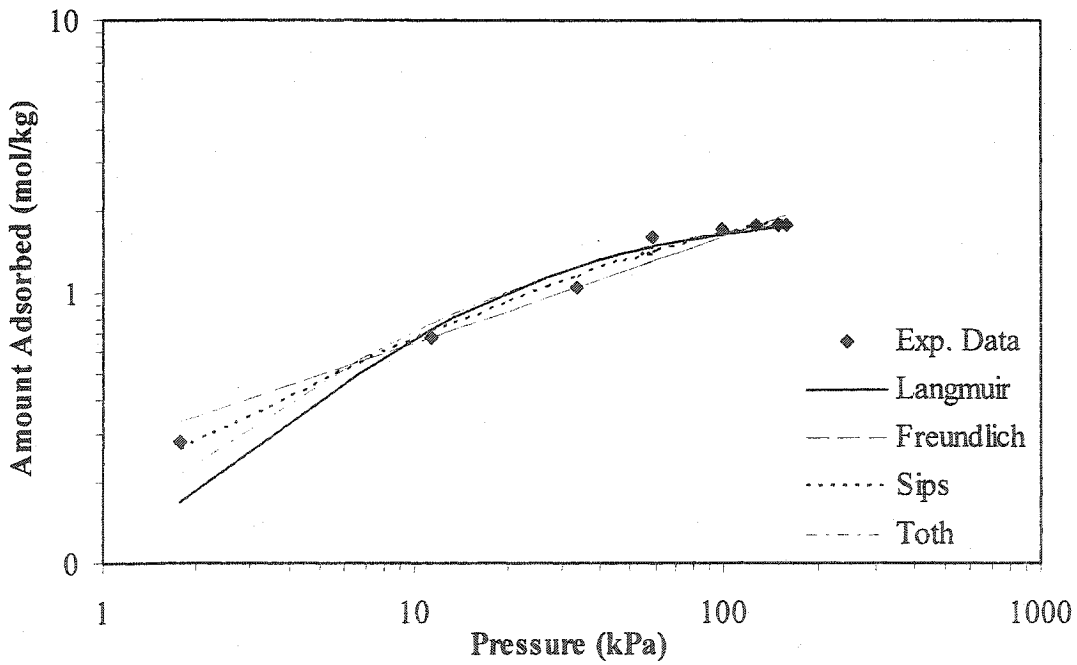

Figure A6: Adsorption isotherm of methyl chloride with HiSiv-3000 and fitted models at 80°C at logarithmic scale.

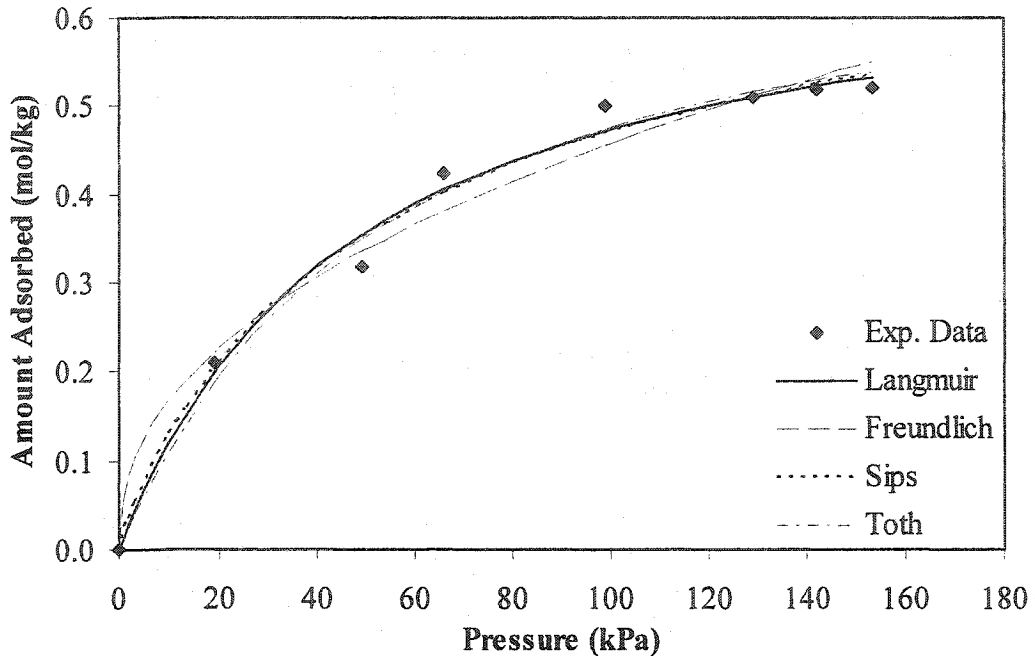

Figure A7: Adsorption isotherm of nitrogen with HiSiv-3000 and fitted models at 40°C.

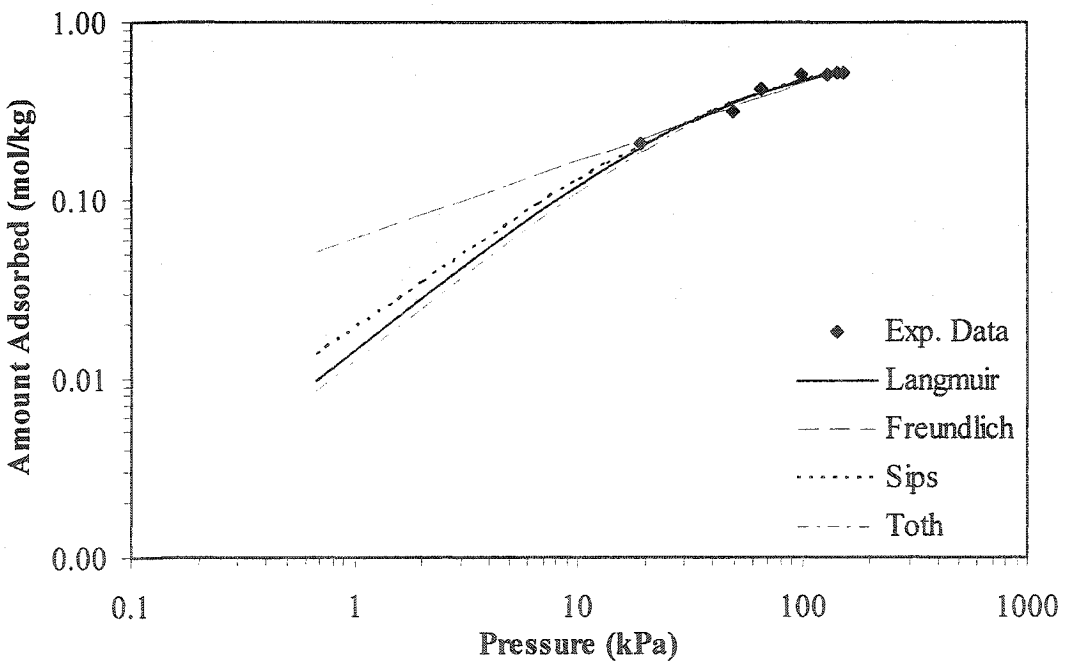

Figure A8: Adsorption isotherm of nitrogen with HiSiv-3000 and fitted models at 40°C at logarithmic scale.

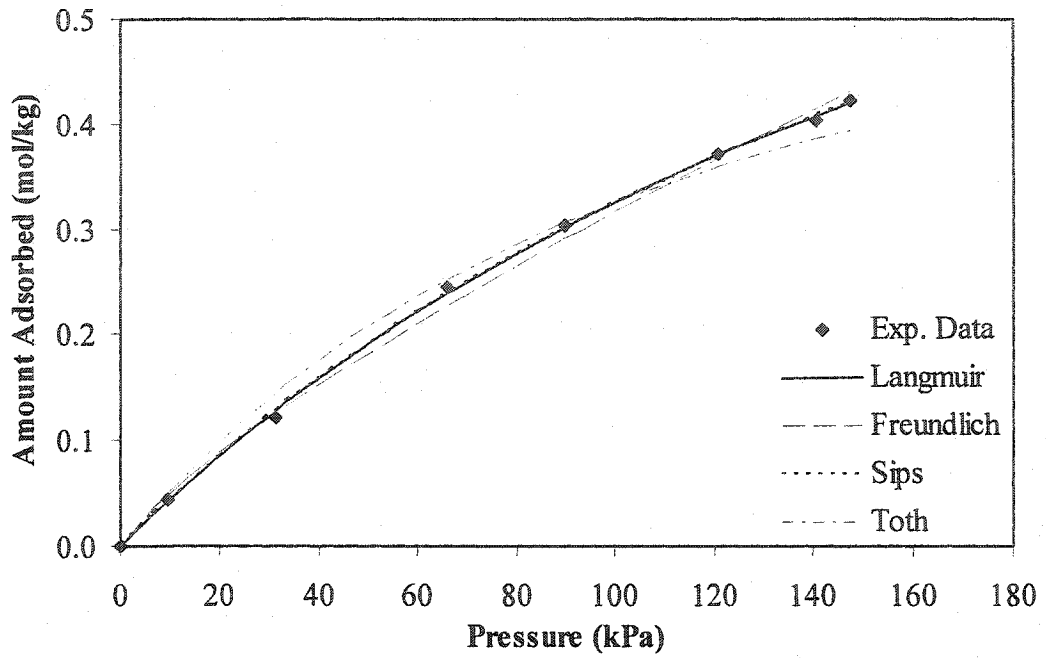

Figure A9: Adsorption isotherm of nitrogen with HiSiv-3000 and fitted models at 60°C.

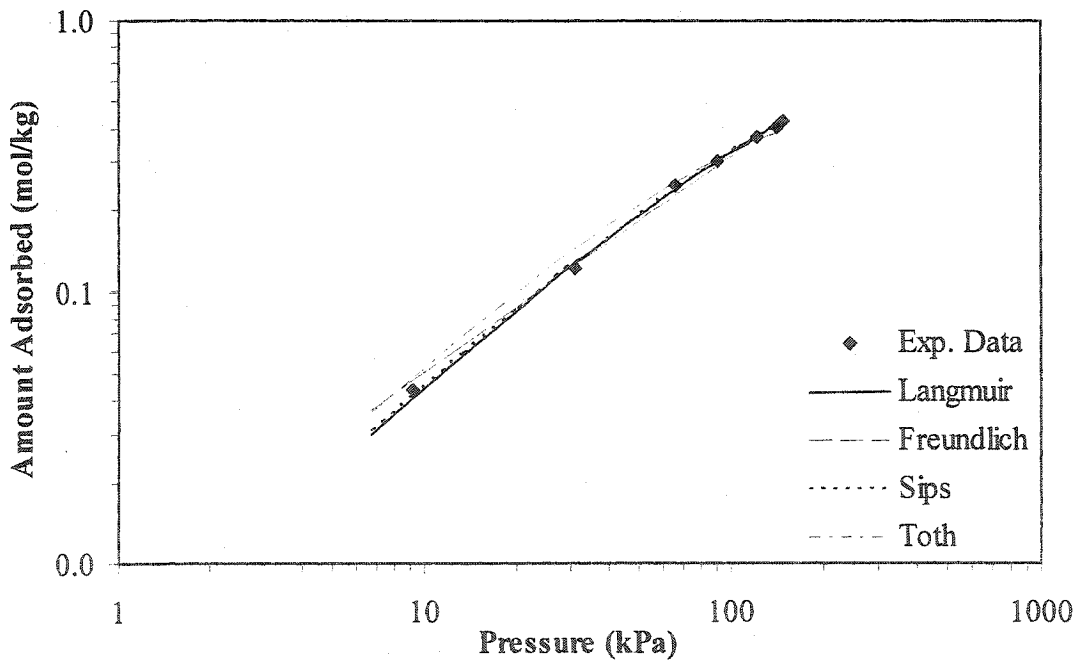

Figure A10: Adsorption isotherm of nitrogen with HiSiv-3000 and fitted models at 60°C at logarithmic scale.

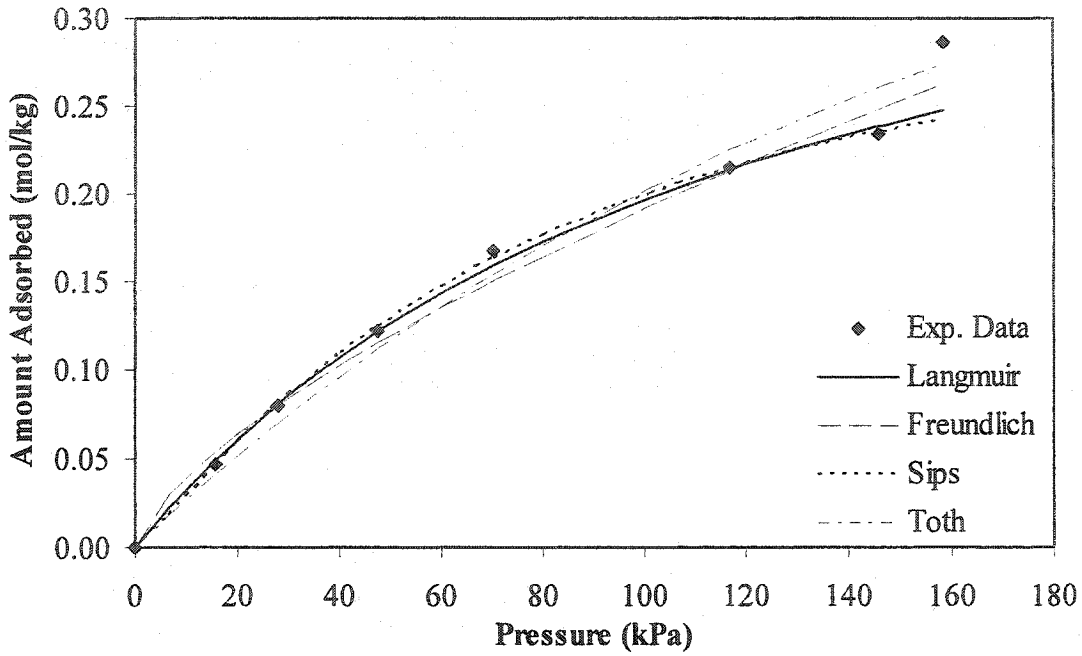

Figure A11: Adsorption isotherm of nitrogen with HiSiv-3000 and fitted models at 80°C.

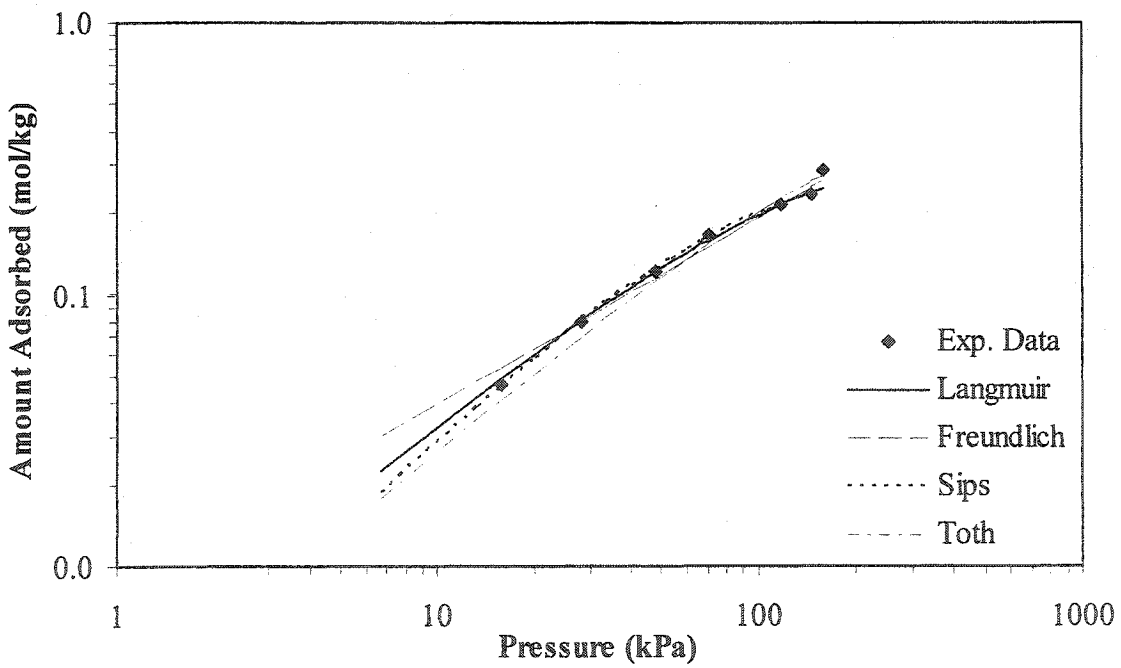

Figure A12: Adsorption isotherm of nitrogen with HiSiv-3000 and fitted models at 80°C at logarithmic scale.

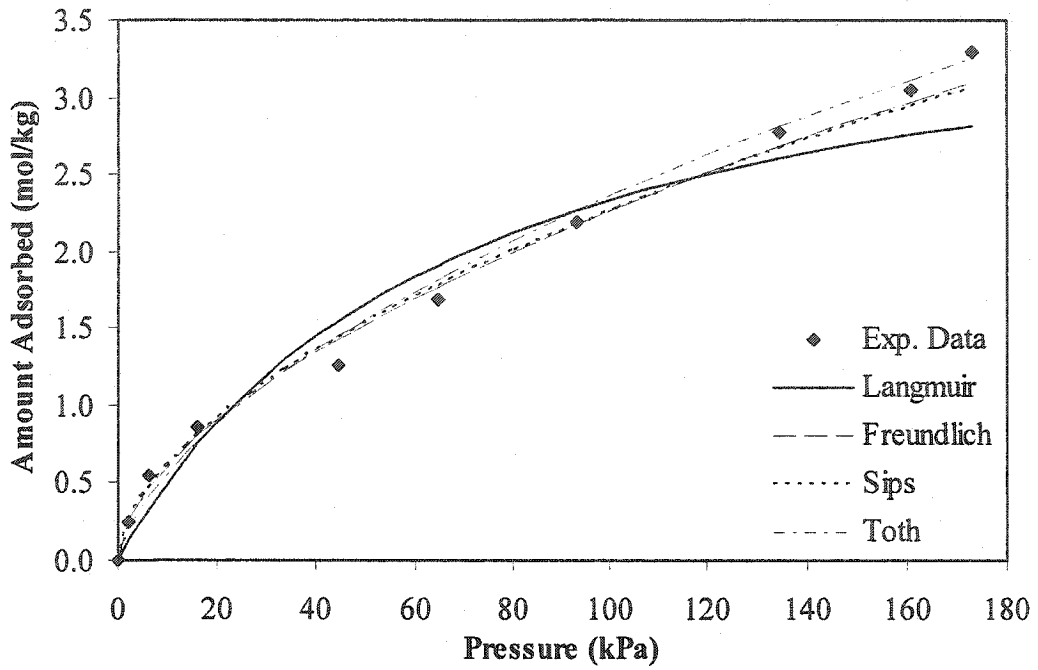

Figure A13: Adsorption isotherm of methyl chloride with SBA-15 and fitted models at 40°C.

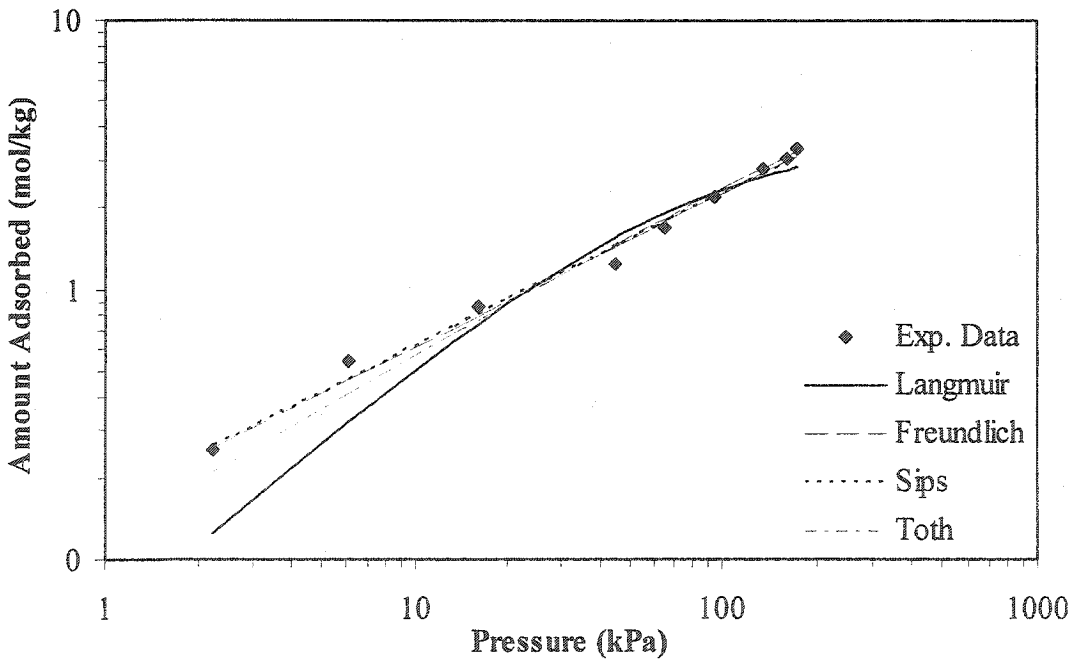

Figure A14: Adsorption isotherm of methyl chloride with SBA-15 and fitted models at 40°C at logarithmic scale.

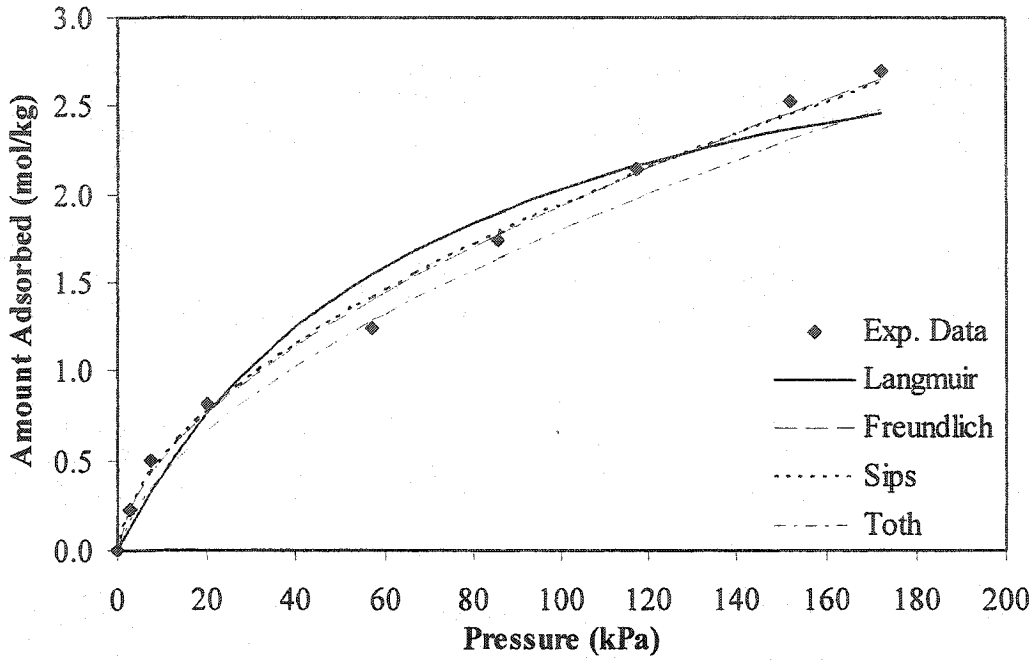

Figure A15: Adsorption isotherm of methyl chloride with SBA-15 and fitted models at 60°C.

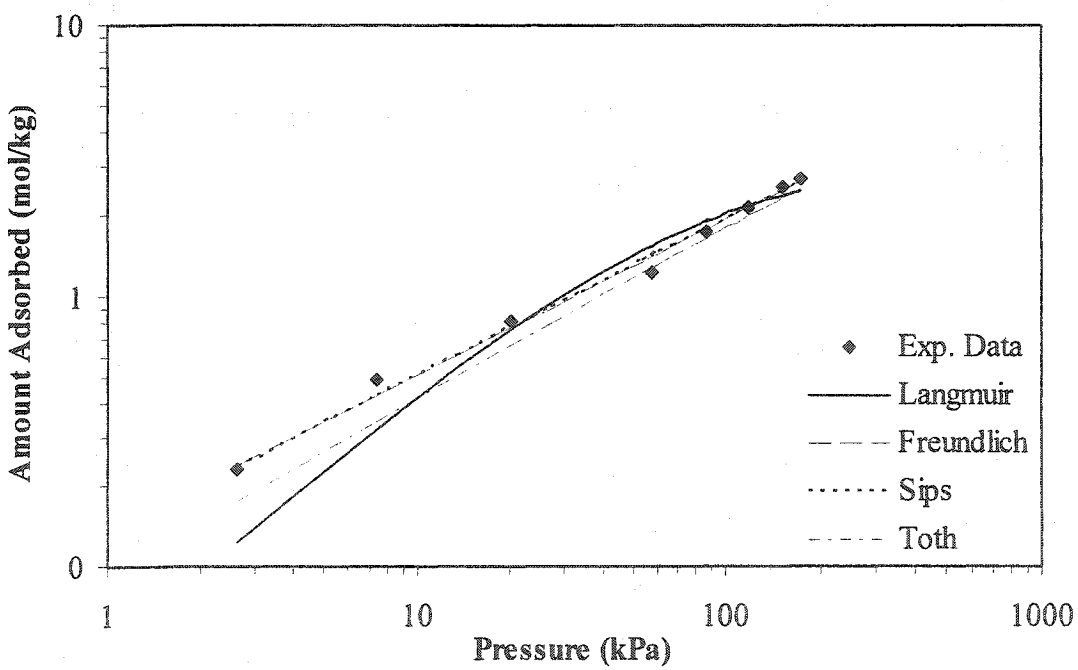

Figure A16: Adsorption isotherm of methyl chloride with SBA-15 and fitted models at 60°C at logarithmic scale.

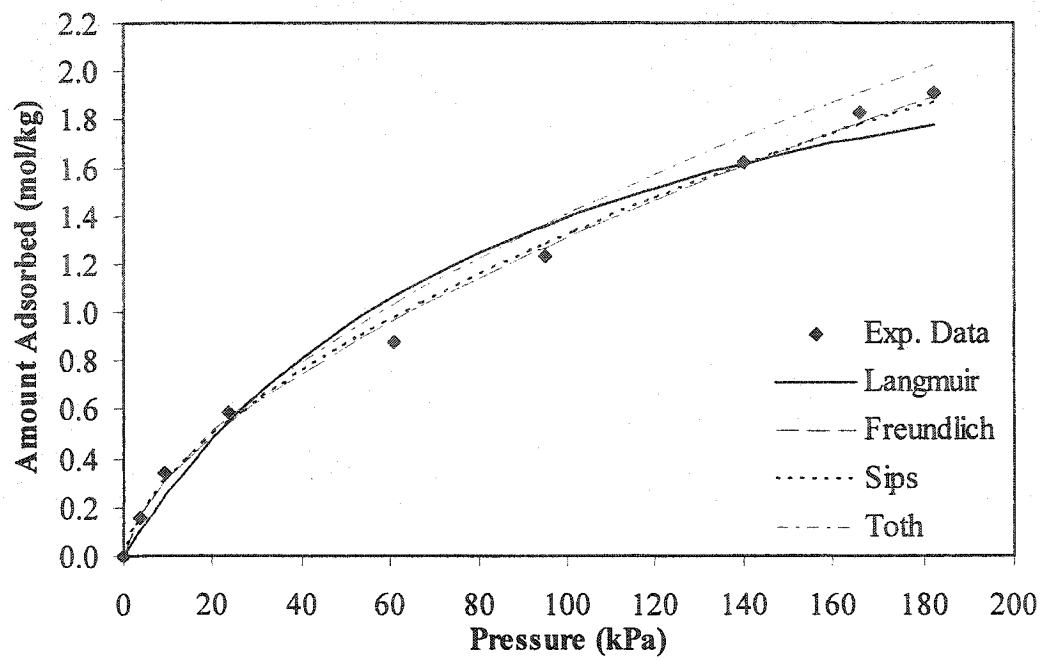

Figure A17: Adsorption isotherm of methyl chloride with SBA-15 and fitted models at 80°C.

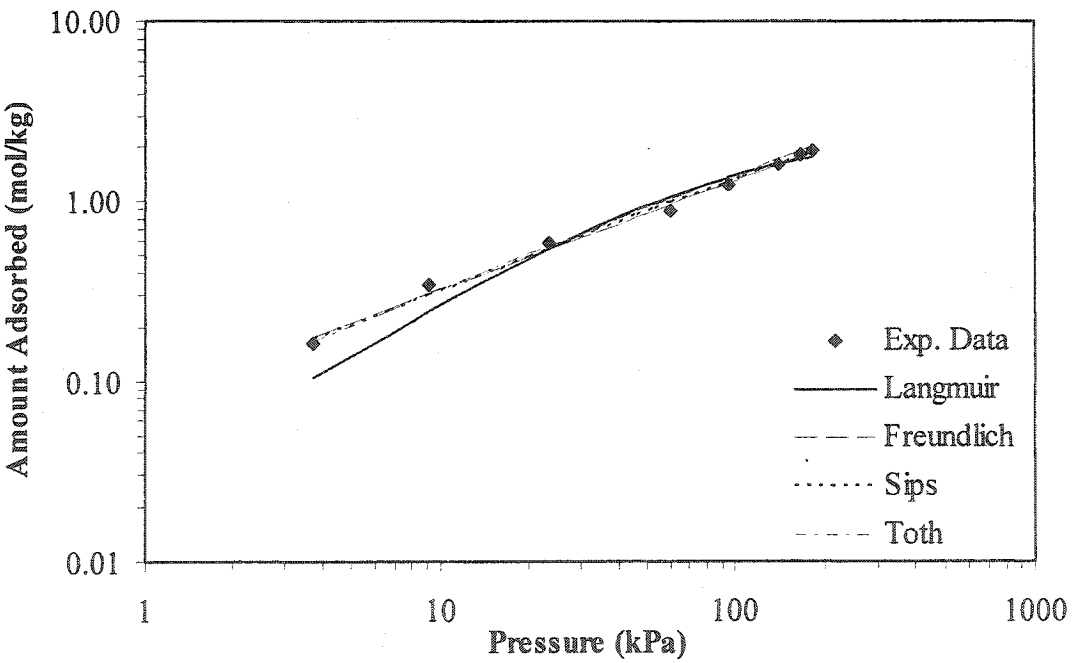

Figure A18: Adsorption isotherm of methyl chloride with SBA-15 and fitted models at 80°C at logarithmic scale.

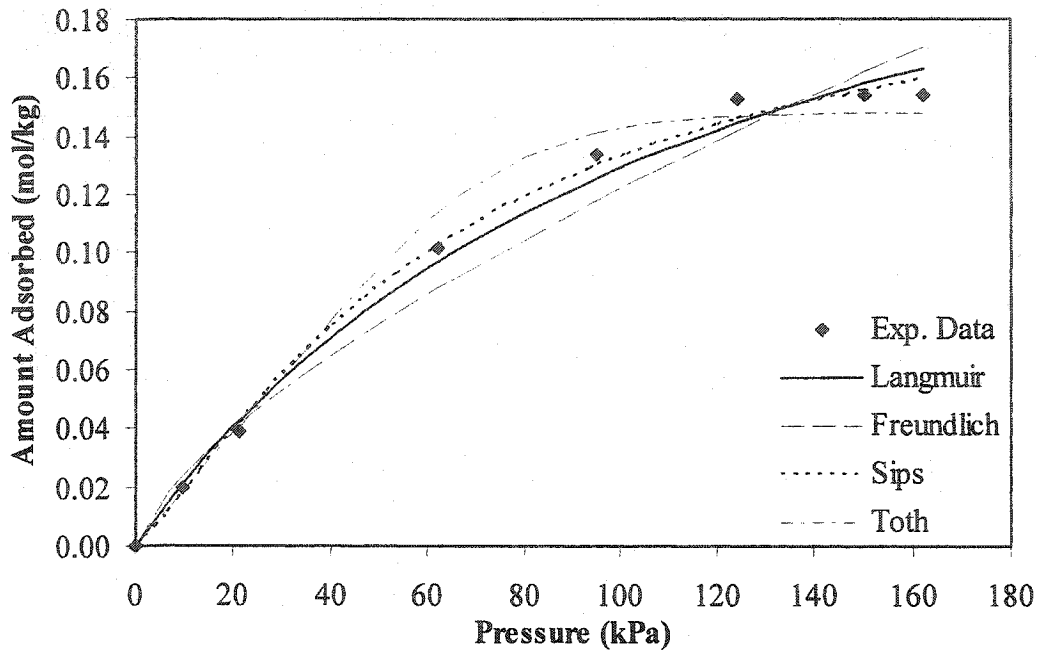

Figure A19: Adsorption isotherm of nitrogen with SBA-15 and fitted models at 40°C.

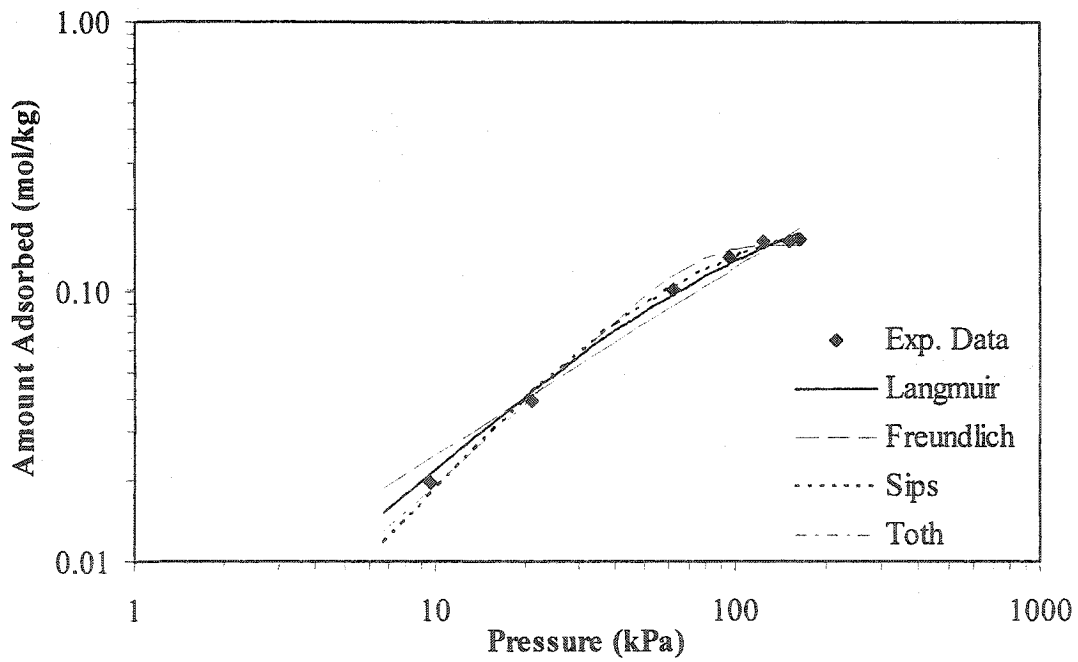

Figure A20: Adsorption isotherm of nitrogen with SBA-15 and fitted models at 40°C at logarithmic scale.

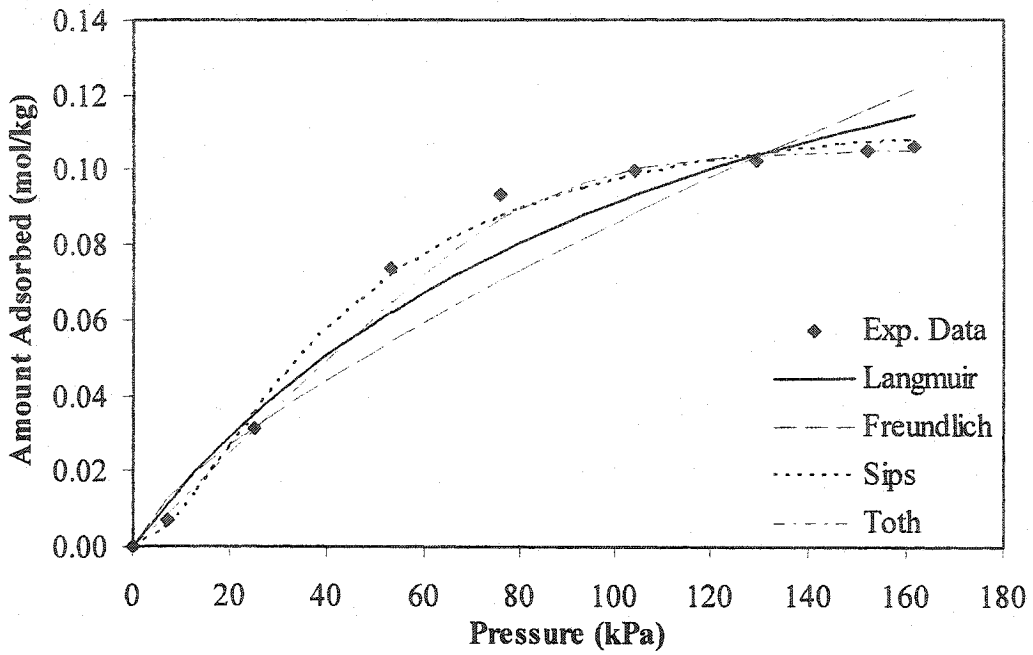

Figure A21: Adsorption isotherm of nitrogen with SBA-15 and fitted models at 60°C.

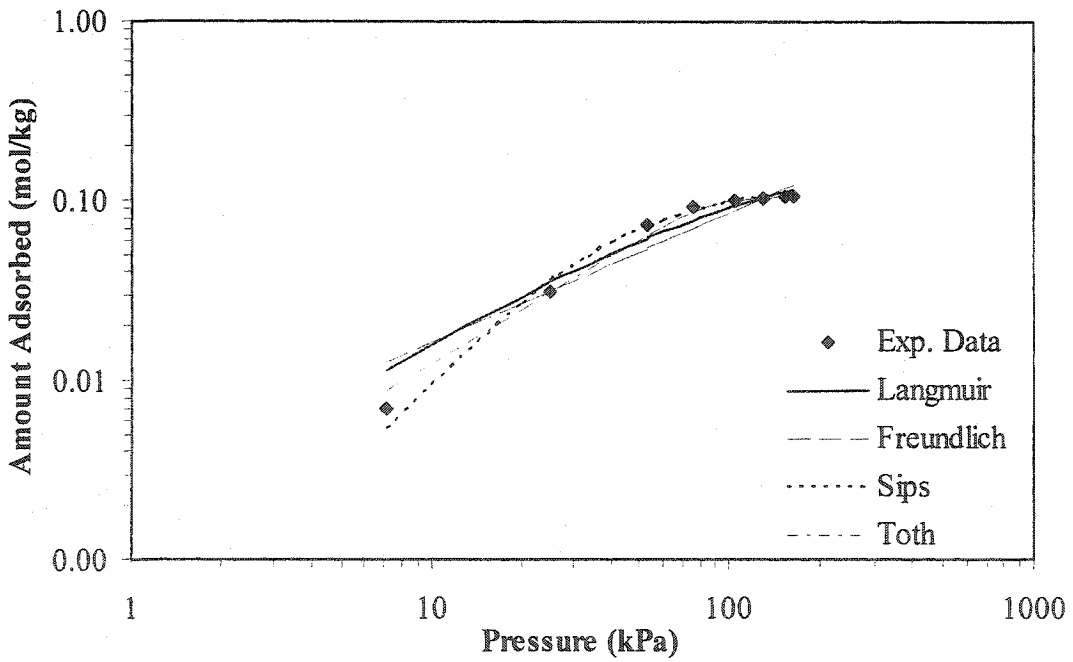

Figure A22: Adsorption isotherm of nitrogen with SBA-15 and fitted models at 60°C at logarithmic scale.

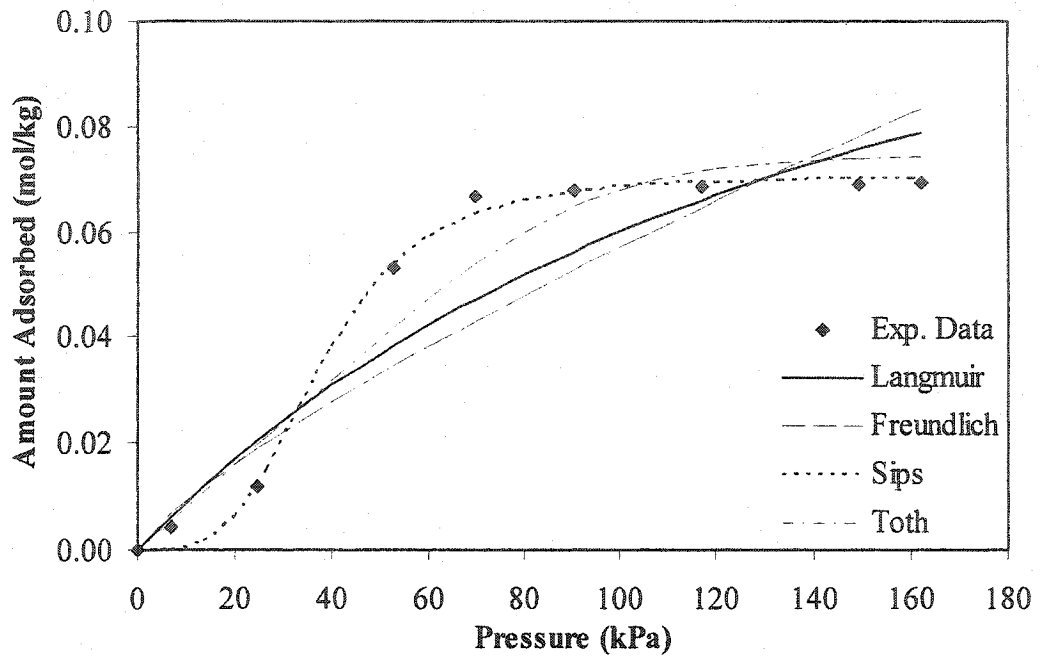

Figure A23: Adsorption isotherm of nitrogen with SBA-15 and fitted models at 80°C.

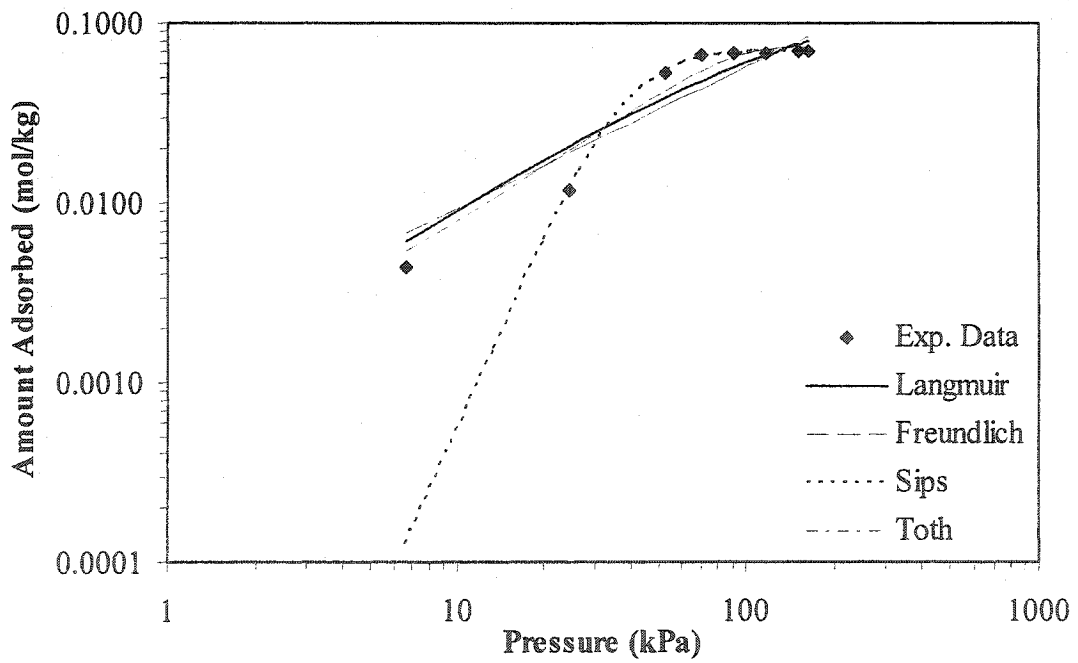

Figure A24: Adsorption isotherm of nitrogen with SBA-15 and fitted models at 80°C at logarithmic scale.

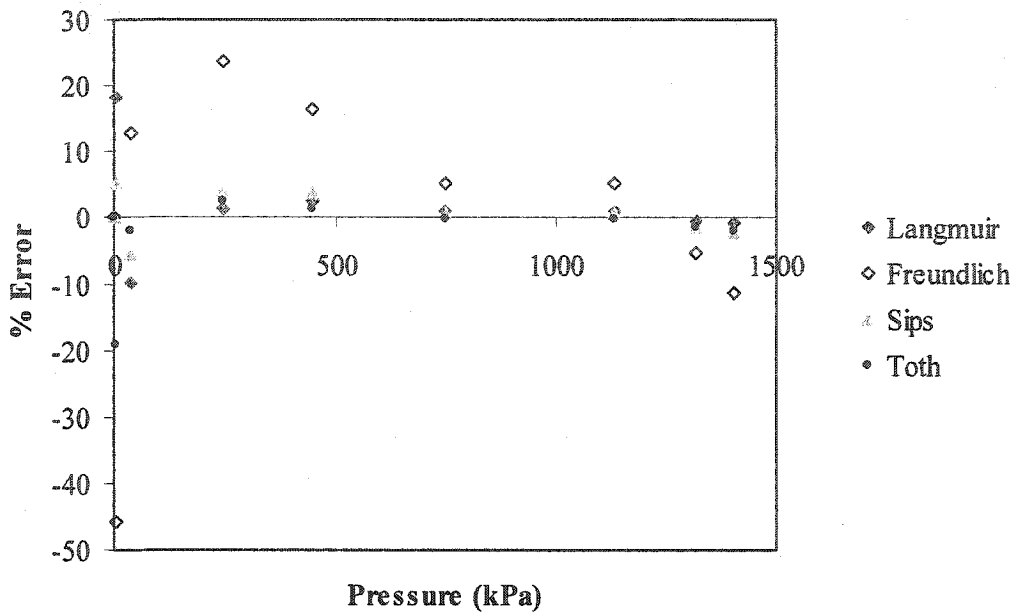

Figure A25: Residual plot for model fits of methyl chloride adsorption with HiSiv-3000 at 40 °C.

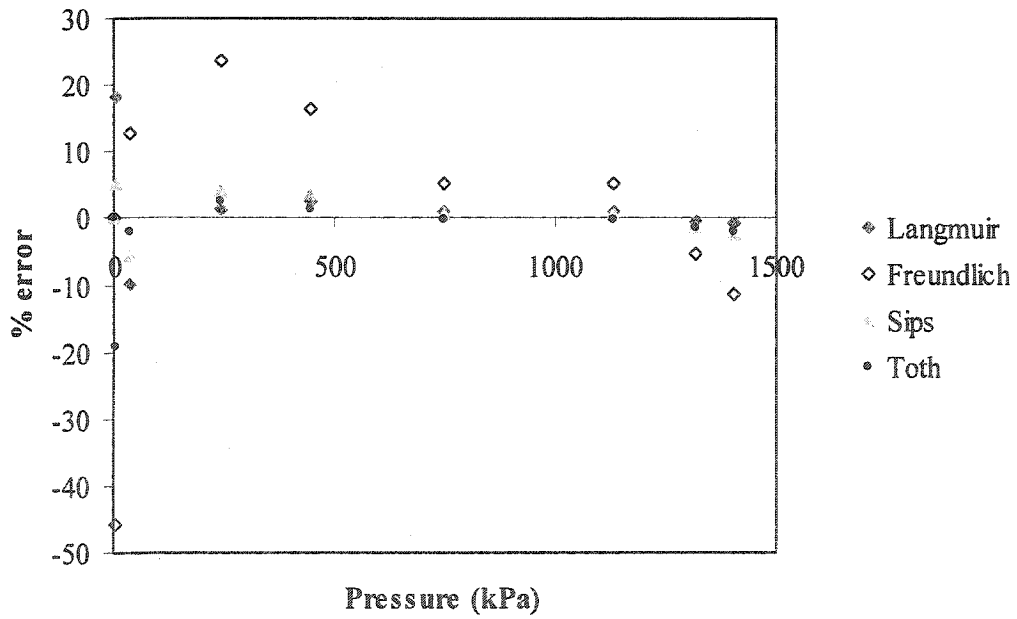

Figure A26: % Error of residual plot for model fits of methyl chloride adsorption with HiSiv-3000 at 40 °C.

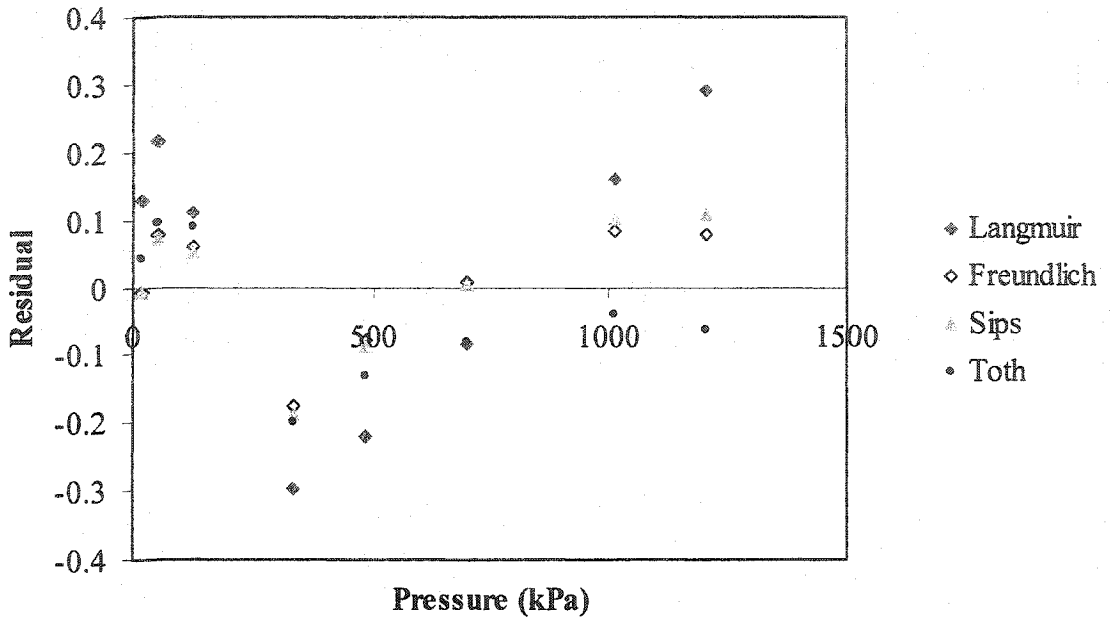

Figure A27: Residual plot for model fits of methyl chloride adsorption with SBA-15 at 40 °C.

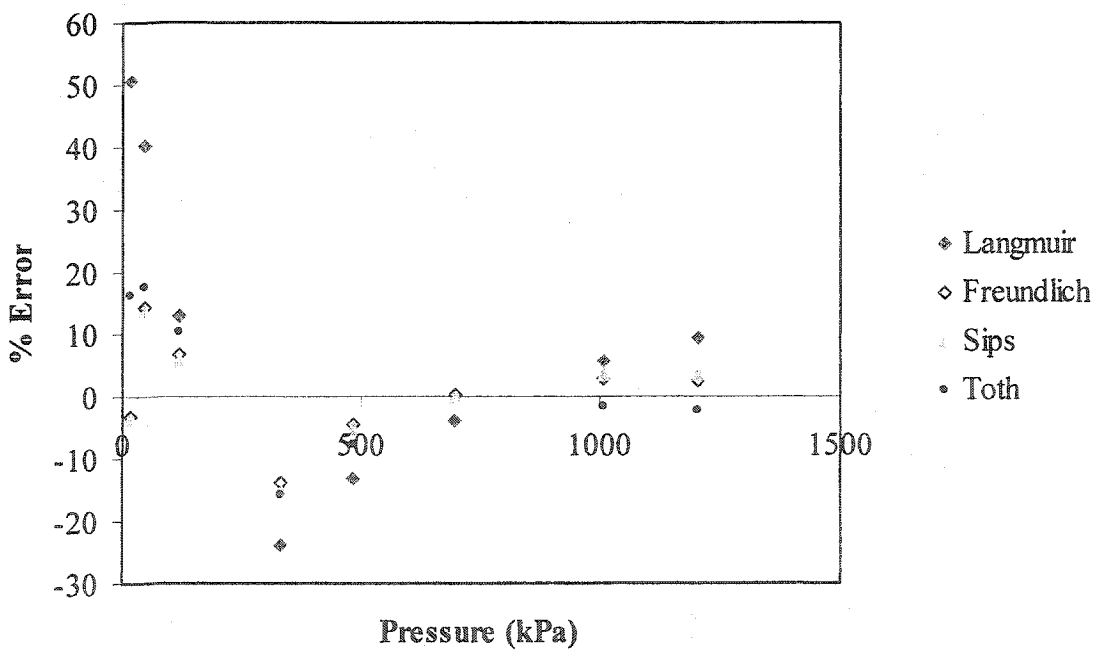

Figure A28: % Error of residual plot for model fits of methyl chloride adsorption with SBA-15 at 40 °C.

APPENDIX B: EXTRA FIGURES FOR CARBON CLOTH AND MESOCARBON ADSORPTION

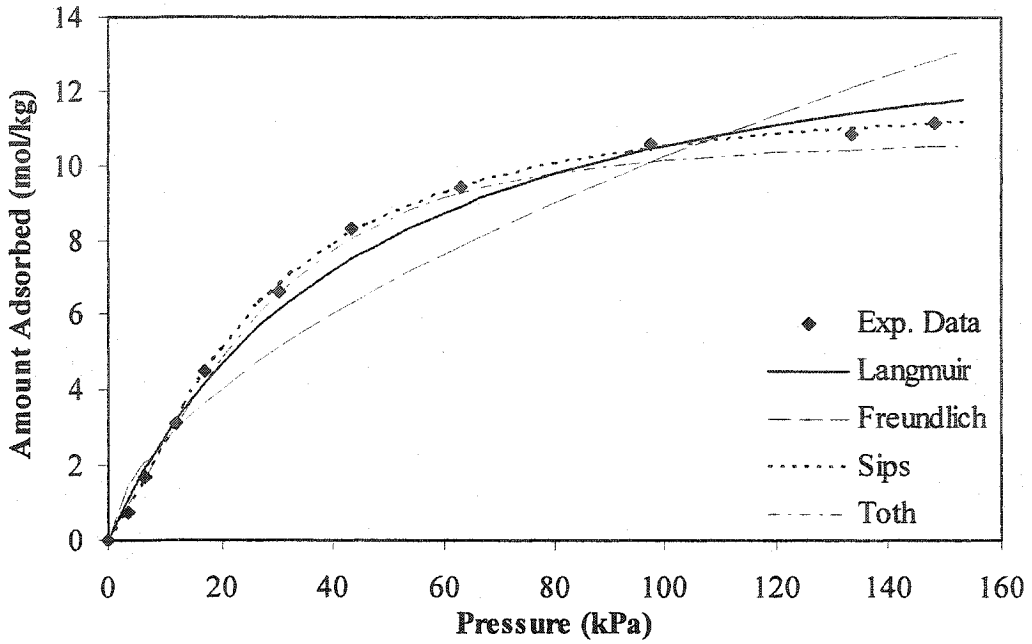

Figure B1: Adsorption isotherm of methyl chloride with carbon cloth and fitted models at 21.5 °C.

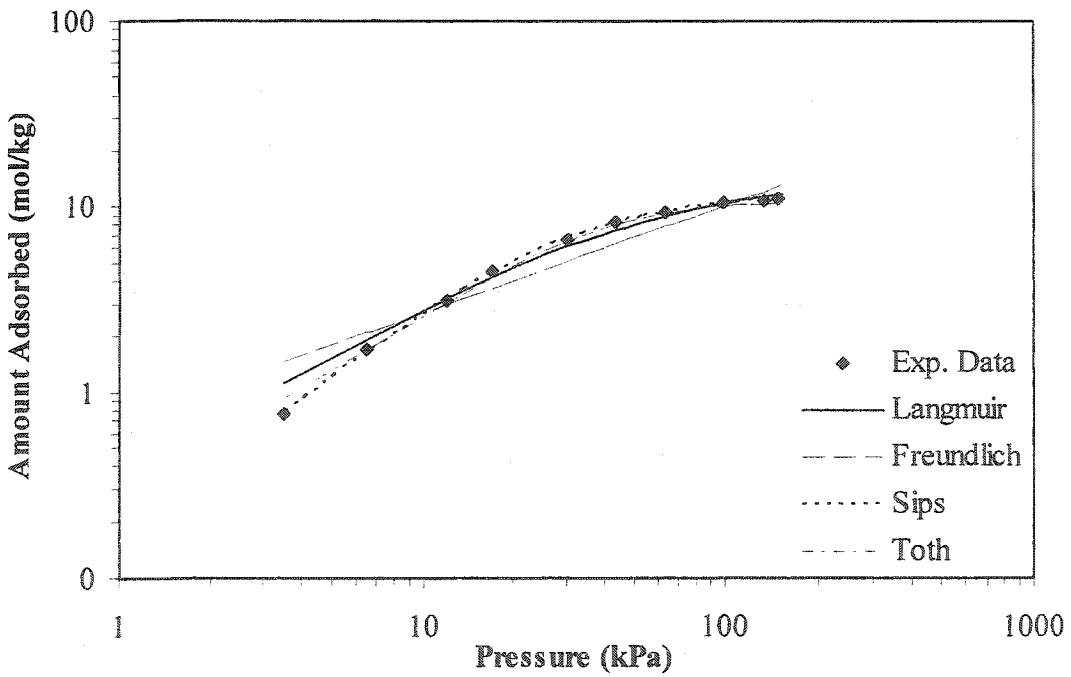

Figure B2: Adsorption isotherm of methyl chloride with carbon cloth and fitted models at 21.5°C at logarithmic scale.

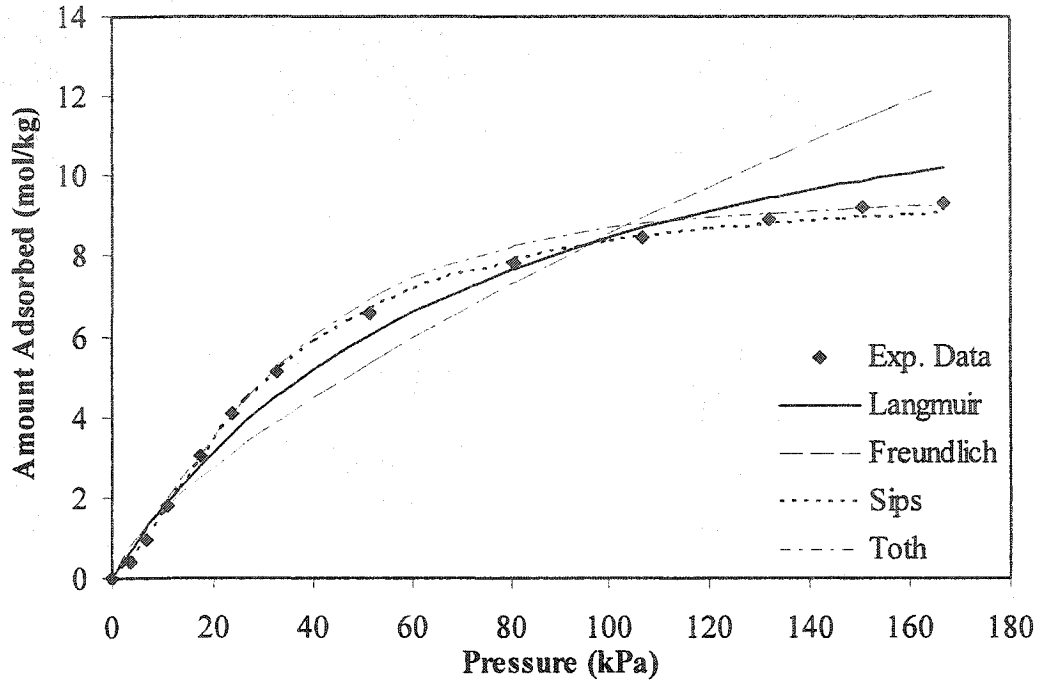

Figure B3: Adsorption isotherm of methyl chloride with carbon cloth and fitted models at 40°C.

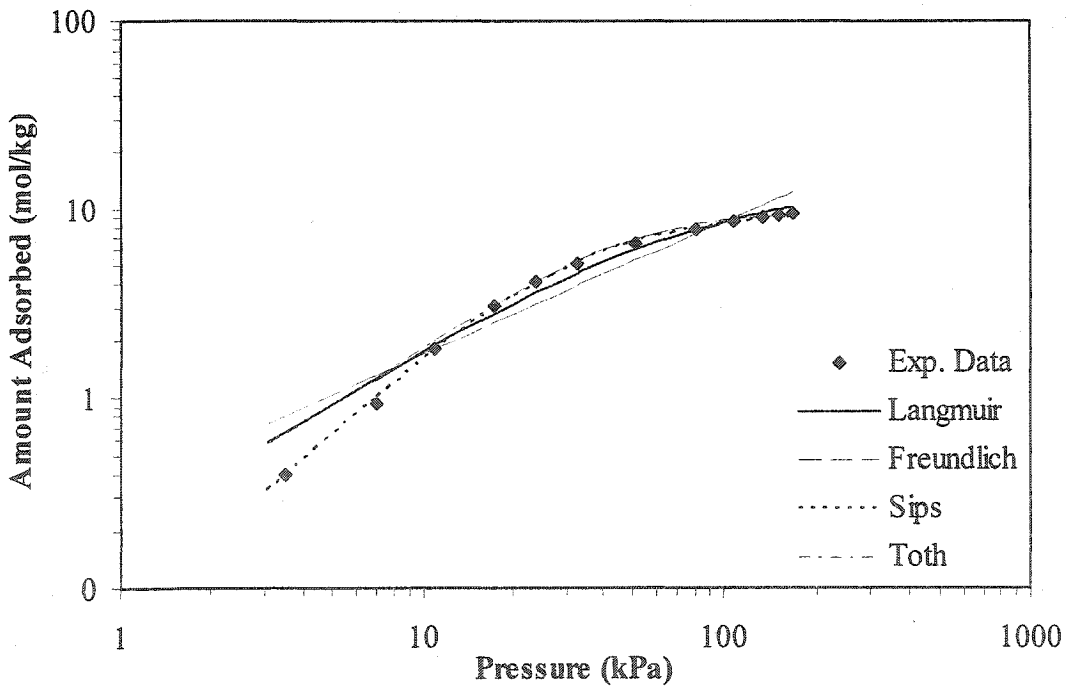

Figure B4: Adsorption isotherm of methyl chloride with carbon cloth and fitted models at 40°C at logarithmic scale.

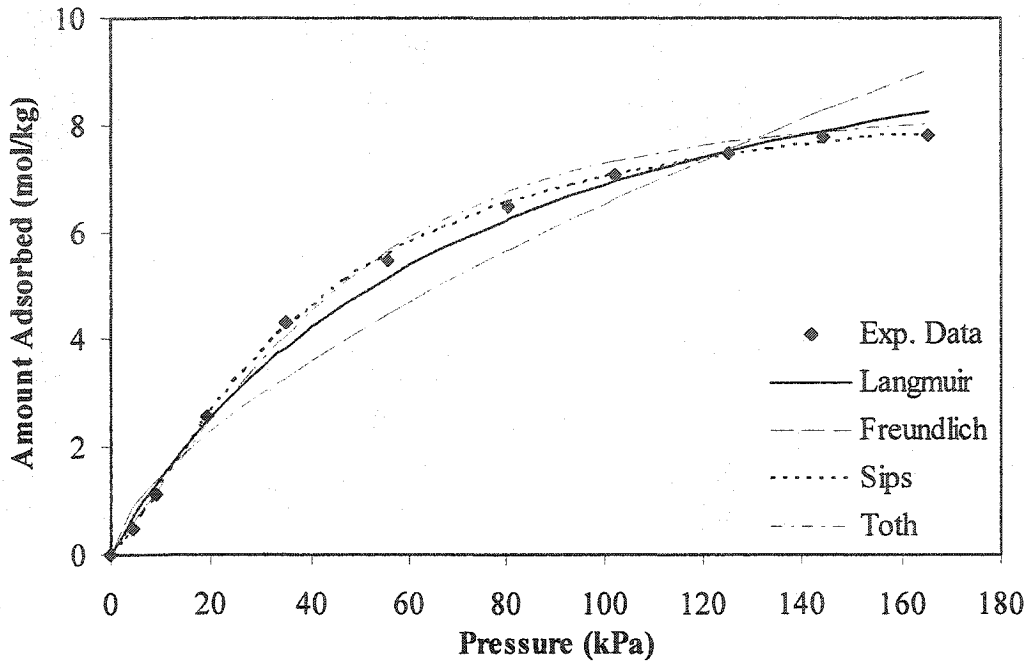

Figure B5: Adsorption isotherm of methyl chloride with carbon cloth and fitted models at 60°C.

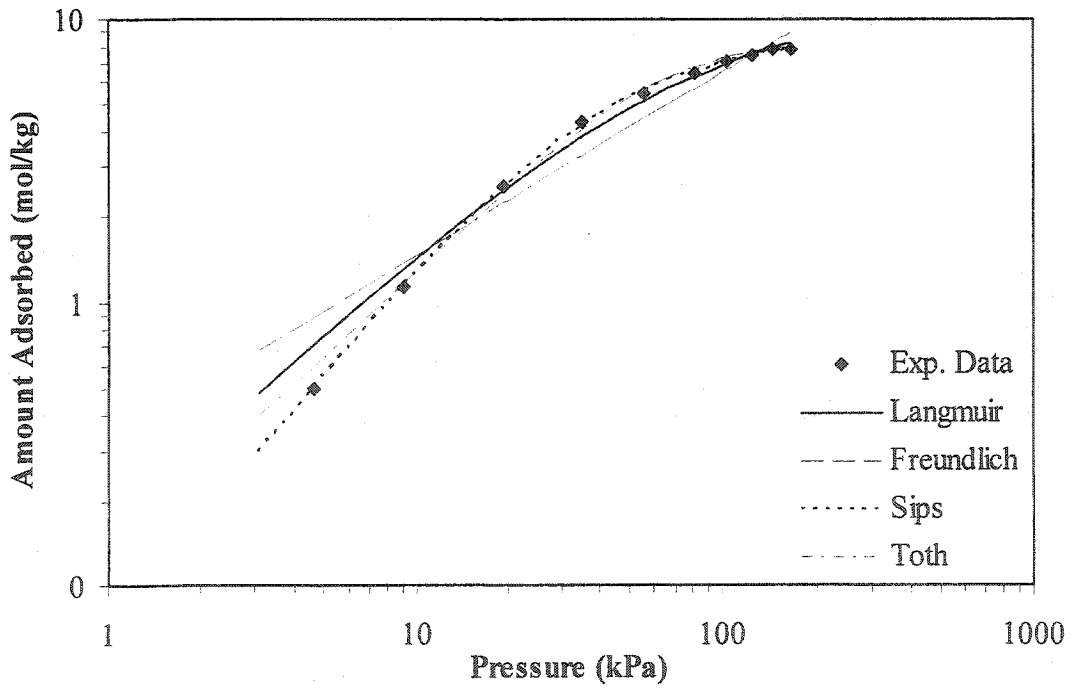

Figure B6: Adsorption isotherm of methyl chloride with carbon cloth and fitted models at 60°C at logarithmic scale.

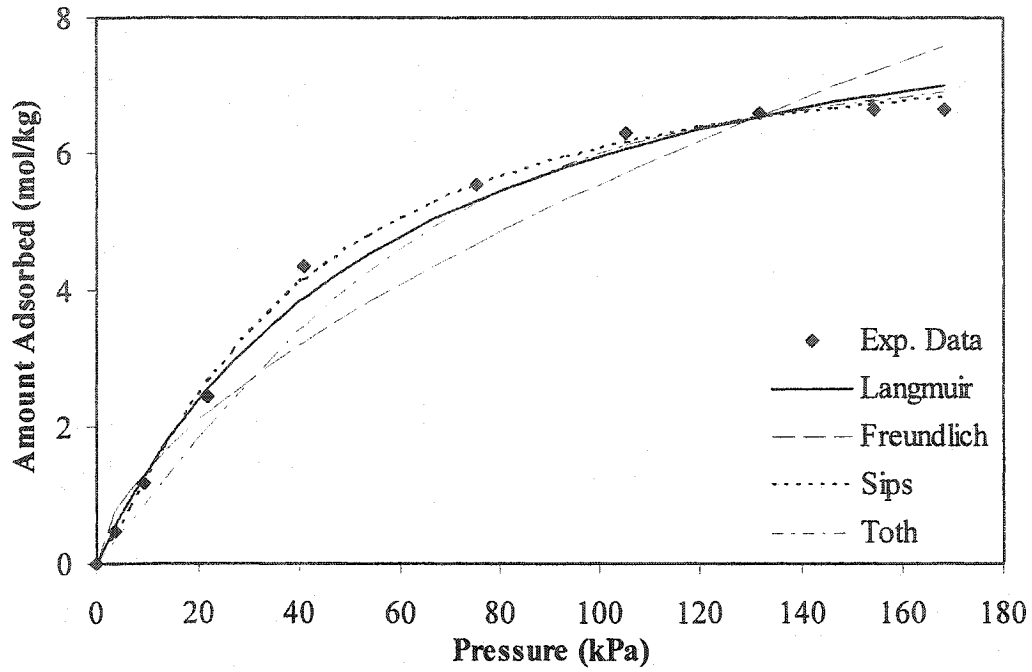

Figure B7: Adsorption isotherm of methyl chloride with carbon cloth and fitted models at 80°C.

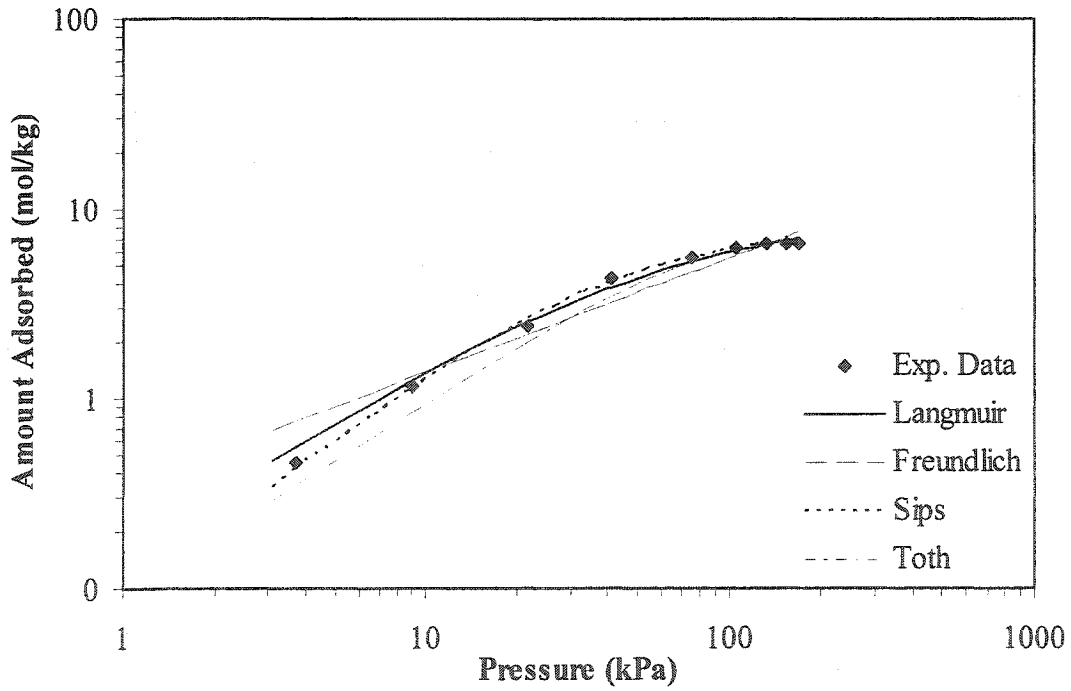

Figure B8: Adsorption isotherm of methyl chloride with carbon cloth and fitted models at 80°C at logarithmic scale.

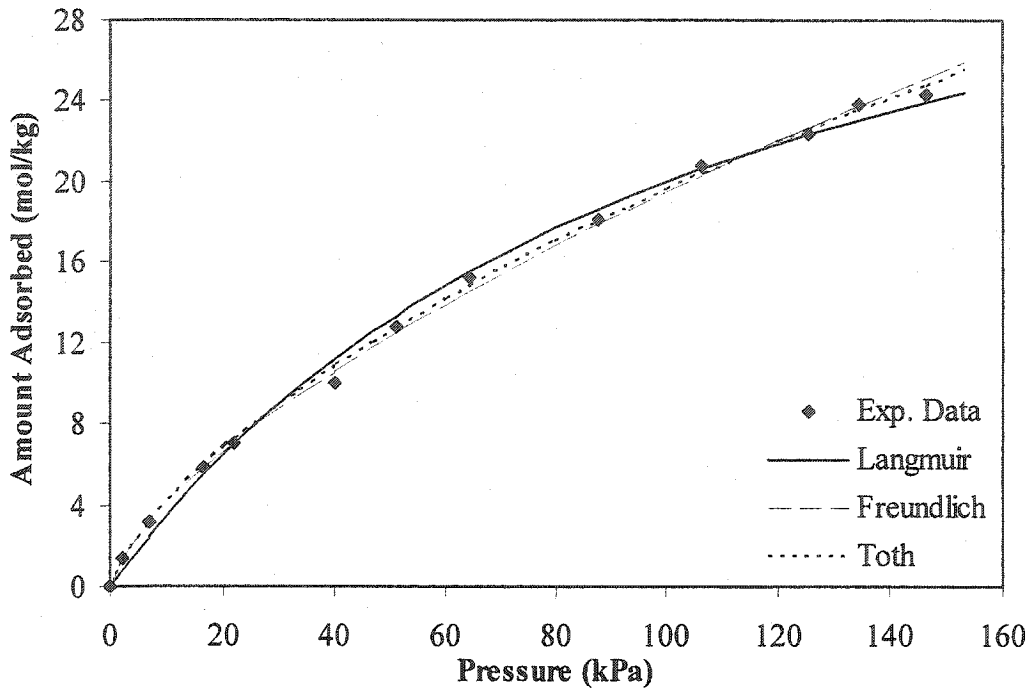

Figure B9: Adsorption isotherm of methyl chloride with mesocarbon and fitted models at 21.5°C.

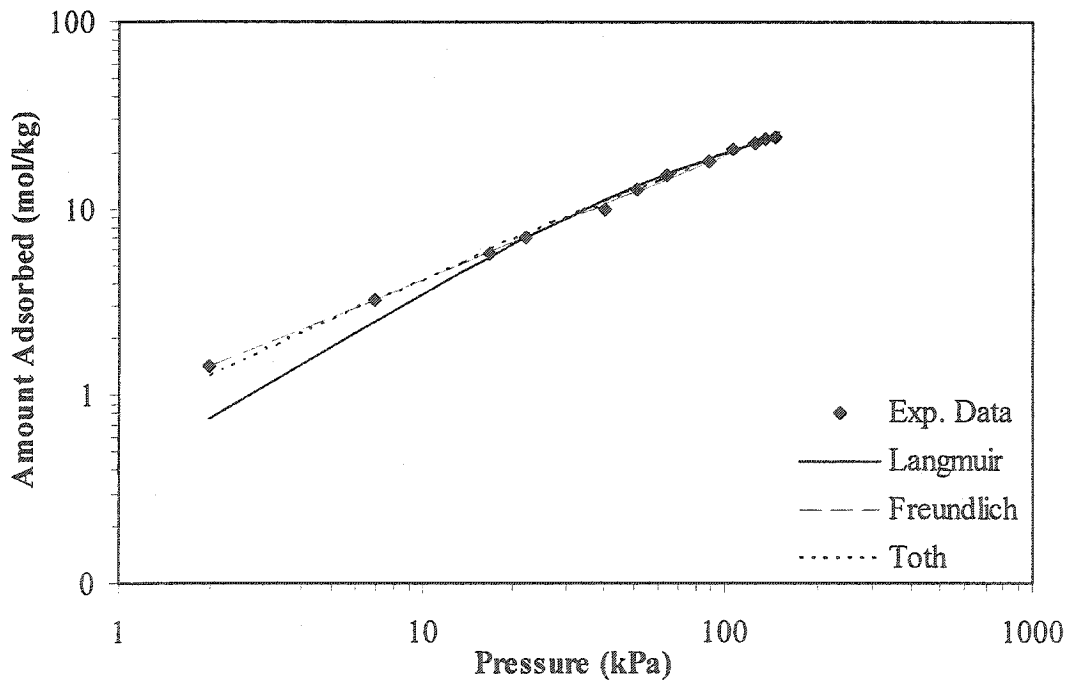

Figure B10: Adsorption isotherm of methyl chloride with mesocarbon and fitted models at 21.5°C at logarithmic scale.

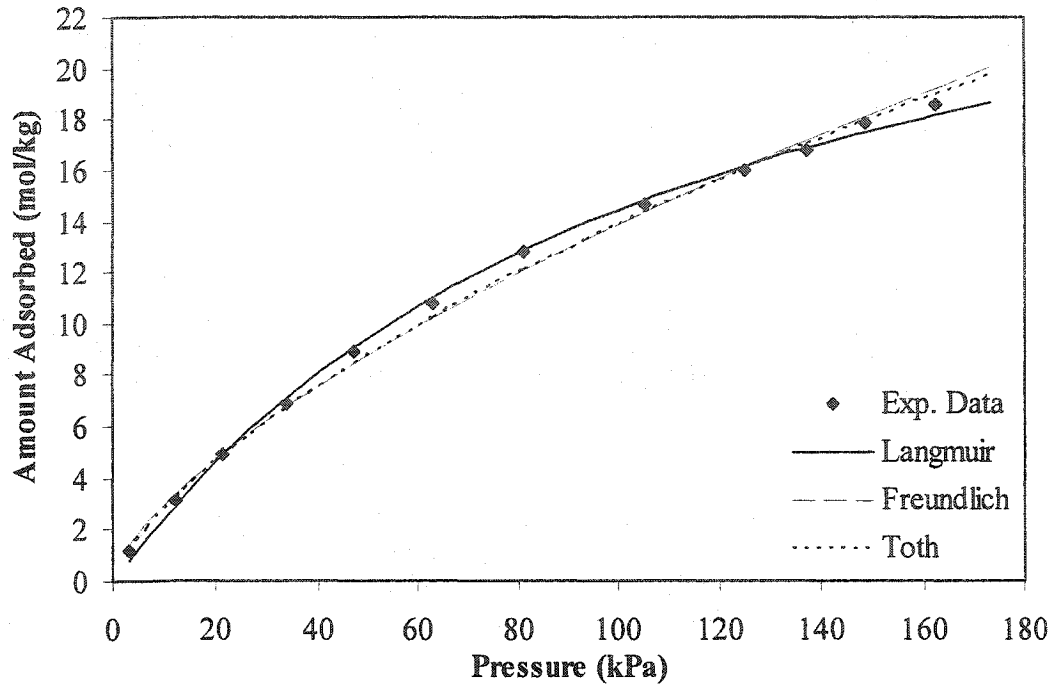

Figure B11: Adsorption isotherm of methyl chloride with mesocarbon and fitted models at 40°C.

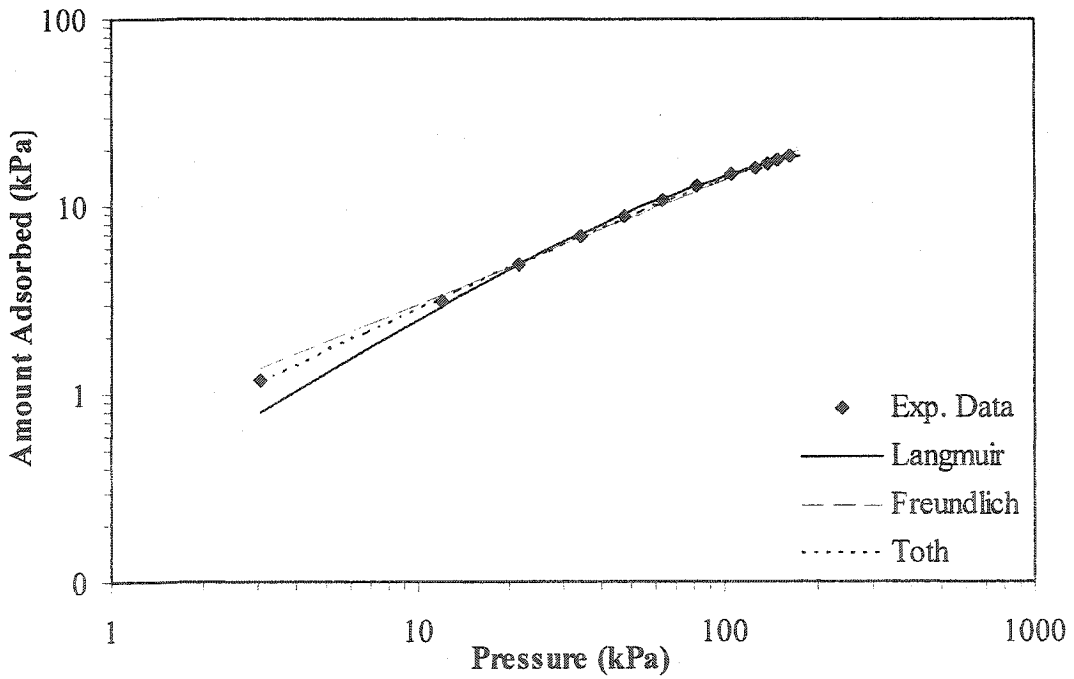

Figure B12: Adsorption isotherm of methyl chloride with mesocarbon and fitted models at 40°C at logarithmic scale.

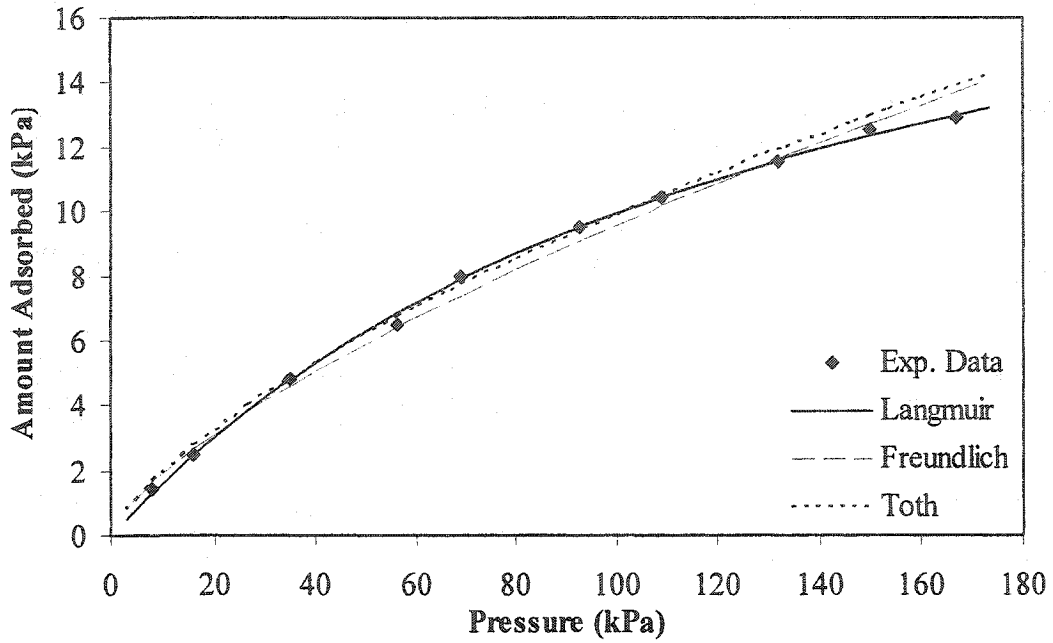

Figure B13: Adsorption isotherm of methyl chloride with mesocarbon and fitted models at 60°C.

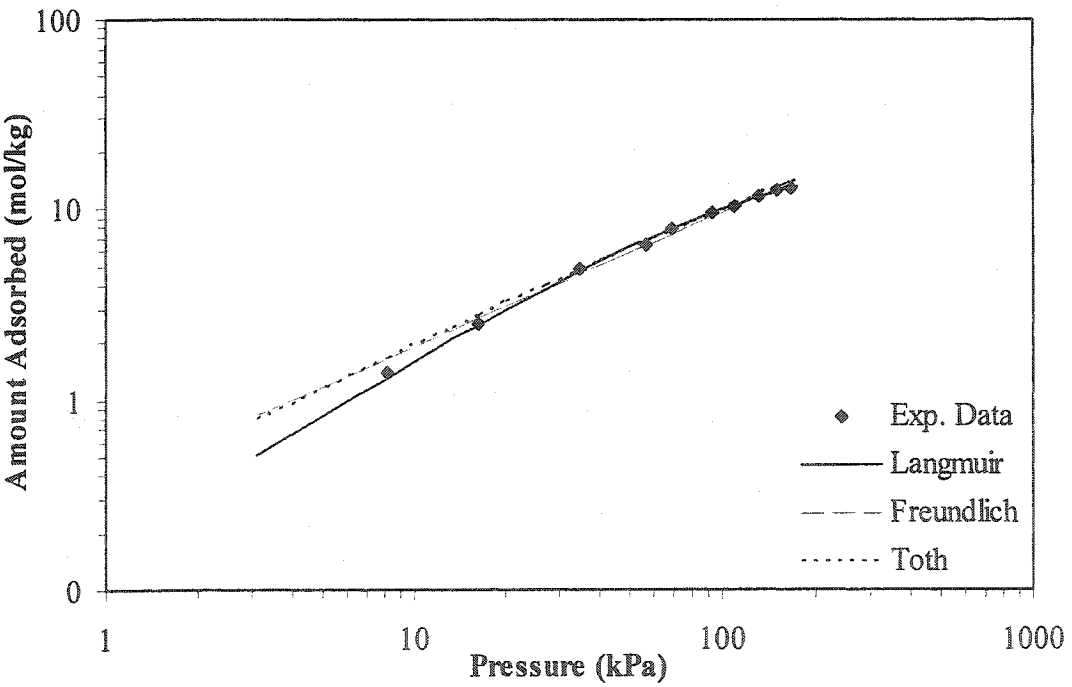

Figure B14: Adsorption isotherm of methyl chloride with mesocarbon and fitted models at 60°C at logarithmic scale.

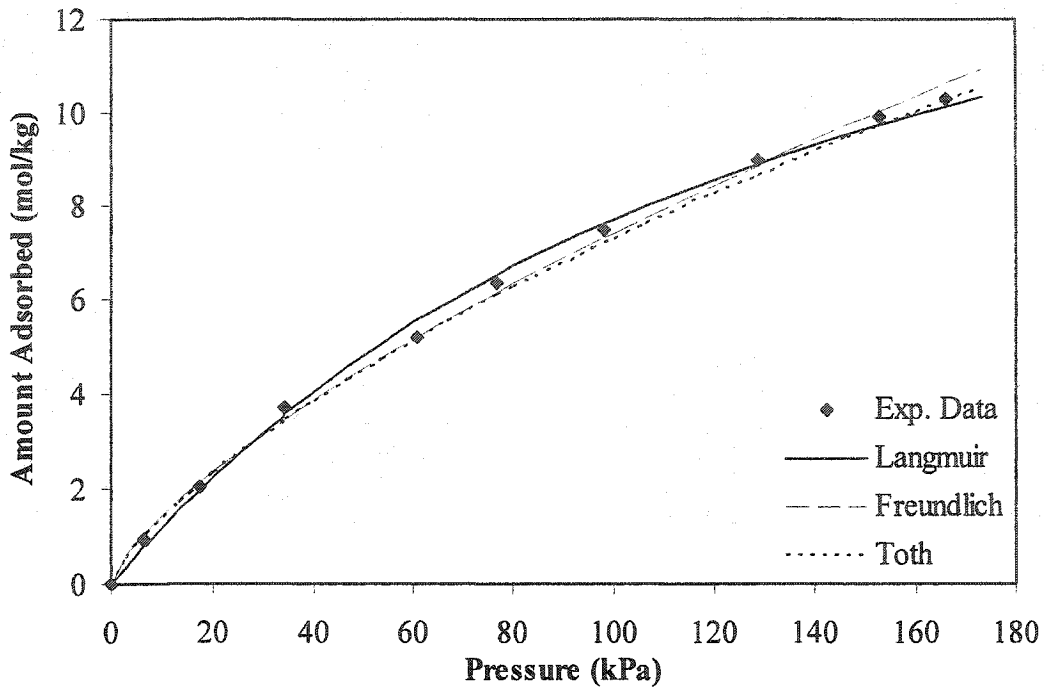

Figure B15: Adsorption isotherm of methyl chloride with mesocarbon and fitted models at 80°C.

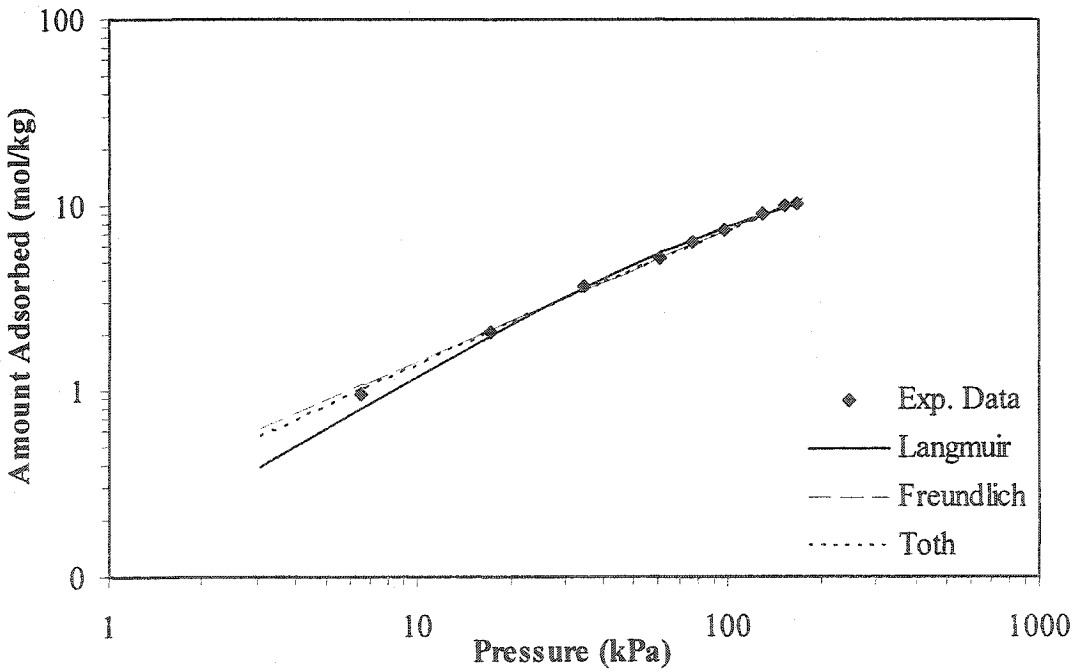

Figure B16: Adsorption isotherm of methyl chloride with mesocarbon and fitted models at 80°C at logarithmic scale.

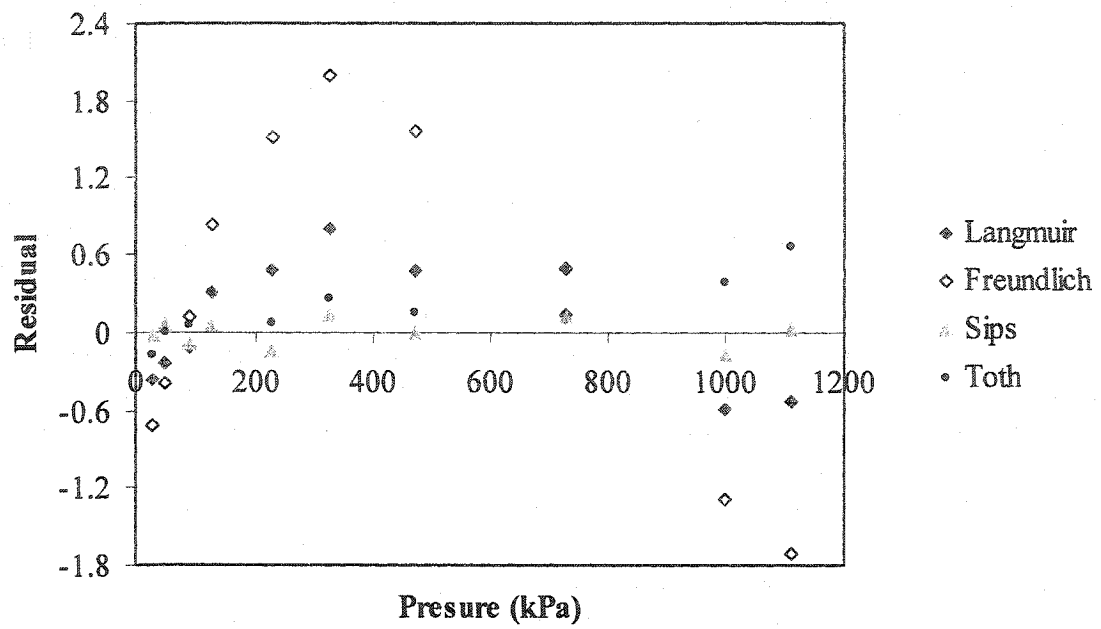

Figure B17: Residual plot for model fits of methyl chloride adsorption with carbon cloth at 40 °C.

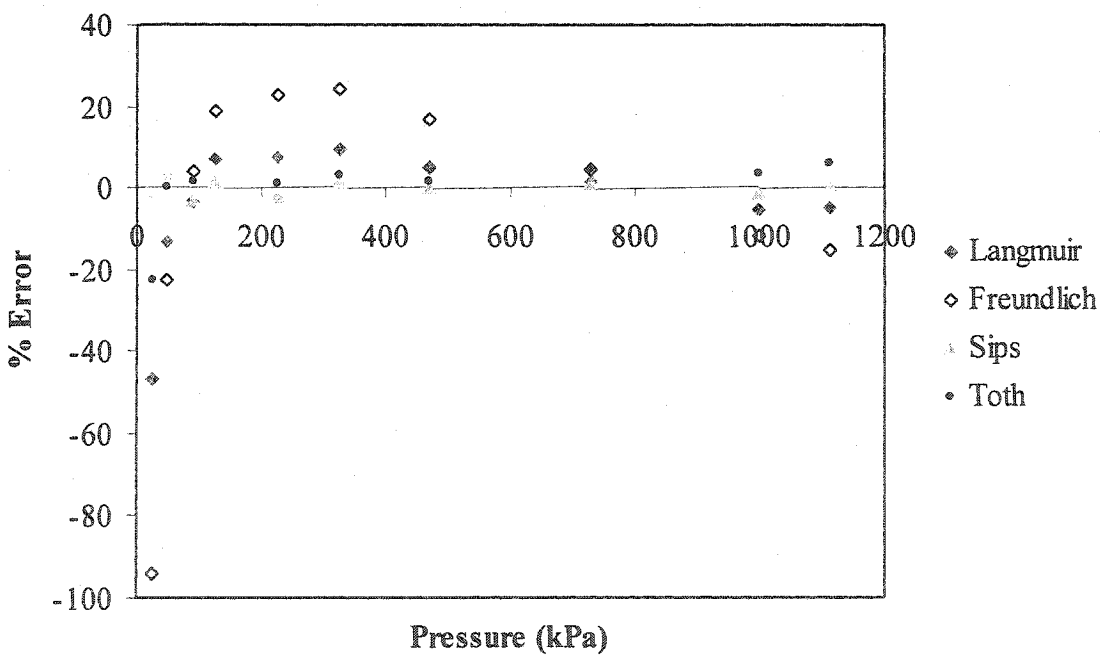

Figure B18: % Error of residual plot for model fits of methyl chloride adsorption with carbon cloth at 40 °C.

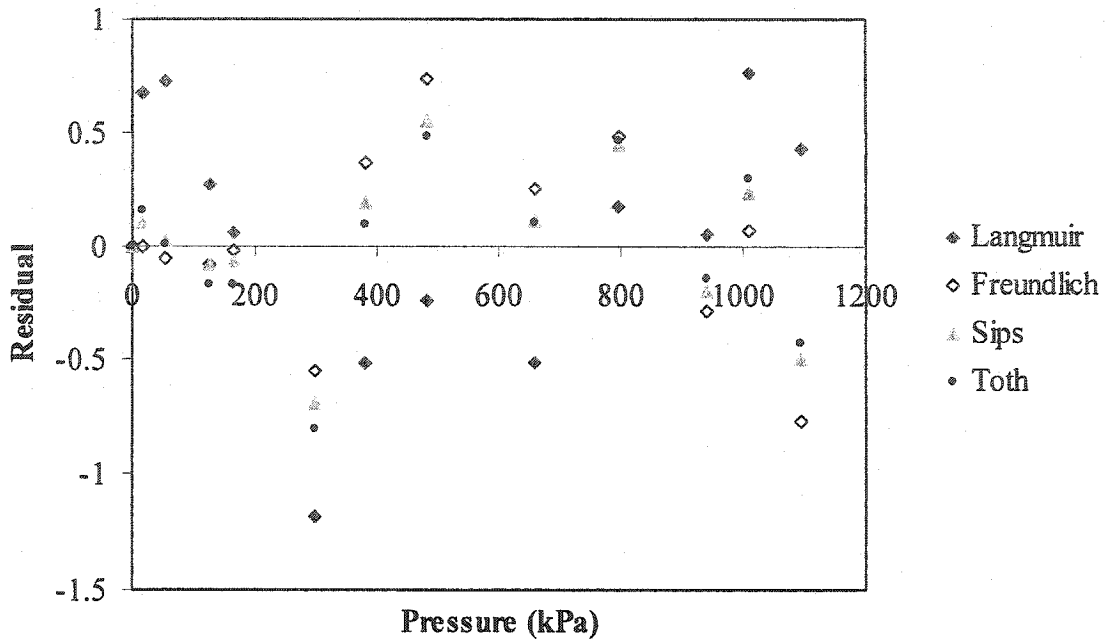

Figure B17: Residual plot for model fits of methyl chloride adsorption with mesocarbon at 40 °C.

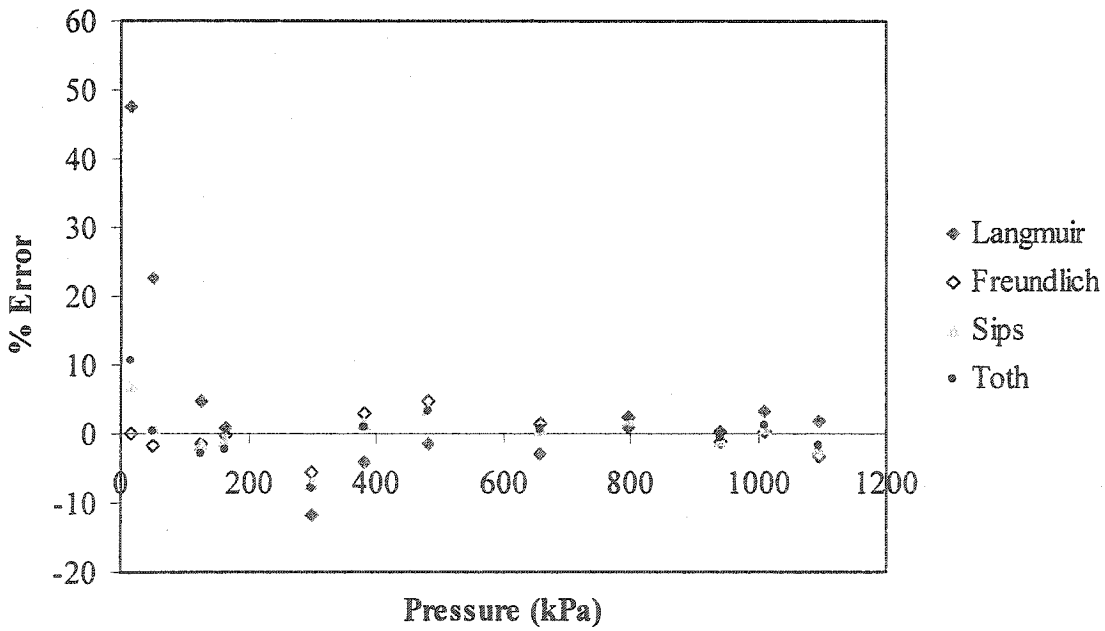

Figure B20: % Error of residual plot for model fits of methyl chloride adsorption with mesocarbon at 40 °C.